RELIABILITY-BASED ANALAYSIS OF CRACK CONTROL IN REINFORCED CONCRETE BEAMS

By

RIMA ZAHALAN

A Thesis submitted to the

Graduate School-New Brunswick

Rutgers, The State University of New Jersey

in partial fulfillment of the requirements

for the degree of

Master of Science

Graduate Program in Civil and Environmental Engineering

written under the direction of

Dr. Hani Nassif

and approved by

_____

_____

_____

New Brunswick, New Jersey

May 2010

ABSTRACT OF THE THESIS

Reliability-Based Analysis of Crack Control in Reinforced Concrete Beams

By RIMA ZAHALAN

Thesis Director:

Dr. Hani H. Nassif

This thesis is a study on reliability-based analysis of reinforced concrete beams at the crack control limit state. Past approaches to crack control and crack widths predictions in various codes are discussed. The limit state considered in this study is the maximum flexural crack width of reinforced concrete structures. Reliability index, β, is calculated to assess the level of safety in the ACI 318-08 Building Code.

Resistance prediction equations for the flexural crack control limit state as well as load equations are researched and developed in terms of the stress in the reinforcing steel. Statistical properties of variables are obtained from available literature. The effects of several parameters on the reliability index are also studied. The equation by Frosch (1999) provided the most accurate crack width predictions for various beam data obtained and is used as the resistance model in the limit state function. The live load model used is based on statistical information provided in the study by Nowak et. al (2008) which was also used in the calibration of the ACI318-08 building code. Monte Carlo simulation is performed using statistical parameters obtained for each variable. A total of 1290 beams are designed using the ACI 318-08 Building Code and included in a detailed parametric study.

It is concluded that the spacing of steel reinforcement and the concrete cover had the most significant effects on the reliability of crack width predictions. When spacing of reinforcement and concrete cover are increased, the reliability index decreases. However, increasing beam effective depth and area of reinforcement did not significantly increase the reliability index. Additionally, using a larger number of bars with smaller diameters yields higher reliability indices than using a small number of bars with larger diameters. Furthermore, an overall trend was observed that as steel yield strength increases and concrete strength decreases, the reliability index decreases. This study can be considered as a prelude to a future code calibration process of the ACI 318-08 Building Code at the serviceability limit state of crack control.

ACKNOWLEDGEMENTS

I would like to start by thanking Dr. Hani H. Nassif for his continuous support, encouragement, motivation, and guidance throughout my graduate study at Rutgers University. Thank you for providing me with the inspiration to achieve success. Your support is gratefully acknowledged. I am proud to be your student.

I would also like to thank Dr. Husam S. Najm and Dr. Kaan Ozbay for being on my committee and for providing me with indispensable advice and instruction.

I am very thankful to Dan Su, Carl Fleurimond, and Patrick Dougherty who facilitated the formation and continuance of this thesis. Your help was invaluable. I thank you for being patient with me and always being available and willing to help me with open arms. I will always remember you.

I would like to thank my family for their constant encouragement and support throughout my education. You are proud of me and I am also proud of you and to be part of this family. Thank you for your love. I love you all.

I would like to thank the Graduate School for its support and cooperation. With every little request made, you have always come through. I appreciate all your help.

I would also like to thank all my teachers, professors, and friends here at Rutgers University. Without you, my experience at Rutgers would have not been filled with a strong core and supported by the necessary foundation to achieve success. Thank you very much.

Thanks are given to all others who have provided help along the way.

TABLE OF CONTENTS

LIST OF TABLES

LIST OF FIGURES

CHAPTER 1 THESIS OVERIEW

1.1 PROBLEM STATEMENT

The factors influencing cracking in concrete have been debated throughout recent history. Crack width prediction models have been presented and various codes have implemented crack control provisions. These codes have been based on statistical analysis which is in turn based on collected crack width data. Reinforced concrete structures are considered here. The properties of the variables used in the previous analyses have all been deterministic, which are quantities that are assumed to be perfectly known. However, properties of structures are inherent to natural variability. Therefore, absolute safety, or zero probability of failure, cannot be achieved. Thus, a reliability-based approach will be taken which considers the probability of failure of a structure. This probability of failure is measured in terms of a reliability index, β. Extensive research has been performed on ultimate limit states, but not enough has been done on serviceability limit states with regard to reliability index. With a reliability-based approach, the variables used in the prediction equations will be considered as random variables and not deterministic. Consequently, the reliability-based model makes the resulting designs more real and more consistent than the currently used deterministic models. An attempt to control cracking using the reliability index as an input variable, which varies based on the designer's desired probability of failure, is made here to account for the inherent variability found in the material properties of structures. Different variables will be analyzed using a reliability-based approach to determine which ones will have the most effect on the probability of failure.

1.2 RESEARCH OBJECTIVES AND SCOPE

The principal objective of this research is to perform a reliability-based analysis to determine the reliability index of crack width in reinforced concrete structures. Control of cracking in concrete is important for aesthetics and durability. The crack control limit state is addressed. The most important variables influencing cracking in reinforced concrete will be determined using a reliability-based analysis. Provisions will be recommended based on these influencing parameters. Probabilistic analysis using random variables is becoming more prevalent and models real world situations better than a deterministic analysis. A limit state function is used with a crack width prediction equation as the resistance and a distributed live load for an office building will be used as the load. This model will be simulated using the Monte Carlo method. The results of the Monte Carlo simulation will output a reliability index for each case studied. Evaluation of these reliability indices will determine how selected parameters influence reliability and safety. Parameters included in the study are beam width, beam effective depth, concrete cover, steel yield strength, concrete compressive strength, area of reinforcement, spacing of reinforcement, and reinforcement bar size. Reliability indices will also be evaluated to see if the designed beams meet the selected target reliability index.

1.3 THESIS ORGANIZATION

This thesis consists of six chapters described briefly as follows:

Chapter I covers the introduction consisting of the problem statement, research objective and scope, and thesis organization.

Chapter II covers the literature review dating back to the 1950s of the history of crack width theory, causes and mechanism of cracking, the most influential variables on crack width, and a collection of crack width equations. Theories of various investigators are presented chronologically. A comparison of international code provisions is also presented along with a summary of the most important crack width equations, identified by simplicity and historical use.

Chapter III covers an introduction to the reliability-based approach and how considering variables as random as opposed to deterministic is becoming more prevalent in structural design. The inherent variability of material properties must be taken into account and the resulting realization that the capacity may not be the same for every structure with the same design parameters.

Chapter IV covers the test method and procedure. A validation of the resistance and load equations is provided and proven using data of measured crack widths available in literature. Statistical parameters of the variables are also presented, which include mean, standard deviation, and coefficient of variation.

Chapter V covers the results of the Monte Carlo simulations, the most influential parameters affecting the reliability index, an analysis of these results, and a discussion.

Chapter VI covers the conclusions, recommendations, and appendices.

CHAPTER 2 CAUSES AND MECHANISM OF CRACKING IN CONCRETE

2.1 INTRODUCTION

Control of cracking in concrete structures is controversial but must be controlled for aesthetic purposes, durability, and corrosion resistance. Cracking can reduce the serviceability of a structure. Cracking can primarily be caused by flexural and tensile stresses, but also from temperature, shrinkage, shear, and torsion. Although researchers do not agree on any one specific crack formula, the most significant parameters to control cracking have been widely agreed upon. The most sensitive factor is the reinforcing steel stress, followed by concrete cover, bar spacing, and the area of concrete surrounding each bar. It has been agreed upon that the bar diameter is not a major variable.

2.2 CAUSES OF CRACKING IN CONCRETE

Cracking in concrete is subject to an inherent variability. Concrete cracks simply because it has low tensile strength and lacks ductility i.e. it is brittle. The following lists the factors that cause cracking according to Abdun-Nur (1983). The first factor is a too high water content in the concrete mixture which increases drying shrinkage and causes tensile stresses due to shrinkage movement. The second is excessively high cement content which requires more water and leads to the aforementioned cracking result. Next, when higher cement content is used than needed, extra heat is generated through the hydration of cement which leads to thermal stresses that exceed the tensile strength of concrete at early ages. Fourth, cycles of drying and wetting due to rain and sun cause dimensional expansion and contraction and lead to stresses that again exceed the tensile strength of concrete. Fifth, temperature changes also cause expansion which leads to

excess stresses. Next, freezing and thawing not only brings temperature and dimensional changes that introduce tension, but also freezing of the water in pores creates additional tensile stresses that cause cracking. Also, deicing salts to increase safety for moving traffic on pavements leads to forces of crystallization of the salt out of solution which increases tensile stresses. Furthermore, the effect of chloride ions on the reinforcing steel causes rusting and expansion of the steel which brings tensile stresses. Eighth, dry hot winds during placing remove the surface water quickly and cause surface shrinkage which leads to cracking. Ninth, structural adjustments due to foundation movements by settlement or expansive soils lead to cracking. Next, the reaction between the alkalies in the cement and certain types of silica in aggregates bring about the formation of a gel that leads to internal pressures which cause concrete to break up in tension. Lastly, sulfate attack of the concrete produces calcium sulfoaluminate which occupies a large space and leads to internal pressure which causes cracking. Abdun-Nur maintains that these are some of the major causes of cracking he has experienced throughout his career but there certainly may be more causes.

2.3 HISTORY OF CRACK WIDTH THEORY

Since the 1950s, various researchers have been conducting investigations on cracking in concrete. Previous research using statistical evaluation has been performed on reinforced concrete beams where crack widths were recorded at two primary locations- the bottom tension surface and the side face at the level of reinforcement. The crack width at the bottom of the beam is typically larger than on the side of the beam because of the larger extension of the bottom face than at the level of the steel. Due to the random

nature of cracking and currently accepted models that become invalid when concrete cover is large, there is an ever-growing need for investigators to find compromise on crack width equations that will accurately determine width values and provide insight on specific parameters that will prevent large crack widths. Figure 1 shows a cracked section, where S_c denotes crack spacing and f_s denotes reinforcement stress.

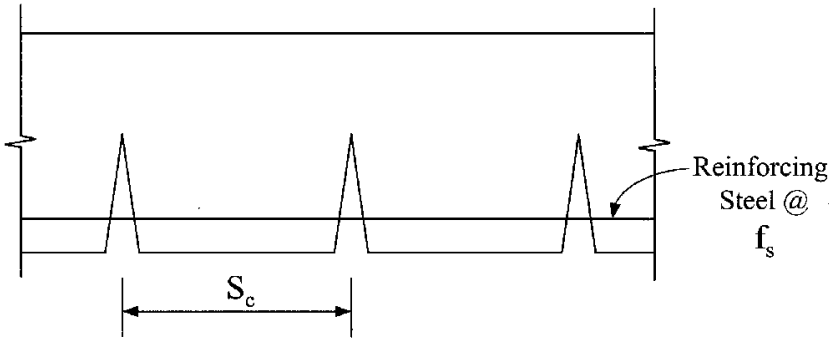

Figure 2.1: Cracked Section (Frosch, 1999)

2.3.2 EQUATION BY CLARK (1956)

Clark (1956) conducted tests to enable engineers to estimate crack width and spacing in flexural members of varying design and stresses in reinforcement. He maintained that the low tensile strength of concrete, its low extensibility, and the stresses brought on by drying shrinkage all result in cracks in the tensile zone of loaded reinforced concrete flexural members. The data provided in this experiment will be elaborated on later in this thesis as it was used to test the accuracy of existing crack width equations. The study included 58 reinforced concrete beams and slabs of varying dimension. The specimens were loaded with two point loads at quarter points and Tuckerman gages were used to measure the width of cracks.

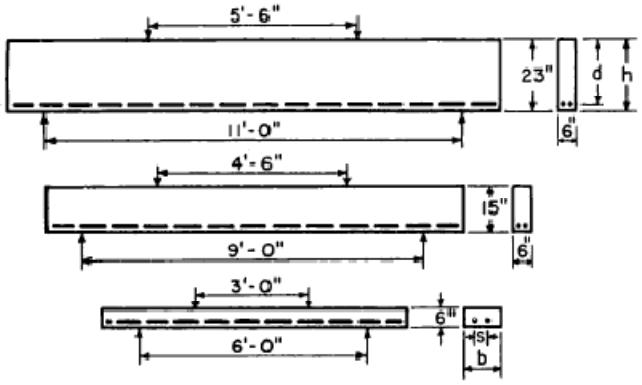

Figure 2.2: Dimensions of Clark's Specimen and Type of Loading (Clark, 1956)

Figure 2.3: Typical Crack Pattern at Failure (Clark, 1956)

Clark (1956) concluded that the average width of cracks was found to be proportional to the product of the quantities D/p and (h-d)/d. Furthermore, he stated that average width was also found to be proportional to the increase of steel stress beyond that causing initial cracking. Clark (1956) also insisted that the width of cracks can be reduced by using a large number of small bars and by increasing the ratio of reinforcement. However, the aforementioned investigators disagree. Broms (1965), Gergely-Lutz (1968), and Frosch (1999) indicate that the ratio D/p is not a good correlation variable, especially for T beams, and that bar size plays a minimal role in reducing crack widths. The coefficients in Clark's (1956) equation are specific to a set of data and thus his equation is not the simplest applicable formula. Nevertheless, Clark

(1956) concluded that his equation gave reasonable values for average crack width and that the maximum crack width is 1.64 times the average crack width:

$$w_{ave} = C_1 \frac{D}{p} [f_s - C_2 \left(\frac{1}{p} + n\right)] \quad (2.1)$$

where:

w_{ave} = average width of cracks, in

C_1, C_2 = coefficients, the values depend on distribution of bond stress, bond strength, and tensile strength of concrete, for Clark's study $C_1 = 2.27 \times 10^{-8}$(h-d)/d, $C_2 = 56.6$

D = diameter of reinforcing bar, in

p =A_s/A_e =cross-sectional area of reinforcement/cross-sectional area of concrete = bd, in^2

f_s = computed stress in reinforcement, psi

n = ratio of modulus of elasticity of steel to concrete (assumed to be 8 in Clark's study)

h = overall depth of beam/slab, in

d = distance from compressive face of beam/slab to centroid of longitudinal tensile reinforcement

2.3.3 EQUATION BY KAAR AND MATTOCK (1963)

Kaar and Mattock (1963) also developed a well-known crack width equation for bottom face cracking using the same variables as the Gergely-Lutz (1965) equation discussed later:

$$w_b = 0.115 \beta f_s \sqrt[4]{A} \quad (2.2)$$

where:

w_b = maximum crack width, 0.001 in

β = ratio of distances to neutral axis from extreme tension fiber and from centroid of reinforcement

f_s = steel stress calculated by elastic crack section theory, ksi

d_c = bottom cover measured from center of lowest bar, in

A = average effective concrete area around a reinforcing bar, having same centroid as reinforcement, in²

The equation of Kaar and Mattock (1963) was derived from a curve fit of limited data primarily from Hognestad and Kaar-Mattock. The equation fits the test data well for the range of covers considered. However, for covers greater than 2.5 inches, the equation no longer fits data well (Frosch, 1999).

2.3.4 EQUATION BY BROMS (1965)

Broms (1965) attempts to construct a rather uncomplicated method for calculating crack width and crack spacing in reinforced concrete members. Using reinforcement with higher strength levels in reinforced concrete members is partially limited by the crack width which can be permitted without endangering reinforcement. Generally, increasing steel stress and crack spacing also increases the crack width at the level of reinforcement. Plain bars associated with crack spacing for reinforced concrete members is large, thus prompting steel stress levels to be kept lower to control crack widths. Analysis of the stress distribution in cracked reinforced concrete members has shown that assuming a linear or uniform distribution of stress may lead to larger and more significant errors

when the calculated crack spacing or the main cracks approach two times the thickness of the concrete cover or the individual spacing of reinforcing bars (Broms, 1965).

Broms carried out tests on 37 tension members and 10 flexural members all having reinforced high strength bars in order to analyze crack width and crack spacing. It was found that the length of new cracks that develop in a member that has been reinforced with several bars depends primarily on the spacing of the individual bars and on the initial crack spacing. The study concluded that the absolute minimum visible crack spacing will be the same distance from the surface to the center of the bar that is located nearest to the surface of the member, defined as distance t. Therefore, the theoretical minimum crack spacing is equal to the thickness of the concrete cover (Broms, 1965).

Based on his study, Broms (1965) developed a formula to calculate average crack width w_{max}, neglecting the elongation of concrete and assuming crack spacing equal to twice the distance t_e (the effective concrete cover) where ϵ_s is the strain in the reinforcement. In the figure below, $t = t_e$, the distance to the nearest reinforcing bar to the point in question (e.g. C). Broms' equation for maximum crack width is as follows:

$$w_{max} = 4t_e\epsilon_s \text{ when } t > 1.0 \tag{2.3}$$

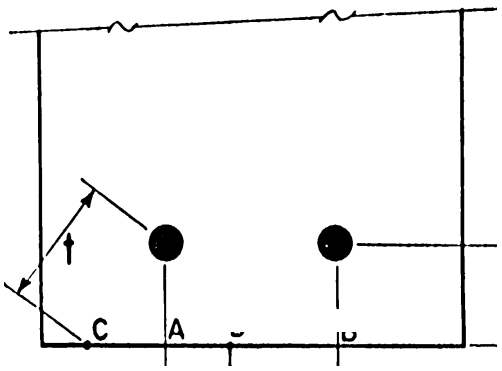

Figure 2.4: Reinforced concrete member showing terms used to define the effective cover, t_e (Gergely and Lutz, 1968)

This equation is only applicable when the nominal steel stress exceeds 20,000 to 30,000 psi at cover thicknesses ranging from 1.25 to 3.0 in and about 50,000 psi at a cover thickness of 6.0 inches. Thus, the equation is not a reasonably applicable one for all situations.

It was also shown that the widths of the initial cracks present at low levels of stress in the reinforcement, usually less than 20,000 psi were almost the same at the surface of the members closest to the reinforcement. The crack widths positioned at the surface were two to three times greater than the widths closer to the reinforcement at stresses larger than 30,000 psi (Broms, 1965).

2.3.5 EQUATION BY GERGELY AND LUTZ (1968)

Peter Gergely and Leroy Lutz (1968) examine information from six experiments by Broms (1965), Hognestad (1962), Kaar and Mattock (1963), Kaar and Hognestad (1965), Clark (1956), and Rüsch and Rehm (1964) for the side and bottom crack width of flexural members. In order to obtain equations for bottom and side face cracks that best fit the data, a large number of equations and variables were analyzed. Gergely and Lutz present an equation that best fit the experimental data. These equations were used to predict the most likely bottom and side face crack widths in reinforced concrete flexural members.

Others have proposed a myriad of semi-theoretical and experimental equations that contain several different variables. Because the width of cracks can be subjected to large scatter, it is more difficult to ascertain which equation is better for predicting such quantities. The primary variable is the steel stress, f_s. Bar diameter was concluded to be insignificant when determining crack widths while the number of bars was extremely important since it indirectly determines concrete cover. Some other variables considered were the average effective concrete area around a reinforcing bar (A), bar spacing s, concrete cover t_s or t_b, and the ratio of bar diameter D to reinforcement ratio p. Crack width was found to directly change depending on the distance from the nearby bar (Gergely and Lutz, 1968).

The larger extension of the bottom face allows the crack width at the bottom of the beam to be generally larger than on the side of the beam as opposed to the level of steel. “Regression analysis was used where the coefficients of a linear expression that best fits a given set of experimental data are determined by a least squares of deviations

criterion" (Gergely and Lutz, 1968). When considering individual variables of certain investigations, the basis for evaluation remained in the standard error. When comparing various investigations, the magnitude of the regression coefficient was quintessential.

Based on their study, Gergely and Lutz (1968) recommend the following equation for calculating bottom crack width:

$$w_b = 0.076\beta f_s \sqrt[3]{Ad_c} \tag{2.4}$$

where:

w_b = maximum crack width, 0.001 in

β = ratio of distances to neutral axis from extreme tension fiber and from centroid of reinforcement

f_s = steel stress calculated by elastic crack section theory, ksi

d_c = bottom cover measured from center of lowest bar, in

A = average effective concrete area around reinforcing bar, having same centroid as reinforcement, in² and is equal to 2b'(h-d)/m, where b' is the width of the beam at the centroid of tensile reinforcement, h is the depth, d is the effective depth, and m is the number of tensile reinforcing bars

They did this only after taking into consideration that the Rüsch -Rehm and Kaar-Mattock data are biased. They compared the results to other studies and concluded that Clark's test program was more comprehensive than other American studies.

In conclusion, Gergely and Lutz found that the steel stress is the most important factor. The cover thickness is an important factor as well but not the only thing that

should be taken into consideration. The bar diameter is not a detrimental factor and that the ratio D/p is not a good variable in any form. The proximity of the compression zone in flexural members reduces the size of the crack width. As the strain gradient increases, so does the bottom crack width and that the major variables are the effective concrete area A_e, the number of bars m, the side or bottom cover, and the steel stress (Gergely and Lutz, 1968).

2.3.6 ACI FALL CONVENTION: MODERATED BY DARWIN (1984)

To discuss the aforementioned crack width theories, the ACI fall convention met in 1984 in New York, NY. It was sponsored by ACI committees 222, Corrosion of Metals in Concrete, and 224, Control of Cracking of Concrete Structures and supervised by David Darwin. David G. Manning, Eivind Hognestad, Andrew W. Beeby, Paul F. Rice, and Abdul Q. Ghowrwal. The participants at the convention all shared their views, reflected below. A debate was conducted to question current design tactics and provisions. They connected crack width to steel stress, bar spacing, exposure conditions, and cover thickness. According to these provisions, a thinner crack width can be acquired by reducing the cover in order to provide protection against severe exposure conditions. Corrosion resistance can be decreased by a reduced cover.

According to Manning (1984), there are two varied theories about the effect of cracking on the corrosion of steel in concrete. “Theory No. 1 states that cracks significantly reduce the service life of structures by permitting aces of chloride ions, moisture, and oxygen to reinforcing steel, not only accelerating the onset of corrosion but

providing space for the deposition of corrosion products. The opposing argument, Theory No. 2 states that while cracks may accelerate the onset of corrosion, such corrosion is localized and confined to the intersected reinforcing bars" (Manning, 1984). Because chloride ions eventually diffuse through concrete that has not been cracked and further develop more corrosion, after several years of service there is little ability to tell the difference the amount of corrosion in cracked and uncracked concrete. Manning, Beeby, and Maylan all believe that Theory No. 2 is closest to the actual situation than the first theory. Most codes outline certain provisions to deal with crack width at the surface of the concrete. However, the crack width at the bar is not related to the surface cracks. The crack width at the bar is a function of where the crack originated, the amount of cover, the steel stress, the arrangement and diameter of the bars, the reinforcement ratio, and the depth of the tensile zone.

Hognestad (1984) outlines current provisions at the time of the meeting. The 1971 ACI Building Code was created to accommodate the use of reinforcing steels with yield strength of 60,000 to 80,000 psi. Rules introduced the issue of crack control and were made to distribute reinforcement and controlled limitations on steel stress at service loads. When the ACI Code was written in 1971, it was not known the limits beyond which crack widths and steel would lead reinforcement to corrode. Therefore, the Gergely-Lutz term for crack width was chosen as the main basis for the provisions relating to distribution of flexural reinforcement. In preference to other equations at the time, this choice was made on the basis of simplicity and reasonable accuracy, considering that crack width is subject to large scatter. The equations for Gergely-Lutz crack width and

reinforcement distribution z are as follows, where exterior denotes structures exposed to outside environment and interior denotes structures not exposed to outside environment:

$$w = 0.076\beta\sqrt[3]{d_c A} < 0.013 \text{ in (exterior)},0.016 \text{ in (interior)} \quad (2.5)$$

$$z = f_s\sqrt[3]{d_c A} < 145 \text{ k/in (exterior) } 175 \text{ k/in (interior)} \quad (2.6)$$

The z factor has been modified several times for different structures, such as pipes or slab-type structures, to produce correct results since the cod provisions are too general. Committee 224 has been concerned about using the z factor to reduce cover in order to reduce crack width under conditions with potentially high corrosive levels. Numerous researchers concur that the z value is not as significant as has been previously suggested. The committee has stated that the crack width, or the crack width as seen through the z value, will not provide protection for reinforcement against corrosion. Hognestad deduced that the provisions set forth in the code control steel corrosion through six major factors. The quality of concrete, adequate cover, limited chlorides, sound reinforcing details, steel stress limitations, and prestressing in must all be considered. One of the Committee's recommendations calls for limiting the value of the cover that is used for the calculation of z to 2 in. Manning and Beeby believe there is no legitimate relationship between crack width and corrosion. Therefore, the crack provisions in most codes of practice are more likely to lessen in durability than to improve it. "The road toward design criteria for the future could be to differentiate between various exposures, types of member, and types of service" (Beeby, Darwin, Hognestad, & Manning, 1984).

2.3.7 EQUATION BY FROSCH (1999-2001)

The ACI Building Code calls for the control of flexural cracking in reinforced concrete members. Since 1971, the code has used the z-factor method, which is a tailored form of the Gergely-Lutz crack width equation that was derived from a statistical assessment of experimental data. Thicker concrete covers coupled with the use of high-performance concrete are becoming increasingly popular because of their durability. These thicker covers are necessary for maintaining crack control. They result in unrealistic bar spacing and prevent the use of contemporary crack control practices that are based on statistical reasoning. Research is becoming increasingly significant to determine if increasing covers can still provide reasonable crack control, the effect of epoxy-coated reinforcement on crack width, and the validity of the z-factor approach for thicker concrete covers. Frosch (1999) discusses the validity of the crack width equation and introduces a new formulation of the equation based on the physical phenomenon The physical model allows a designer to choose any limiting crack width (2001).

Gergely and Lutz (1968) developed a well-known crack width equation for the critical bottom tension face that was previously mentioned. The concrete cover d_c is of interest and the range covered in the Gergely-Lutz study considered a maximum cover of only 3.31 in, where only three test specimens had covers greater than 2.5in. The fit for the equation is best seen with covers less than 2.5 in. However, it is perfectly legitimate to question both equations outside the parameters of the covers already considered. The Kaar-Mattock (1963) and Gergely-Lutz (1968) equations displayed a divergence in the tabulated crack widths as the covers increased, as seen in Figure 2.5. This did not allow for a “correct” equation to exist because test data for thicker covers is unavailable.

Another approach needs to be taken in order for the calculation of crack widths to converge for covers greater than 2.5 in.

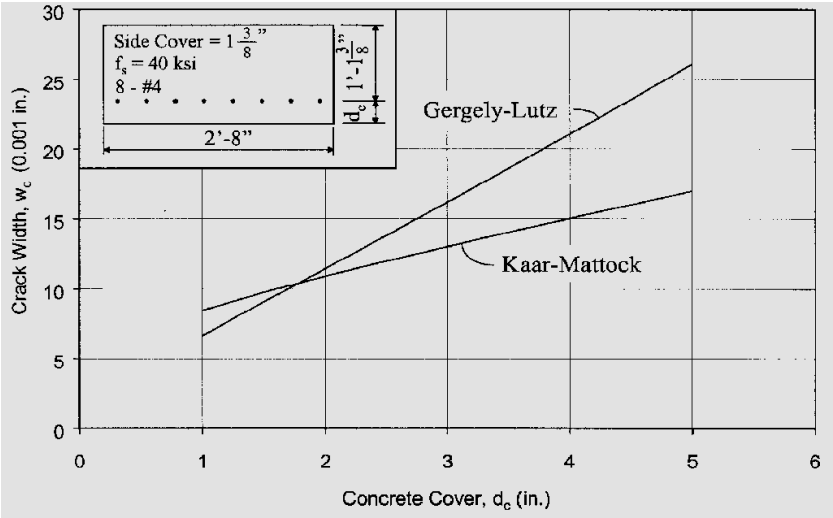

Figure 2.5: Comparison of Equations of Gergely-Lutz (1968) and Kaar-Mattock (1963), (Frosch, 1999)

The physical model for cracking is considered to provide more perception on crack width calculations. This can be shown in the following figures which illustrate a cracked section and an assumed linear strain gradient profile.

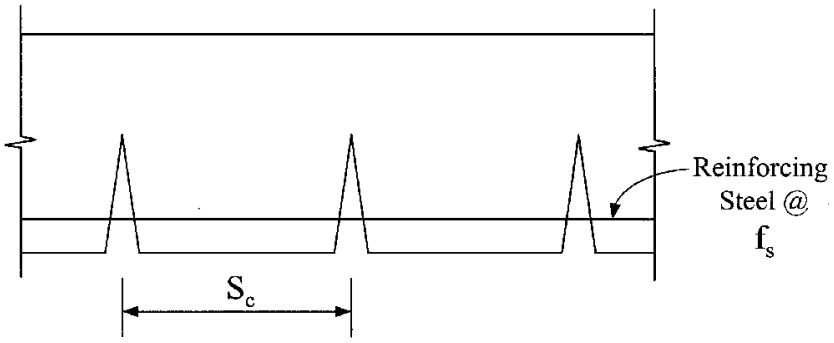

Figure 2.1: Cracked Section (Frosch, 1999)

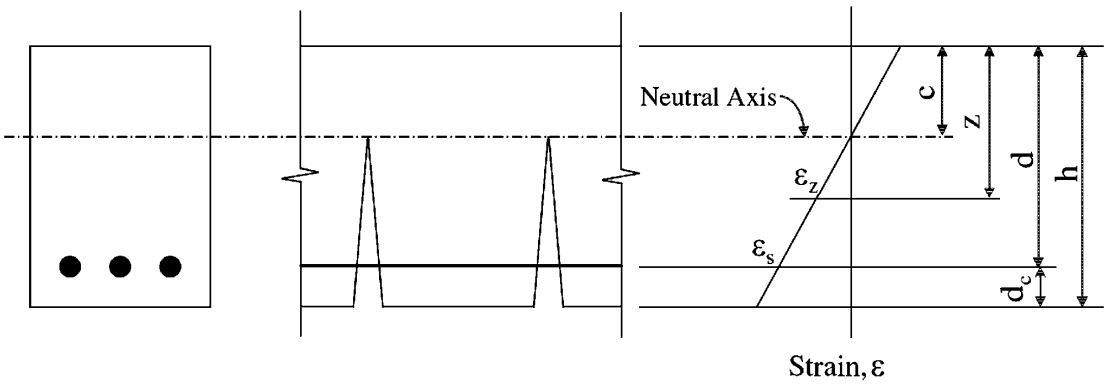

Figure 2.6: Strain Gradient (Frosch, 1999)

Flexural cracking was studied where crack width is calculated at the level of reinforcement by the following equation:

$$w_c = \varepsilon_s S_c \tag{2.7}$$

where:

w_c = crack width

ε_s = reinforcing steel strain = f_s / E_s

S_c = crack spacing

f_s = reinforcing steel stress

E_s = reinforcing steel modulus of elasticity

To determine crack width at the beam surface, the above equation can also be multiplied by an amplification factor β = ε2/ε1 = (h-c)/(d-c) to account for the strain gradient.

Crack widths were generated based on the physical model. These results were compared to test data mainly used in the Kaar-Mattock and Gergely-Lutz study except that of Rusch-Rehm. The crack width model clearly shows that the crack spacing and width are functions of the distance between the reinforcing steel. Limiting the spacing of the steel contributes to crack control. Placing reasonable limits on crack widths results in provisions for maximum bar spacing. Based on the physical model, the equation to calculate the maximum crack width for uncoated reinforcement is as follows:

$$w_c = \frac{2f_s}{E_s}\beta\sqrt{\left(d_c^2 + \left(\frac{s}{2}\right)^2\right)} \tag{2.8}$$

For epoxy coated reinforcement, the formula should be multiplied by a factor of 2. The equation can also be rearranged to solve for the allowed bar spacing, s:

$$s = 2\sqrt{\left(\left(\frac{w_c E_s}{2f_s\beta}\right)^2 - d_c^2\right)} \tag{2.9}$$

where:

s = maximum permissible bar spacing, in

w_c = limiting crack width, in. (0.016 in, based on ACI 318-95)

E_s = 29000 ksi

f_s = reinforcement steel stress; 2/3f_y, ksi (ACI 318-08 recommended, accounts for service stress)

$\beta = 1.0 + 0.08\,d_c$

d_c = bottom cover measured from center of lowest bar, in

Based on the physical model, the following design recommendation is presented that accommodates the use of both coated and uncoated reinforcement. The primary purpose of these recommendations serve is to unify the design criteria for controlling cracking in side face and bottom face cracking. As the thickness of the cover increases, the reinforcement spacing decreases:

$$s = 12\alpha\left[2 - \frac{d_c}{3\alpha_s}\right] \leq 12\alpha_s \tag{2.10}$$

where:

$\alpha_s = \frac{36\gamma_c}{f_s}$ (reinforcement factor)

d_c = thickness of concrete cover measured from extreme tension fiber to center of bar or wire located closest thereto, in

s = maximum spacing of reinforcement, in

γ_c = reinforcement coating factor: 1.0 for uncoated reinforcement; 0.5 for epoxy-coated reinforcement, unless test data can justify a higher value

According to Frosch (1999), there is a disadvantage for the current use of crack width expressions. They are based solely on statistical reasoning and any covers beyond 2.5 in. are limited. For covers less than 3 in., a limited bar spacing of 12 in. should be used for Grade 60 reinforcement. This is reduced to 9.6 in. for Grade 75 reinforcement. Gergely maintains that limiting surface cracks is for the sole purpose of improving aesthetics. Test data corroborates the aforementioned formulation for calculating crack width and is based on the physical phenomenon observed. Frosch (1999) maintains that

the crack width model clearly shows that crack width is a function of the distance between reinforcing steel. Therefore, crack control can be maintained by limiting the distance between reinforcing steel.

The ACI 318-08 Building Code also states that deep beams must have distributed reinforcement in order to control crack widths. Typically, crack widths are expected only at the extreme tensile face of the beam because that is where the largest cracks are mostly anticipated. However, Beeby has conducted studies that showed the largest crack widths occurring in the web along the beam side face with the maximum widths occurring at about mid-height. This is supported by Frosch (2005). Frosch (2005) also states that research has shown that the ACI 318-08 provisions in Section 10.6.4 are sufficient to control side face cracking. The largest crack width occurs at the bottom face and decreases to zero at the neutral axis. This is based upon the assumption that crack spacing is constant over the depth of the beam. On the contrary, the crack spacing varies over the depth of the beam and forms cracks near the neutral axis. In effective depths greater than 36 in., ACI requires skin reinforcement to limit side face crack width in larger beams. Thicker covers coupled with high performance concrete provide durability to concrete structures. Concrete cover is a primary component used to control crack width which leads to questions arising as to whether current code provisions based on the work of Frantz and Breen are adequate enough to control side face cracking (Frosch, 2002).

For any section that contains only primary reinforcement, the maximum crack spacing will occur at the largest distance from the reinforcement, this being at the neutral axis. Minimum crack spacing will occur at the level of reinforcement. The model tested showed that crack width in beams having a larger depth can be greater than the crack

width at the bottom surface. Therefore, the skin reinforcement provides a decline in crack spacing along the depth of the cross section. This occurs by reducing the distance from the closest reinforcement. The model reasonably calculated crack widths but overestimated the average crack widths by 11% and underestimated them by 14%. Increasing maximum side width cracks by 33% can lend to more accuracy as shown through histograms with results of the physical model. The side cover varied yet the results were within range (Frosch, 2002).

The crack model allows crack width to be calculated at any part along the cross section. A profile of the crack width through the depth of the section is more easily created and allows for information regarding optimum locations for placing skin reinforcement for the purpose of controlling side face cracks.

Results from tests conducted on the physical model correlate with the results set forth by Beeby (1971) and Frantz and Breen (1978) (Frosch, 2002). No crack widths were seen in beams having only primary reinforcement and no crack widths existed at the neutral axis. They began just below the neutral axis and increased toward the bottom face until a maximum was reached. Crack widths were minimized at points where skin reinforcement was added. Therefore, understanding crack width profiles for both sections including and not including reinforcement allows for maximum crack control. This occurs where maximum crack widths can be expected as well (Frosch, 2002). The following figure illustrates the crack width profile with and without skin reinforcement:

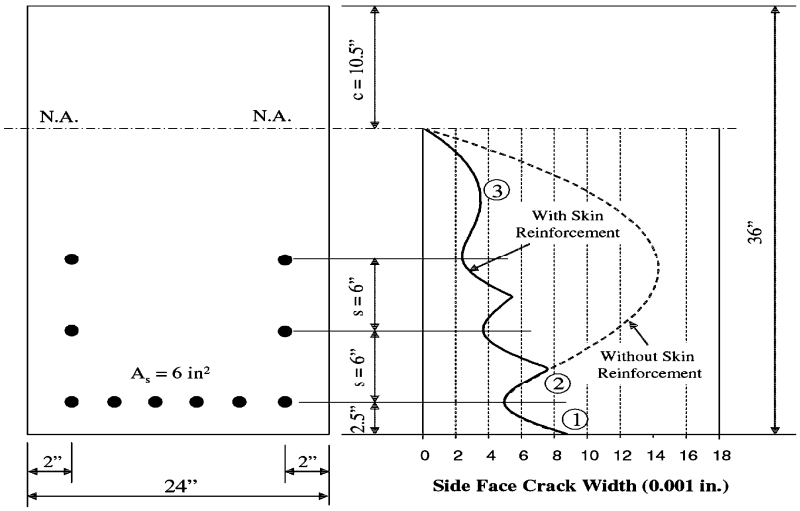

Figure 2.7: Side Face Crack Width Profile (Frosch, 2002)

The cracking model shows that the crack spacing and crack width along the side face are functions of the distance from the reinforcement. Therefore, crack control can be achieved after adding skin reinforcement and limits the reinforcement spacing. A crucial facet is placing the concrete cover over the skin reinforcement. Depending on the accepted limit for crack widths and the depth of the section, skin reinforcement may not be a necessary component. Since the maximum crack width was previously stated to be halfway between the reinforcement and neutral axis, the following equation can be used to solve for the crack width at x = (d-c)/2:

$$w_c = \varepsilon_s \sqrt{d_s^2 + \left(\frac{1}{2}(d-c)\right)^2} \tag{2.11}$$

This equation can be solved for d as a function of d_s. The study of the physical model states that for a 36 ksi reinforcement stress level and where the concrete side faces covers up to 3 in., it is possible to build sections having an effective depth of 36 in. without using skin reinforcement. For thicker covers, the maximum effective depth not requiring

skin reinforcement should be decreased. Moreover, there is a reduction is maximum effective depth for covers thicker than 3 in. for Grade 60 reinforcement. This results in a maximum d = 36 in. These values are consistent with the current design requirements set forth by ACI 318-99.

According to Frosch (2002), the placement of the first bar is the most critical for constant spacing of skin reinforcement. Studies concluded that the maximum skin reinforcement spacing is a function of the concrete cover over the skin reinforcement. It was also shown that a maximum bar spacing of 12 in. will provide reasonable crack control for concrete covers up to 3 in. The provisions concerning reinforcements confirm the presence of adequate control of cracking along the side face. ACI provisions for bottom face reinforcement can also be utilized for the design of skin reinforcement. Unification can help to simplify the current design provisions and takes into account the effect concrete covers have. The following figure shows the required skin reinforcement spacing:

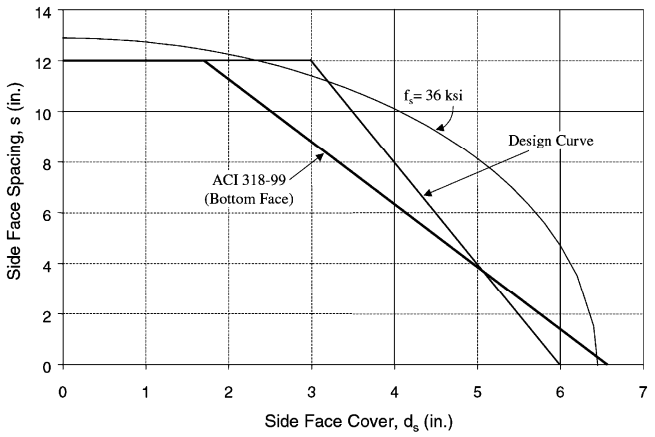

Figure 2.8: Required Skin Reinforcement Spacing (Frosch, 2002)

It is necessary to determine the location in the section where the reinforcement can no longer be used in sections where reinforcement exists. Because crack widths are controlled by skin reinforcement below its end point, it is necessary to calculate the maximum distance s_{na} where the skin reinforcement can be eradicated. The maximum crack width will occur approximately halfway between the neutral axis and the location of the first layer of skin reinforcement at a distance $x = s_{na}/2$ from the neutral axis (Frosch, 2002). Although Frosch maintains that his 1999 equation is more conservative, the maximum crack width using skin reinforcement can be calculated by the following:

$$w_s = s_{na}\left(\frac{\varepsilon_s}{d-c}\right)\sqrt{d_s^2 + \left(\frac{s_{na}}{2}\right)^2} \tag{2.12}$$

Only the bottom 40% of the cross section requires skin reinforcement in the physical model. Similar studies were conducted for varying concrete cover dimensions ranging from 1 to 4 in.

These analyses present the notion that changes in concrete cover dimensions do not significantly change the results. For 50% of the effective depth, it is traditional to require skin reinforcement in the tension zone, which is consistent with current ACI code provisions. Furthermore, it was shown that reinforcement bar size does not tremendously affect crack widths. The tests that were performed with varying bar sizes resulted in approximately the same crack widths. The bar size only impacted the dimension d. As long as the skin reinforcement provides sufficient bond transfer to the concrete itself, a bar of any size can be used with a high success rate. Again, it has been verified that the

spacing used on skin reinforcement is the primary parameter in controlling side face crack widths. This can also be done for controlling side face cracks (Frosch, 2002). Skin reinforcement shall be required along both side faces of a member for a distance d/2 nearest the flexural tension reinforcement if the effective depth exceeds the value

$$d = 42\alpha_s - 2d_c \leq 36\alpha_s \tag{2.13}$$

where:

$d =$ effective depth, in.;

$d_c =$ thickness of concrete cover, in., for bottom-face reinforcement, measured from extreme tension fiber to center of bar, and for skin reinforcement, measured from side face to center of bar.

2.4 REVIEW OF DESIGN CODES

A comparison of international provisions for crack control is discussed here. This was done in an endeavor to acquire other crack width prediction equations and theory. In regard to both, it was determined that for simplicity and agreement of theory, that the American codes are deemed most suitable.

2.4.1 ACI CODE SPECIFICATIONS (2008)

ACI 318-08 requirements for flexural crack control in beams and thick one-way slabs are based on the statistical analysis (Gergely and Lutz, 1968) of maximum crack width data from several sources. ACI maintains that crack control is particularly important when reinforcement with yield strength in excess of 40,000 psi is used. Good

detailing practices such as concrete cover and spacing of reinforcement should lead to adequate crack control even when reinforcement of strength 60,000 psi is used. ACI 318-99 and 318-08 Section 10.6 does not make a distinction between interior and exterior exposure since corrosion is not clearly correlated with surface crack widths in the range normally found with reinforcement stresses at service load levels. ACI 318-08 only requires that the spacing of reinforcement closest to a surface in tension, s, shall not exceed that given by

$$s = 15\left(\frac{40{,}000}{f_s}\right) - 2.5c_c \tag{2.14}$$

but not greater than $12(\frac{40{,}000}{f_s})$, where c_c is the least distance from surface of reinforcement or prestressing steel to the tension face. If there is only one bar or wire nearest to the extreme tension face, s used in equation (1) is the width of the extreme tension face. These provisions are not sufficient for structures subject to very aggressive exposure or designed to be watertight. Special investigation is required for such structures. ACI 318-99 also limited the maximum spacing to 12in, but this limitation has been removed in ACI 318-08 (ACI Committee 224, 2001). ACI also recommends the use of several bars at moderate spacing rather than fewer bars at larger spacing to control cracking. These provisions were updated in 2005 to reflect the higher service stresses that occur in flexural reinforcement with the use of the load combinations introduced in the 2002 Code. The maximum bar spacing is specified to directly control cracking. Similar recommendations have been stated for deep beams with the requirement of skin reinforcement.

2.4.2 AASHTO LRFD SPECIFICATIONS (2008)

AASHTO LRFD (2008) also provides provisions to control flexural cracking through spacing of reinforcement. Similar to the equation adopted in ACI, AASHTO emphasizes the importance of reinforcement detailing and that smaller bars at moderate spacing tend to be more effective than larger bars of equivalent area. AASHTO also agrees with ACI on the most important parameters affecting crack width and specifies a formula for distribution of reinforcement to directly control cracking. The equation is based on the physical crack model of Frosch 2001 rather than on the statistically-based model used in previous editions. The equation limits bar spacing rather than crack width as is as follows:

$$s \leq \frac{700\gamma_e}{\beta_s f_{ss}} - 2d_c \tag{2.15}$$

in which $\beta_s = 1 + \frac{d_c}{0.7(h-d_c)}$ (geometric relationship between crack width at tension face versus crack width at reinforcement level)

where:

γ_e = exposure factor = 1.00 for Class I exposure, 0.75 for Class II exposure

d_c = thickness of concrete cover measured from extreme tension fiber to center of the flexural reinforcement located closest thereto (in.)

f_{ss} = tensile stress in steel reinforcement at the service limit state (ksi)

h = overall thickness of depth of the component (in.)

As seen above, unlike ACI, AASHTO specifies exposure conditions to meet the needs of the authority having jurisdiction. Class I exposure condition is based on a crack width of 0.017in and applies when cracks can be tolerated due to reduced concerns of appearance and/or corrosion and can be thought of as an upper bound in regards to crack width for appearance and corrosion. Class II exposure condition applies to transverse design of segmental concrete box girders for any loads applied prior to attaining full nominal concrete strength and is used when there is increased concern of appearance and/or corrosion such as in substructures exposed to water and decks. The exposure factor can also vary to meet the user's needs. AASHTO LRFD also specifies requirements for skin reinforcement based on ACI 318 standards. The AASHTO equation (15) also applies to both reinforced and prestressed concrete, with specifications on the steel stresses used.

2.4.3 EUROCODE 2 AND COMITE EURO-INTERNATIONAL DU BETON (CEB)/FEDERATION INTERNATIONAL DE LA PRECONTRAINTE (FIP) MODEL SPECIFICATIONS (1990)

2.4.3.1 CEB/FIP MODEL SPECIFICATIONS

The Comite Euro-International du Beton and the Federation International de la Precontrainte (CEB/FIP) Model Code 1990 (CEB 1990) for concrete structures uses a different approach than ACI for crack control. The CEB/FIP technique examines the transfer of stress from the concrete and the reinforcement and estimates the width and spacing of the crack. The tensile load is applied to the beam prior to cracking and causes the beam to produce equal strains in the concrete and steel. As the load increases, so does

the strain until cracks develop in the concrete. This results in the steel resisting the entirety of the tensile load. There is a slip between the concrete and the steel. This occurs adjacently to the cracks. This slip is the most important factor in controlling crack widths because it causes some of the force in the steel to transfer through the bond stress and affecting the perimeter of the bar. Thus, the concrete between the cracks is forced to carry tensile force. The steel strain is a maximum at a crack and the concrete strain is zero. With the CEB/FIP approach, the crack width is related to the distance over which the slip occurs and to the difference between the steel and concrete strains in the slip zones on either side of the crack (Carino and Clifton, 1995). The CEB/FIP 1990 equation to calculate crack width with low probability of being surpassed is as follows:

$$w_k = l_{s,max} (\varepsilon_{sm} - \varepsilon_{cm} - \varepsilon_{cs}) \quad (2.16)$$

where w_k = characteristic crack width

$l_{s,max}$ = maximum distance over which slip between concrete and steel occurs and is equal to $\phi/(3.6\rho_{s,ef})$, where ϕ = bar diameter, $\rho_{s,ef}$ = area of steel divided by effective concrete area in tension (similar to ACI's value A, but calculated differently)

ϵ_{sm} = average steel strain within $l_{s,max}$

ϵ_{cm} = average concrete strain within $l_{s,max}$

ϵ_{cs} = concrete shrinkage strain (negative value)

In this approach, the bond stress is assumed to be uniform over the slip distance and equal to 1.8 times the concrete tensile strength, f_t. According to this bond-slip model, intermediate cracks can occur only when the spacing between the cracks exceeds $l_{s,max}$. According to Beeby (1979) and Base (1976) it has been argued that the slip mechanism is not the only issue affecting crack width. According to this, there should be significant differences between the spacing of the cracks in members with smooth bars as opposed to members with deformed bars. According to the Beeby (1979), the width of real cracks is more than likely due to a combination of these two mechanisms. The location of a neutral axis in a flexural member is another factor affecting the surface crack width. As the distance from the neutral axis increases, so does the flexural crack. The ACI approach takes this into account through the use of the β-value in equation 25 (Carino and Clifton, 1995).

2.4.3.2 EUROCODE 2 AND CEB/FIP MODEL SPECIFICATIONS

The CEB-FIP Model Code and Eurocode 2 crack width formulas are based on the idea that the dominating parameter affecting crack widths is crack spacing (Tammo and Thelandersson, 2009). Crack spacing is assumed to be proportional to bar diameter and reinforcement area, which in turn depends greatly on the concrete cover. This implies that crack width increases with concrete cover. These codes also predict that crack width is affected by bar diameter, but that contradicts the authors' current test results. Beeby (2004) supports the findings that the ratio of bar diameter to the effective reinforcement ratio should not be a governing parameter to determining crack widths. Gergely and Lutz (1968) also corroborate this. Even in these codes, when concrete cover is increased, these

codes do not agree on exactly how the crack width will change, emphasizing the disagreement on this issue by the international community.

In 2008, the ACI code revised its crack control formula based on a model developed by Frosch (2001), where the concrete strain is ignored and the crack spacing is determined differently than the CEB-FIP Model Code and Eurocode 2. Broms (1965) concludes that crack spacing is thought to be proportional to maximum concrete cover. Thus, the limitation of surface crack width can be achieved by reducing the spacing between reinforcing bars. ACI does not limit crack widths for fear of reinforcement corrosion. However, DeStefano et al. (2003) conducted a study that concluded concrete cover does not influence crack spacing or crack width.

2.5 SUMMARY OF CRACK WIDTH EQUATIONS

The following section presents a summary of crack width equations that are simple and accurate to calculate maximum crack width. Other more complex equations are not considered due to the difficulty of applicability, such as the ones presented in international codes.

Clark (1956) concluded that the average width of cracks was found to be proportional to the product of the quantities D/p and (h-d)/d. Furthermore, he stated that average width was also found to be proportional to the increase of steel stress beyond that causing initial cracking. Clark (1956) also insisted that the width of cracks can be reduced by using a large number of small bars and by increasing the ratio of reinforcement. However, the aforementioned investigators disagree. Broms (1965),

Gergely and Lutz (1968), and Frosch (1999) indicate that the ratio D/p is not a good correlation variable, especially for T beams, and that bar size plays a minimal role in reducing crack widths. Nevertheless, Clark concluded that his equation gave reasonable values for average crack width and that the maximum crack width is 1.64 times the average crack width. This is given by Equation 2.1

Kaar and Mattock (1963) also developed a well-known crack width equation for bottom face cracking using the same variables as the Gergely-Lutz equation. This is given by Equation 2.2. The equations of Kaar and Mattock (1963) and of Gergely and Lutz (1968) fit the test data well, especially with covers less than 2.5 in, but it is reasonable to question these equations outside the range of the covers considered. The equations intersect around a cover of 1.625 in. As the covers increased, the two equations showed a divergence in calculated crack widths, and thus a "correct" equation cannot be determined since test data for thicker covers is unavailable. An alternate approach is needed to calculate crack widths with covers greater than 2.5 in.

Broms' (1965) derived an expression for maximum crack width from tensile tests for high stresses. Broms' study demonstrated the shortcomings of using the average effective concrete area around a reinforcing bar as a variable. Instead, Broms used the variable t_e as the effective cover thickness defined as the effective distance from any point on the beam surface to the centroid of the nearest reinforcing bar and $\in_s$ is in milli in/in; t_e is difficult to acquire. This is given by Equation 2.17.

Gergely-Lutz (1968) developed a well-known crack width equation for the critical bottom tension face. This is given by Equation 2.4. The concrete cover d_c is of interest and the range considered in the Gergely-Lutz study tested a maximum cover of only 3.31 in, where only three test specimens had covers greater than 2.5in.

Frosch (1999) recommends Equation 2.8, which is based on the physical model, to determine maximum crack width for uncoated reinforcement from an experiment including a physical model. For epoxy coated reinforcement, the formula should be multiplied by a factor of 2. The crack width model developed shows that the crack spacing and width are functions of the distance between the reinforcing steel. Crack control can be achieved by limiting the spacing of this steel. Maximum bar spacing can be achieved by placing reasonable limits on crack widths. Frosch attempts to determine bottom face and side face crack widths in a single equation.

CHAPTER 3 RELIABILITY-BASED ANALYSIS

3.1 INTRODUCTION

Society expects that structures are designed with a reasonable level of safety. There are many sources of uncertainty inherent to structural design. These include natural causes of uncertainty such as wind, earthquake, snow, live loads, etc, and human causes such as calculation errors, design approximations, etc. As a result, it is necessary to consider the variation of load, resistance and material properties, estimation of parameters due to limited sample size, and uncertainty due to simplifying assumptions and unknown boundary conditions. Throughout history, basic variables, such as materials properties, section geometry, etc, of structures have been taken to be deterministic variables. This leads to the idea that a structure is designed so that its theoretical capacity is greater than the estimated design loads. However, this is not always the case when materials are created or acquired from resources. In recent advances, it is becoming increasingly accepted that the design variables are actually random variables. With this, the design capacity of a section may not actually be larger than the design loads. Therefore, designers attempt to find a balance between cost, safety, economy, service, performance, and durability (Corotis, 1985). Because of this, it is necessary to consider the design variables as random variables with probabilistic values.

Reliability-based analysis takes into account the inherent uncertainty associated with structural design. The reliability of a structure is its ability to fulfill its design purpose to a certain level of probability specified by the designer or a code. It is often understood as the probability that a structure will not fail to perform its intended function. Failure does not denote collapse or catastrophic failure. Rather, it denotes the inability of

a structure to perform its intended function. This makes the resulting design model more applicable to real world circumstances and more consistent that the currently used deterministic model since it factors in variable uncertainty and prediction errors of variables and equations (Siriaksorn and Naaman, 1980). Reliability-based analysis utilizes a safety index, also called a reliability index, β, to be applied as an input variable in the design process. This index corresponds to a probability of failure that can be applied based on the designer's preference.

A limit state can be defined as the instance where the performance of a structure has to be checked to ensure safety according to specific load requirements (Siriaksorn and Naaman, 1980). It is the set of performance criteria that must be met when a structure is subjected to loads. Limit state design entails the satisfaction of the ultimate limit state or the serviceability limit state. Ultimate limit states address failure of a structure in regard to moment, shear, ductility, etc. Serviceability limit states address usability of a structure in regard to deflection, fatigue, cracking, etc and are less critical than ultimate limit states. In this thesis, the serviceability limit state of cracking will be addressed. Provisions from the ACI 318-08 code will be used.

3.2 RELIABILITY-BASED ANALYSIS

Structural safety has been an important theory and practice since ancient times. Throughout history, design methods have taken structural parameters to be deterministic. However, more recently these statistical approaches have been evolving into probabilistic approaches. The first mathematical formulation of structural safety was considered by Mayer (1926), Streletzki (1947), and Wierzbicki (1936). They recognized that load and

resistance parameters are random variables that have an associated probability of failure. Freudenthal developed these ideas further in the 1950s. These investigators formulated convolution functions that were too difficult to solve by hand. It wasn't until the work of Cornell and Lind in the late 1960s and early 1970s that the application of reliability analysis was feasible by hand. Hasofer and Lind created a definition of the reliability index in 1974 while Rackwitz and Fiessler developed an efficient economical procedure for its evaluation in 1978. Others have made contributions to the reliability approach and by the 1970s it became a well developed theory. Only some codes have incorporated reliability analysis to structural members. According to Nowak and Collins (2000), application of the reliability approach to ultimate limit states has been seen more recently, but not much has been done toward serviceability limit states with respect to this (An endeavor is made in this thesis to establish the significance of reliability-based approaches to the serviceability limit states in building codes, specifically the cracking limit state.

3.3 DEVELOPMENT OF THE LIMIT STATE

The idea of the crack control limit state will be used to help define failure in regard to structural reliability. It is the boundary between a desired and undesired level of performance of a structure. The limit state function must be derived to identify a safety margin. Failure is denoted when the "load" on the beam, whether it is actual loads such as live load or dead load, or a serviceability "load" such as deflection or cracking, exceeds the "resistance" of a structure, such as moment capacity, shear capacity, or code accepted levels of deflection or cracking. A structure is considered safe when the load effect is less

than or equal to the resistance. In this thesis, the crack created by an applied live load and the self weight of the beam will be evaluated by the accepted ACI 318-08 crack width limit of 0.016 inches. Let R represent the resistance and Q represent the load side of the limit state function, G. The limit state function would be defined as follows:

$$G\ (R, Q) = R - Q \tag{3.1}$$

The limit state would be when G = 0. If G ≥ 0, the structure is considered safe. If G < 0, the structure is considered unsafe for the desired level of performance. The reliability of a structure can be measured using the reliability index which depends on the limit state function G. Not only will G have to be greater than 0, it will have to be at a certain level to achieve a desired reliability index, β. The reliability index corresponds to a probability of failure, P_f, which is equal to the probability that the undesired performance will occur. Mathematically, this is stated as follows:

$$P_f(R - Q < 0) = P_f(G < 0) \tag{3.2}$$

The probability of failure can be derived when considering the continuous variable's probability density function (PDF). The PDF for resistance is denoted $f_R(r)$ and the PDF for the load is denoted $f_Q(q)$. Mathematically, this can be expressed as:

$$P_f = \int_{-\infty}^{+\infty} f_R(q_i) f_Q\ (q_i) dq_i \tag{3.3}$$

This integration is not straight forward and requires numerical techniques to evaluate. Therefore, the probability of failure, which corresponds to a reliability index, is calculated using other methods. The reliability index, β corresponds to the probability of failure with the following equation, if the variables are normally distributed and

uncorrelated, where ϕ^{-1} is the inverse of the standard normal cumulative distribution function:

$$\beta = -\phi^{-1}(P_f) \ or \ P_f = \phi(-\beta) \tag{3.4}$$

Table 3.1 illustrates how β varies with the probability of failure and vice versa based on the aforementioned formula.

Table 3.1: Reliability Index β and Probability of Failure P_f

P_f	β
10^{-1}	1.28
10^{-2}	2.33
10^{-3}	3.09
10^{-4}	3.71
10^{-5}	4.26
10^{-6}	4.75
10^{-7}	5.19
10^{-8}	5.62
10^{-9}	5.99

The limit state function G involves random variables, as discussed earlier with a reliability-based approach. Converting these random variables to their "standard form," which is a nondimensional form of the variables, has been shown to provide a convenient understanding of the approach. For the basic variables R and Q, the standard forms can be expressed as

$$Z_R = \frac{R - \mu_R}{\sigma_R} \tag{3.5}$$

$$Z_Q = \frac{Q - \mu_Q}{\sigma_Q} \tag{3.6}$$

where Z_i is sometimes referred to as a reduced variable

μ_i = the mean of the variable

σ_i = the standard deviation of the variable

The variables R and Q can be expressed in terms of the reduced variables as follows:

$$R = \mu_R + Z_R\sigma_R \tag{3.7}$$

$$Q = \mu_Q + Z_Q\sigma_Q \tag{3.8}$$

The reliability index can be defined as the inverse of the coefficient of variation of the function G or as the shortest distance from the origin of reduced variables to the line $G(Z_R, Z_Q) = 0$, as introduced by Hasofer and Lind (1974) (Nowak and Collins, 2000). As stated earlier, first order second moment analysis will be used for the reliability approach. The reliability index is called a second-moment measure of structural safety because only the first two moments (mean and variance) are required to calculate β. For this thesis, using a Monte Carlo simulation, which will be discussed later, the reliability index is calculated as follows and shown in the figure below:

$$\beta = \frac{\mu_R - \mu_Q}{\sqrt{\sigma_R^2 + \sigma_Q^2}} = \frac{\mu_G}{\sigma_G} \tag{3.9}$$

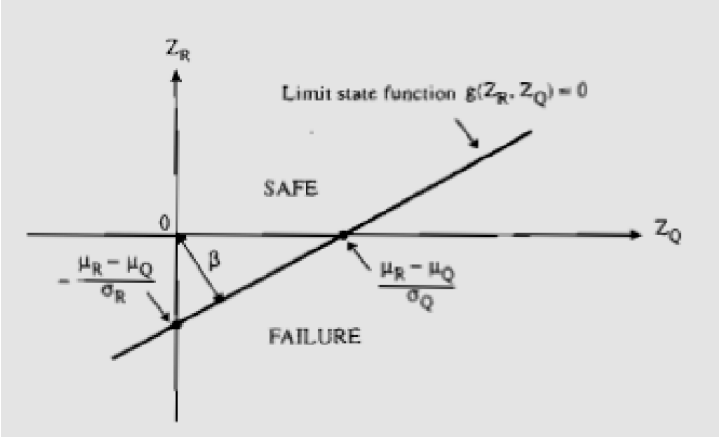

Figure 3.1: Reliability Index Defined As the Shortest Distance in the Space of Reduced Variables (Nowak and Collins, 2000)

3.4 SIMULATION PROCEDURE

The reliability index of reinforced concrete beams is sought to be determined from a reliability-based approach to assess the effect of primary variables on flexural crack width prediction. As discussed before, in the past, code provisions have utilized statistical analysis to predict and control crack width. A reliability-based approach will be used to analyze crack width prediction and enable designers to seek a level of safety corresponding to a probability of failure. A generalized procedure is presented here, while details of the steps will be presented later. Singly reinforced rectangular concrete beams were designed using ACI 318-08 code provisions to provide flexural adequacy. Beams were designed for all possible combinations of three different values for four input variables- span length, steel yield strength, concrete strength, and concrete cover. For beams with depth (h) greater than 36, skin reinforcement as #3 bars are provided up to h/2 as required by the ACI 318-08 code. This reinforcement does not influence maximum crack width at the bottom of the beam since only the bottom layer of tension

reinforcement directly affects crack width. All beams have a 1 inch cover on each side for reinforcement. The span lengths included are 20 ft, 30 ft, and 40 ft; the steel yield strengths are 40 ksi, 60 ksi, and 80 ksi; the concrete strengths are 4 ksi, 6 ksi, and 8ksi (normal weight concrete); the concrete covers considered are 1 inch, 2 inches, and 3 inches. The spacing between all beams is 10 ft. For this base case, there are 81 possible combinations of beams. A distributed live load pertaining to office buildings was then placed on these beams for analysis.

To analyze the effect of each major design variable on crack width reliability index, one parameter was varied while all others were held constant. The variables studied were beam width, beam depth, concrete cover, concrete strength, steel yield strength, area of reinforcement, ACI design spacing, and ACI maximum spacing. This yielded over 700 beams to be used in the Monte Carlo simulation. The effect of bar size on reliability index was tested for each beam by using an adequate amount of ASTM deformed #5 bars and #10 bars. Technically, this doubles the amount of beams used in the simulation, to total around 1450 beams with input variations.

Literature review has been performed to assess the most credible and accurate crack width equations. Once a crack width formula was chosen, the limit state function was derived using the aforementioned techniques. For this study, the limit state was in terms of reinforcement steel stress. The chosen crack width equation, along with sectional analysis of the beams, was solved for in terms of the steel stress. This derivation will be presented later. Statistical data was also obtained for each variable used in the limit state function, since the first moment second order analysis requires the mean and variance. This will also be presented in detail later.

After all the necessary parameters were obtained, a Monte Carlo simulation was performed to obtain a reliability index for each beam. The Monte Carlo simulation is a technique used to generate results numerically without actually doing any physical testing. The basis of all Monte Carlo simulations is the generation of random numbers from 0 to 1. Information from other tests regarding the variables in the limit state, such as mean, coefficient of variation, and probability distribution, is used to perform the simulation. For each variable, random number from 0 to 1 are use to generate values for each variable that correspond to the aforementioned information. A substantial amount of simulations must be conducted to obtain enough random numbers that represent the spectra of possible values for the input variables to within a small percent deviation. With this, the results will provide a more accurate testament to the reliability index by narrowing the margin of change.

Once random variables are generated that correspond to the probability distribution, the limit state function G is evaluated for an adequate number of simulations. In this study, it was found that 2000 simulations resulted in a deviation in reliability index of less than 5% for repeated testing. Once 2000 G values are obtained for each beam, the mean and standard deviation of the set of all G values are generated. The reliability index, which corresponds to a probability of failure, is then calculated for each beam using Equation 3.9 where β is the mean of G divided by the standard deviation of G. Once the reliability indices of all beams have been calculated, the results are then analyzed to determine the effect of different variables on the indices, to evaluate current code provisions, and to provide recommendations for designers seeking to achieve a desired level of performance corresponding to a probability of failure. For this study,

Matlab was used to design the beams according to ACI 318-08 code provisions, generate random numbers for each variable, and perform the Monte Carlo simulations to result in a reliability index for each beam. The codes written for these processes are given in Appendix III. A target reliability index should be a consideration factor for designers using this approach. Based on past practices, the target reliability for the beams in this study is 3.5. This value is the same as in other recent code calibrations, such as AASHTO LRFD 2005 (Nowak et al, 2008).

Presented below is the overall procedure summarized in a step-by-step format.

Step 1: Design singly reinforced rectangular beams using Matlab according to ACI 318-08 design provisions. The input variables for this study were span lengths of 20ft, 30ft, and 40ft; concrete strength of 4ksi, 6ksi, and 8ksi; steel yield strength of 40ksi, 60ksi, and 80ksi; and concrete covers of 1 inch, 2 inches, and 3 inches.

Step 2: Formulate the limit state function, G = R-Q, where G is the limit state function, R is the resistance, and Q is the load. For this study, the limit state function is in terms of the stress in the reinforcing steel, f_s.

Step 3: Obtain statistical parameters of all variables in the limit state function to find each variable's distribution, mean, and standard deviation. For this study, this information can be found in Table 1 based on research done by Siriaksorn and Naaman (1980), and by Nowak, Szersen, Szeliga, Szwed, and Podhorecki (2008).

Step 4: Determine which simulation method to use to obtain the reliability index, β, which corresponds to a probability of failure, $p_f = P(G<0) = P(R-Q<0)$, where P(z) = probability function. For this study, the Monte Carlo Method will be used to obtain

randomized values of R and Q based on each variable's probability distribution. For example, random variables, x_i, for a normal distribution can be obtained by $x_i = \mu_X + z_i\sigma_X$ where $z_i = \phi^{-1}(u_i)$; u_i is the randomly generated number from 0 to 1, and ϕ^{-1} is the inverse cumulative distribution function.

Step 5: To obtain random values of R and Q, a random number must be generated for each variable in the limit state function. Matlab was used to generate the random numbers from 0 to 1 for each variable. Based on the variable's probability distribution, these randomly generated numbers will be converted into a random variable corresponding to typical values. For example, the random number 0.925827 will generate a random steel stress of 30,006 ksi for a steel stress of mean 29,000 ksi and standard deviation 696 ksi.

Step 6: After all variables have randomly generated values, the limit state function G = R-Q should be calculated and stored. Repeat Step 4 until a sufficient number of G values have been generated. Matlab was also used for the Monte Carlo Simulation. For this study, 2000 values of G will be obtained for each beam tested to minimize deviation between the mean and standard deviation of G.

Step 7: After a sufficient number of G values have been obtained, the reliability index, β should be calculated. $\beta = \mu G$ (mean of G)/σG (standard deviation of G). The mean and standard deviation of G were obtained based on the 2,000 values of G using Matlab where the input is the 2,000 values of G for each beam. Thus, using the aforementioned equation for β, the reliability index can be calculated for a beam. A target reliability index should be stated. In this study, the target reliability index is 3.5, corresponding to a

probability of failure of 0.00023, or 2.3 x 10^{-4}. The probability of failure, if desired, is the CDF (cumulative distribution function) of $-\beta$. $P_f = \phi(-\beta)$.

3.5 VALIDATION OF THE RESISTANCE EQUATION

A study of the crack control limit state is being pursued to test the reliability of this limit state given by current codes and crack width equations. Extensive literature review of the research done on crack control from the 1950s to present was undertaken. The purpose of the literature review was to assess the influence of important variables on crack control, to gain understanding of background theory, to find the most accurate and widely used crack control equations, and to compare current code provisions. It has been found that steel stress is the most important variable affecting crack width; that the thickness of the concrete cover and the cross sectional area of concrete surrounding each bar are important geometric variables; that the crack width on the tension face is affected by the strain gradient from the level of steel to the tension face; and that the bar diameter is not a major variable. Furthermore, comparison of international codes such as CEB/FIP AASHTO, and Eurocode has been carried out and moreover, comparison of the American code ACI has been conducted and will be used in this study. Major crack width equations have been researched and include the Gergely-Lutz equation previously used in the ACI code, the newly presented Frosch equation in which the current AASHTO code is based on, and others such as Kaar-Mattock, Clark, Beeby, Broms, etc. A summary of these equations is presented in Table 3.2.

Table 3.2: Equations of Maximum Crack Width

Author	Maximum Crack Width Equation	Year
Clark	$w_{ave} = C_1 \frac{D}{p}[f_s - C_2\left(\frac{1}{p} + n\right)]$	1956
Kaar-Mattock	$w_b = 0.115\beta f_s \sqrt[4]{A}$	1963
Broms	$w_s = 4t_e \in_s = 0.133 t_e f_s$	1965
Gergely-Lutz	$w_b = 0.076\beta f_s \sqrt[3]{Ad_c}$	1968
Beeby	$w_m = (K_1 c + K_2 \frac{\phi}{\rho})\varepsilon_m$	1979
CEB/FIP	$w_k = l_{s,max}\,(\varepsilon_{sm} - \varepsilon_{cm} - \varepsilon_{cs})$	1990
Eurocode	$w_k = \left(50 + 0.25 k_1 k_2 \frac{\phi}{\rho_{ef}}\right)\left(1 - \beta_1\beta_2\left(\frac{\sigma_{sr}}{\sigma_s}\right)^2\right)\frac{\sigma_s}{E_s}$	1991
Frosch	$w_c = \frac{2f_s}{E_s}\beta\sqrt{\left(d_c^2 + \left(\frac{s}{2}\right)^2\right)}$	1999

Previous research using statistical evaluation has been performed on reinforced concrete beams where crack widths were recorded at two primary locations- the bottom tension surface and the side face at the level of reinforcement. The crack width at the bottom of the beam is typically larger than on the side of the beam because of the larger extension of the bottom face than at the level of the steel. Due to the random nature of cracking and currently accepted models that become invalid when concrete cover is large, there is an ever-growing need for investigators to find compromise on crack width equations that will accurately determine width values and provide insight on specific parameters that will prevent large crack widths.

A study on the accuracy of the crack width prediction equations in Table 3.2 was conducted to decide on the resistance of the limit state function G. For simplicity, ease of

variable determination, commonly accepted formulae, and applicability purposes, the equations considered in the accuracy study were Kaar-Mattock (1963), Gergely-Lutz (1968), and Frosch (1999). Data on the measured crack width of regular rectangular beams of different dimensions and reinforcement were obtained from Clark (1956), Chi & Kirstein (1958), Hognestad (1962), Kaar & Mattock (1963), and Hutton (1966). Clark (1956) had a total of 54 beams for steel stress levels of 15 ksi, 20 ksi, 25 ksi, 30 ksi, 35 ksi, 40 ksi, and 45 ksi. Chi & Kirstein had a total of 16 beams for steel stress levels of 15ksi, 20 ksi, 25 ksi, 30 ksi, 35 ksi, 40 ksi. Hognestad had a total of 8 beams for steel stress levels of 20 ksi, 30 ksi, 40 ksi, and 50 ksi. Kaar and Mattock had a total of 13 beams for a steel stress level of 40 ksi. Hutton had a total of 3 beams for steel stress levels that vary by no specific category. The three beams, however, have a total of 25 measured crack widths to provide a reasonable amount of data. Using Frosh's, Kaar-Mattock's, and Gergely-Lutz's equations, the data was tested to determine the most accurate equation from various investigators. The specimen data, crack width predictions, and errors for each beam are given in Appendix I.

The error for each case, called absolute error, was calculated as the absolute value of the difference in predictions so when the average of the errors was taken, a true error would be revealed rather than positive and negative values minimizing these average errors. The percent error, also called percent difference, is the absolute error divided by the measured crack width of each investigator's beams. Accuracy of each prediction equation was based on this percent difference. The findings of each crack width prediction equation for each set of data acquired are categorized by steel stress level and presented below. Averages of all steel stress values do not consider any stress level

beyond yield of steel reinforcement since analysis is complicated beyond this point. Nevertheless, all results are presented.

Table 3.3: Comparison of Prediction Equations for Clark (1956)

fs, ksi	Kaar-Mattock Error	Gergely-Lutz Error	Frosch Error
15	50.1%	34.0%	35.3%
20	32.2%	22.4%	21.4%
25	31.4%	21.2%	23.5%
30	32.2%	21.7%	28.4%
35	30.4%	22.1%	31.6%
40	24.6%	19.8%	27.7%
45	21.3%	26.2%	29.4%
All Beams	33.2%	33.2%	22.5%

Table 3.4: Comparison of Prediction Equations for Chi & Kirstein (1958)

fs, ksi	Kaar-Mattock Error	Gergely-Lutz Error	Frosch Error
15	86.4%	78.7%	39.1%
20	49.2%	42.8%	19.4%
25	43.5%	40.9%	24.6%
30	35.1%	33.8%	22.8%
35	28.7%	28.2%	22.5%
40	23.7%	22.4%	23.0%
All Beams	43.5%	40.4%	24.9%

Table 3. 5: Comparison of Prediction Equations for Hognestad (1962)

fs, ksi	Kaar-Mattock Error	Gergely-Lutz Error	Frosch Error
20	41.6%	44.3%	21.3%
30	36.2%	27.0%	19.1%
40	30.3%	26.3%	20.2%
50	33.8%	26.2%	18.2%
All Beams	45.2%	43.1%	24.9%

Table 3.6: Comparison of Prediction Equations for Kaar and Mattock (1963)

fs, ksi	Kaar-Mattock Error	Gergely-Lutz Error	Frosch Error
40	33.6%	35.6%	33.6%

Table 3.7: Comparison of Prediction Equations for Hutton (1966)

fs, ksi	Kaar-Mattock Error	Gergely-Lutz Error	Frosch Error
<20	163.9%	129.0%	38.1%
20-25	262.0%	194.7%	40.8%
25-30	NO FS VALUES IN RANGE		
30-35	358.7%	273.4%	25.0%
35-40	215.3%	167.0%	56.3%
40-45	248.8%	184.0%	42.9%
45-50	155.0%	123.0%	37.6%
50-55	72.5%	66.0%	57.2%
55-60	74.5%	58.5%	16.4%
All Beams	193.8%	149.4%	39.3%

Table 3.8: Comparison of Prediction Equations for All Data Combined

ALL Data	Kaar-Mattock	Gergely-Lutz	Frosch
% Difference	69.9%	60.3%	30.1%

Table 3.8 shows the percent difference, or percent error, for all the data combined. It is seen that Frosch has the least error by far for all the data considered and when considering each set of data alone. In fact, Frosch's error is half that of Gergely and Lutz's equation, the basis for the ACI code on cracking. It is noted that the Gergely-Lutz

equation has a very large error when considering Hutton's data. If this data were eliminated, the Gergely-Lutz equation would have a percent error of 38.1% while Frosch would have an error of 27.8%. This is still a 10% difference between the two equations, which is enough to corroborate the case for Frosch as the resistance in the limit state function G. In addition to Frosch's exceptional percent error, his equation is also based on the physical phenomenon of cracking and not simply on statistical analysis, as explained in detail in the literature review. This has proven to be enough evidence to support Frosch as the resistance equation for the limit state function.

After selecting Frosch's (1999) crack width equation, crack width predictions were also compared to a state of the art program called Response 2000. Response 2000 is a non-linear sectional analysis program used for the analysis of reinforced concrete elements subjected to shear based on the Modified Field Compression Theory. The program was written from 1996-1999 by Evan Bentz, PhD candidate at the University of Toronto, under the supervision of Professor M.P. Collins. Response 2000 is based on a series of biaxial nodes integrated along a line through the cross section. It calculates the strengths and deformations for beams and columns subject to axial load, moment, and shear. The program is considered to be the successor of the program Response and program Smal. Response 2000 includes a method to integrate the sectional behavior for simple prismatic beam-segments. The assumptions used in the program are that plane sections remain plane and that there is no transverse clamping stress across the depth of the beam. Beam dimensions and properties of concrete and reinforcement are input into the program. When the analysis is performed, an entire Moment-Shear interaction diagram, load deflection properties, and crack diagram will be shown for the specimen.

The predicted crack width can be obtained at levels of stress in the reinforcement and levels of stress at the crack itself.

The aforementioned data was used to compare Response 2000 with Frosch's crack width prediction equation. Overall, Response 2000 had an error of 50.4% as compared to the previously mentioned error of Frosch at 30.1%. It can be seen that Frosch still has a better prediction of crack width compared to the other equations and to this program. Since Frosch's equation does not consider the depth of the beam, deep beams were also tested to verify the accuracy of his equation. Comparisons were made with Response 2000. Data was obtained on deep beams with high strength from Moran and Lubell (2008). Nine beams of the same exact cross section but varying reinforcement were evaluated with 55 crack widths. It was found that Response had an overall error of 43.3% while Frosch still had a better prediction with only an error of 34.8%. To further validate Frosch's equation regarding deep beams, his equation was compared to data obtained from Frantz and Breen (1978) in Texas. There were 44 beams presented in this paper with 166 crack widths. Using Frosch's (1999) equation, the error was a low 28.9%. Thus, it is evident that Frosch has the most accurate prediction from the considered equations for crack widths of any beam type.

3.6 LIMIT STATE FORMULATION

The reliability-based approach to the analysis of crack width limit states is based on calculating a reliability index beta, β. Reliability is the probability that a structure will not fail to perform its intended function. The structural parameters are treated as random variables rather than deterministic values. This attempts to account for the many sources of uncertainty that are inherent of structural design. The Monte Carlo method is a technique used to generate some results numerically based on obtained statistical information without doing any physical testing.

The reliability index, β, is based on the mean and standard deviation of a resistance, R, and a load, Q, to generate the limit state function G as stated earlier for the Monte Carlo method. To formulate the crack width limit state using the reliability approach, the function G will be in terms of the steel reinforcement stress, fs, since research has shown this to be the most important parameter influencing crack widths. Thus, the limit state function would appear as such:

$$G = f_{s\,(resistance)} - f_{s\,(load)} \tag{3.10}$$

As the resistance was validated in the previous section, Frosch's (1999) equation was used for the resistance side of the limit state function. This equation is presented below:

$$w_c = \frac{2f_s}{E_s}\beta\sqrt{\left(d_c^2 + \left(\frac{s}{2}\right)^2\right)} \tag{2.8}$$

The limit state function is in terms of steel stress f_s. Solving for f_s yields the following resistance equation to be used in the limit state:

$$f_s = \frac{w_c E_s}{2\beta\sqrt{\left(d_c^2 + \left(\frac{s^2}{2}\right)\right)}} \tag{3.11}$$

The variables E_s, β, and d_c, w_c are random variables with obtained statistical parameters. In this study, the values for reinforcement steel spacing, s, are deterministic parameters based on ACI318-08 regulations. Spacing will be varied to show its influence on maximum crack width. The variations will range from ACI flexural design spacing to the maximum allowable spacing in ACI 318-08 Section 10.6.4 provisions. This maximum spacing is given by the following provisions of Section 10.6.4:

> The spacing of reinforcement closest to the tension face, s, shall not exceed that given by:
>
> $$s = 15\left(\frac{40{,}000}{f_s}\right) - 2.5c_c \tag{2.14}$$
>
> but not greater than $12\left(\frac{40{,}000}{f_s}\right)$, where c_c is the least distance from surface of reinforcement to the tension face. If there is only one bar nearest to the extreme tension face, s is the width of the extreme tension face.

The load, Q, in the reliability approach was derived based on principles of reinforced concrete analysis, as shown in Figure 3.2.

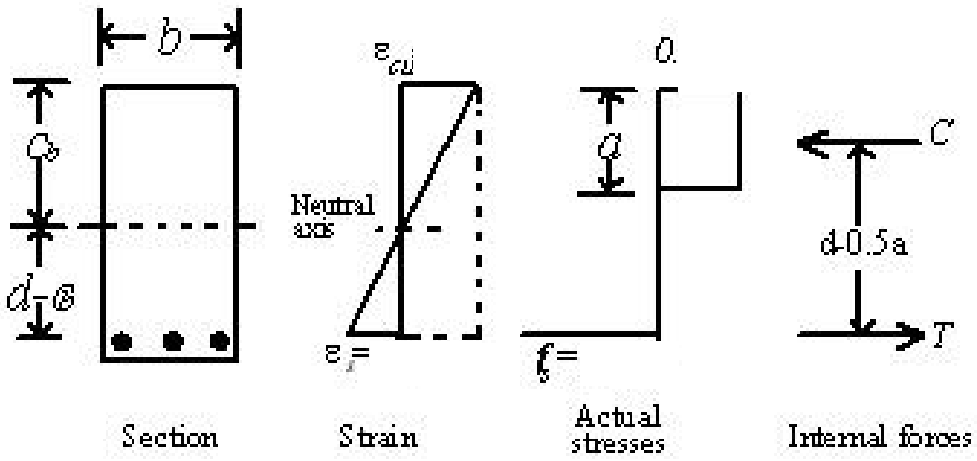

Figure 3.2: Singly Reinforced Concrete Beam with Stress and Strain Distributions

Force and moment equilibrium were used to solve for two unknowns, steel stress f_s and neutral axis, C_{na}. The beams tested in this simulation are assumed to be simply supported and loaded with a distributed live load used in office buildings. The maximum moment for this type of loading as given by the AISC Steel Manual 13th edition is:

$$\frac{wL^2}{8} \tag{3.12}$$

where w = distributed load (lbs)

L = span length (in)

The maximum allowable moment given from the concrete section is:

$$A_s f_s \left(d - \frac{C_{na}}{3}\right) \tag{3.13}$$

where As = area of steel reinforcement

fy = yield stress of the steel

For force equilibrium, the compression force is equal to the tension force. The compression force is as follows:

$$C_c = \frac{f_c C_{na} b}{2} = \frac{\varepsilon_c E_c C_{na} b}{2} \tag{3.14}$$

where f_c = stress in the concrete,

b = width of the concrete section

ε_c = strain in the concrete

E_c = elastic modulus of the concrete

The tension force, T, is as follows, where E_s is the elastic modulus of steel and ε_s is the strain in the steel:

$$T = A_s f_s = A_s E_s \varepsilon_s \tag{3.15}$$

Using force and moment equilibrium, two equations with two unknowns were solved to obtain

the load equation in terms of f_s using Maple 13:

$$f_s = \frac{3\left(A_s E_s + 3E_c bd + \sqrt{A_s^2 E_s^2 + 2A_s E_s E_c bd}\right) wL^2}{8d(4A_s E_s + 9E_c bd)A_s} \tag{3.16}$$

where A_s = area of steel reinforcement, in^2

E_s = elastic modulus of steel, psi

E_c = elastic modulus of concrete, psi

b = width of concrete section, in

d = effective depth of concrete section, in

P = applied load, lbs

L = span length, in

After the load and resistance are combined, the resulting limit state function is as follows:

$$G = \frac{w_c E_s}{2\beta\sqrt{\left(d_c^2 + \left(\frac{s^2}{2}\right)\right)}} - \frac{3\left(A_s E_s + 3E_c bd + \sqrt{A_s^2 E_s^2 + 2A_s E_s E_c bd}\right) wL^2}{8d(4A_s E_s + 9E_c bd)A_s} \quad (3.17)$$

Since a reliability-based approach was taken, most variables are based on statistical information whereas some are merely deterministic. The statistical parameters are presented in the next section.

3.7 STATISTICAL PARAMETERS

To analyze the cracking in reinforced concrete beams probabilistically, the probability distributions and statistical values of mean, coefficient of variation (CoV), and standard deviation of the variables used in the limit state function need to be acquired. Information is limited in regard to these parameters and they can be directly accessed from other sources. If the required data is not available, Ellingwood et al (1974) suggest that the range of variation of the mean values may be estimated and the CoV can be found by assuming a distribution for the mean value over this range. If the mean and CoV are provided, the standard deviation is simply the product of the mean and CoV. Thus, all the necessary parameters would then have been obtained and the Monte Carlo simulation can be executed.

For the resistance case, concrete cover, d_c, elastic modulus of steel E_s, maximum crack width $w_{c,}$ and Frosch's β are all random variables. For the load case, area of reinforcing steel in the bottom most layer near the tension face $A_{s,}$ steel elastic modulus $E_{s,}$ concrete elastic modulus E_c, distributed live load w, concrete section width b, and concrete section effective depth d are all random variables. The deterministic variables for the limit state function are reinforcement spacing s and span length L. Live loads are the loads that can move or be moved, such as occupants, furniture, etc and are inherent to wide variability. The statistical parameters that include the mean and coefficient of variation were obtained from research done by Siriaksorn and Naaman (1980) and by Nowak, Szersen, Szeliga, Szwed, and Podhorecki (2008), which performed an analysis of statistical parameters themselves. They are presented in Table 3.9. The subscript 'n'

denotes a nominal value. As noted earlier, to obtain the standard deviation, one would simply take the product of the mean and CoV.

Table 3.9: Statistical Parameters of Variables Used in the Monte Carlo Simulation

Variable	Distribution	Mean	CoV
b (beam width)	normal	b_n	0.04
h (beam height)	normal	h_n	$\frac{1}{6.4 * h_n}$
d (effective depth)	normal	$0.99d_n$	0.04
d_c (concrete cover)	normal	d_{cn}	0.04
C_Ec (concrete factor)	normal	33.6	0.1217
f'_c (concrete strength)	lognormal Note: Ec = C_Ec* γ_c^1.5$\sqrt{f'c}$	4000: $1.21f_{cn}$' 6000: $1.22f_{cn}$' 8000: $1.09f_{cn}$' (ksi)	4000: 0.155 6000: 0.075 8000: 0.088
γ_c (concrete weight)	normal	150	0.03
f_y (steel yield strength)	lognormal	$1.13f_{yn}$	0.03
A_s (area of reinforcement)	normal	$0.9A_s$	0.015
E_s (steel elastic modulus)	normal	E_{sn}	0.024
w (distributed live load)	Type 1	100 psf (office building occupancy, IBC 2008)	A_I (ft^2) = 400: 0.19 600: 0.18 800: 0.17
w_c (maximum crack width)	normal	0.016 in (ACI 318-08 max allowable)	0.2

As shown in Table 3.9, beam dimensions such as height, width, effective depth are not inherent to wide variability and have a normal distribution. Steel elastic modulus and area of steel reinforcement have a higher variability but still a normal distribution. Steel yield strength and concrete strength have a lognormal distribution. The mean and

coefficient of variation vary with the nominal value of concrete strength. These parameters were obtained directly from Nowak et al (2008). The mean for the maximum crack width was taken from ACI 318-08 limit on maximum allowable crack width and is 0.016 inches. Data from the investigators used to validate the resistance of the limit state function were used to obtain the distribution and coefficient of variation for crack width values at 0.016 inches. The mean and CoV for the distributed live load were also obtained from Nowak et al (2008) and depend on the influence area of the beam, which is twice the tributary area. For this study, the span lengths of 20 ft, 30 ft, and 40 ft, the tributary areas are 200 ft^2, 300 ft^2, and 400 ft^2, respectively since the beam spacing for all beams is 10 ft. Thus, the influence areas become 400 ft^2, 600 ft^2, and 800 ft^2. The values for the CoV were obtained from the equation of the curve in the graph below.

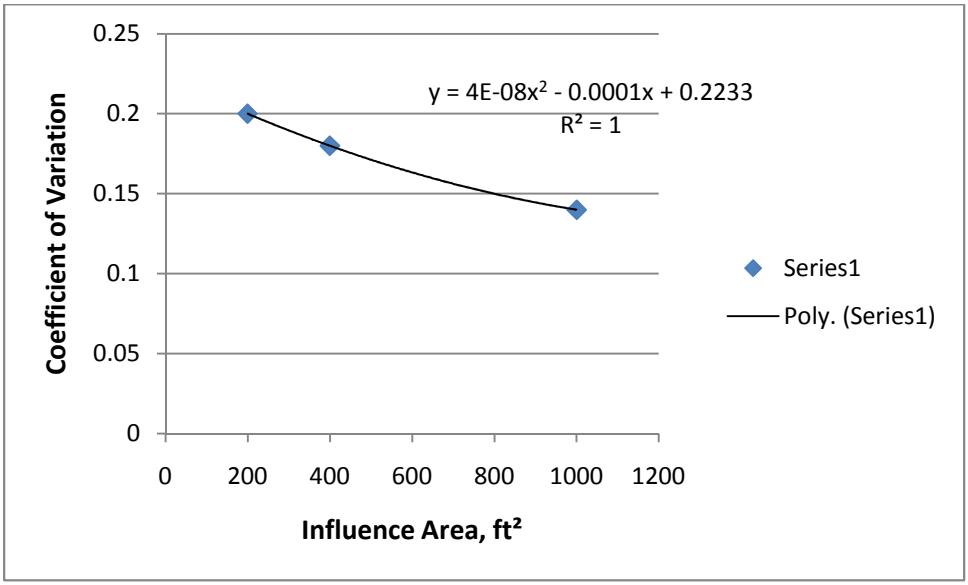

Figure 3.3: Live Load Coefficient of Variation (Nowak et al, 2008)

CHAPTER 4 RESULTS, ANALYSIS, AND DISCUSSION

4.1 EVALUATION OF PARAMETRIC STUDY

The results of the Monte Carlo simulation on the reliability of reinforced concrete beams are presented in this chapter. All beams are rectangular and singly reinforced. The results are categorized by span length, L. For each span length, the variable in question is presented as an average of the values in each span length category. Data is presented for the simulations using the #5 bars and #10 bars. Any designation of "#5"/"#10" indicates use of #5 bars/#10 bars, respectively. The specimen data for each beam and their respective reliability indices for the base case are presented in Appendix II. For the base case, using #5 bars, the average reliability index was 3.27 with a standard deviation of 0.77. Also, 48 out of 81 beams had reliability indices that fell below the target reliability index β_T of 3.5. Using #10 bars, the average reliability index was 2.92 with a standard deviation of 0.85. Also, 60 out of 81 beams had reliability indices that were below β_T. It can be seen that using #5 bars yields a better reliability index than using #10 bars, but not with a very large difference. To achieve the target reliability index of 3.5, ACI must enforce more strict design provisions, which can be applied to a number of variables that will be analyzed in this study.

The variation of the reliability index is presented for the variables of beam width (b), beam depth (d), concrete cover (d_c), steel yield strength (f_y), concrete strength (f_c'), area of reinforcement (A_s), spacing of reinforcement (s), and maximum allowable ACI reinforcement spacing (max s). Tables are presented in this chapter for each variable based on several hundred beams. The number of beams used to obtain the influence of each variable is specified in the respective section. The tables categorize the data by span

length and the variable in question with reliability index in the body of the table. The reliability indices are averages of the aforementioned number of beams classified by span length. This results in 3 reliability indices for each variable and bar size used. Thus, trend lines of these 3 points are logical since they truly represent a series of beams. Horizontal grand total refers to the average of a column while vertical grand total refers to the average of a row with respect to reliability index. Conclusions can be drawn from the graphs and tables.

4.1.1 EFFECT OF BEAM WIDTH

The first variable investigated is beam width, b. A total of 243 beams for each bar size (#5 and #10 to total 486 beams) were used to analyze the effects of this variable. There are 27 beams in each span length. Table 4.1 shows the span length category vertically and the beam widths in inches horizontally with average reliability index in the body. For each span length, the minimum design width is used, and then increased by 4 inches and 8 inches to observe the variation in reliability index with beam width. For example, the minimum design beam width using a span length of 20ft is 8 inches. This was then varied by 4 inches to yield a beam width of 12 inches and then varied by 8 inches to yield a beam width of 16 inches. The same was done for a span length of 30ft (minimum b = 12 inches) and 40ft (minimum b = 15 inches).

As beam width increases within each span length, reliability index shows no trend for both #5 and #10 bars. As span length increases, reliability index increases for #10 bars (vertical grand total), while for #5 bars the indices remain in the same range. No

trend is shown overall for reliability (horizontal grand total) as beam width increases. Using #5 bars yields a higher reliability than #10 bars. The data presented in tables and scatter graphs is to be shown with both #5 bars and #10 bars in the same graph and separate with applied trendlines to provide visual ease of understanding and comparison.

Table 4.1: Influence of Beam Width on Reliability Index

		Variation of Reliability Index with Beam Width (#5 bars)						
	b, in							
L, ft	8	12	15	16	19	20	23	Grand Total
20	3.23	3.22		3.23				3.23
30		3.33		3.33		3.32		3.33
40			3.24		3.25		3.27	3.25
Grand Total	3.23	3.28	3.24	3.28	3.25	3.32	3.27	3.27

		Variation of Reliability Index with Beam Width (#10 bars)						
	b, in							
L, ft	8	12	15	16	19	20	23	Grand Total
20	2.56	2.56		2.57				2.56
30		3.10		3.09		3.10		3.10
40			3.11		3.14		3.13	3.12
Grand Total	2.56	2.83	3.11	2.83	3.14	3.10	3.13	2.93

The average reliabilities with their standard deviations and number of beams with reliability indices less than the target are presented in Table 4.2. Overall, as beam width increases, there seems to be no significant trend or effect on reliability index, its standard deviation, and the number of beams with indices less than the target of 3.5 for both #5 and #10 bars. Around half the beams in each case fail to meet the target reliability index. Beam width does not prove to have a significant influence on reliability index overall.

Table 4.2: Change in Reliability Index with Beam Width Increase

	Average Reliability Index			Standard Deviation of β			Number of $\beta < \beta_T$		
#5 Bars	Base Case	1st Increase	2nd Increase	Base Case	1st Increase	2nd Increase	Base Case	1st Increase	2nd Increase
L = 20 ft	3.23	3.22	3.23	0.81	0.80	0.79	15	15	15
L = 30 ft	3.33	3.33	3.32	0.76	0.76	0.75	16	14	14
L = 40 ft	3.24	3.27	3.26	0.75	0.77	0.76	17	16	16
# 10 Bars	Base Case	1st Increase	2nd Increase	Base Case	1st Increase	2nd Increase	Base Case	1st Increase	2nd Increase
L = 20 ft	2.56	2.56	2.57	0.94	0.95	0.94	23	23	23
L = 30 ft	3.10	3.09	3.10	0.82	0.81	0.81	18	18	18
L = 40 ft	3.10	3.14	3.13	0.68	0.70	0.69	19	18	18

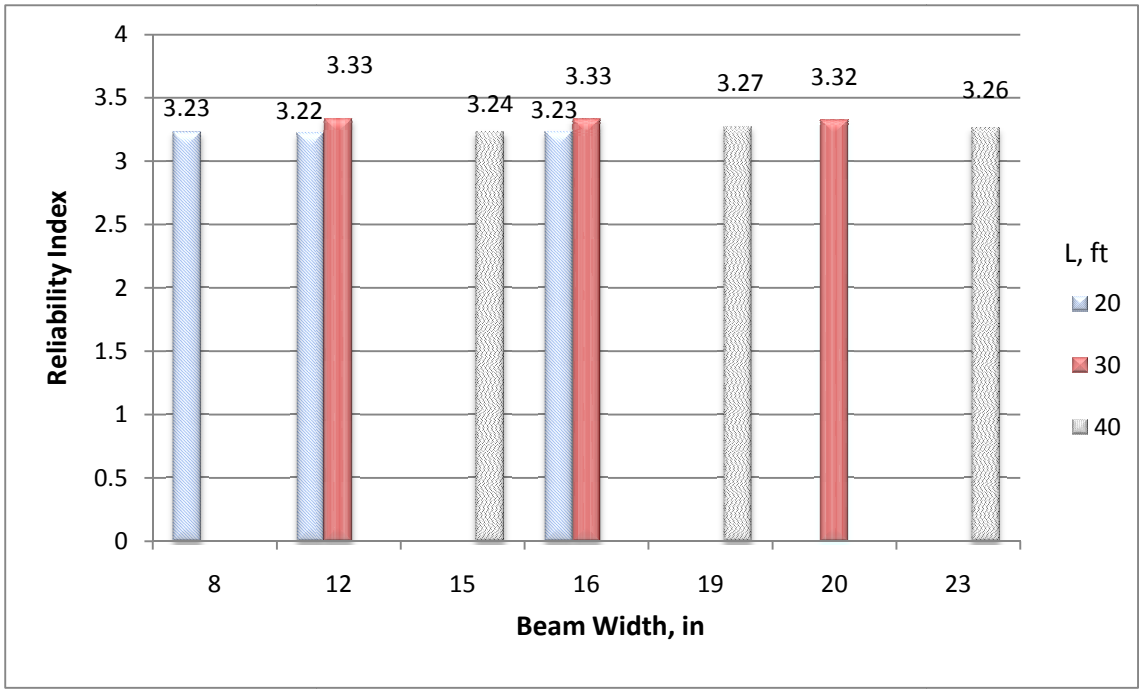

Figure 4.1: Variation of Reliability Index vs. Beam Width for #5 Bars

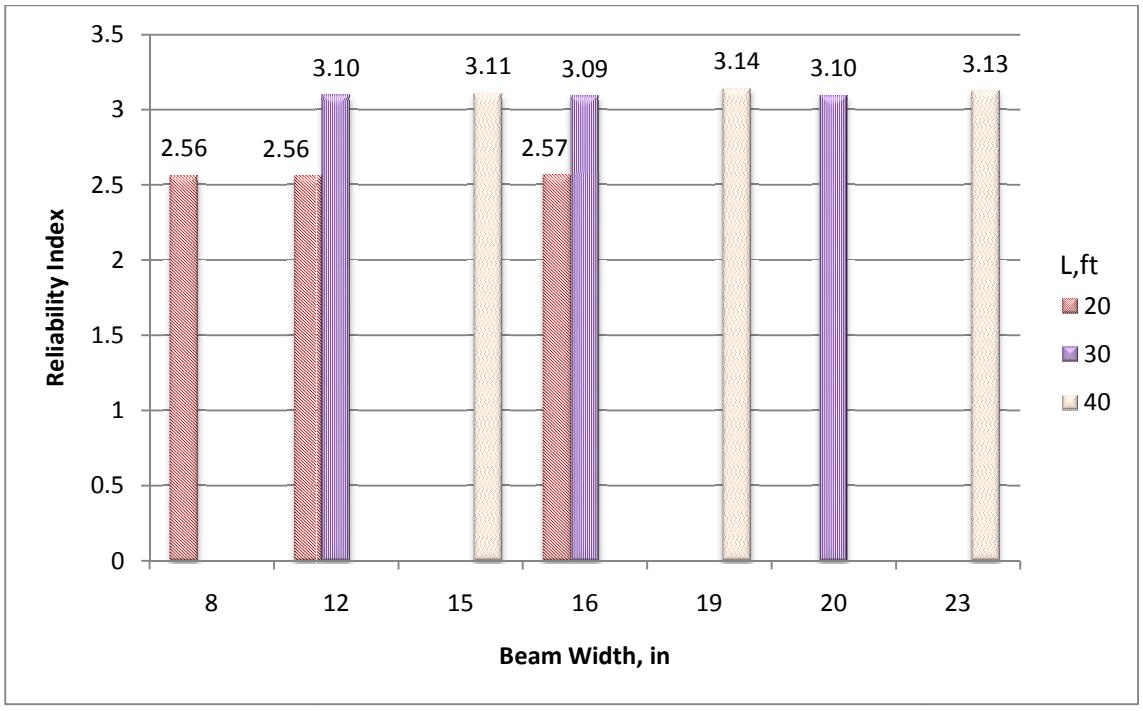

Figure 4.2: Variation of Reliability Index vs. Beam Width for #10 Bars

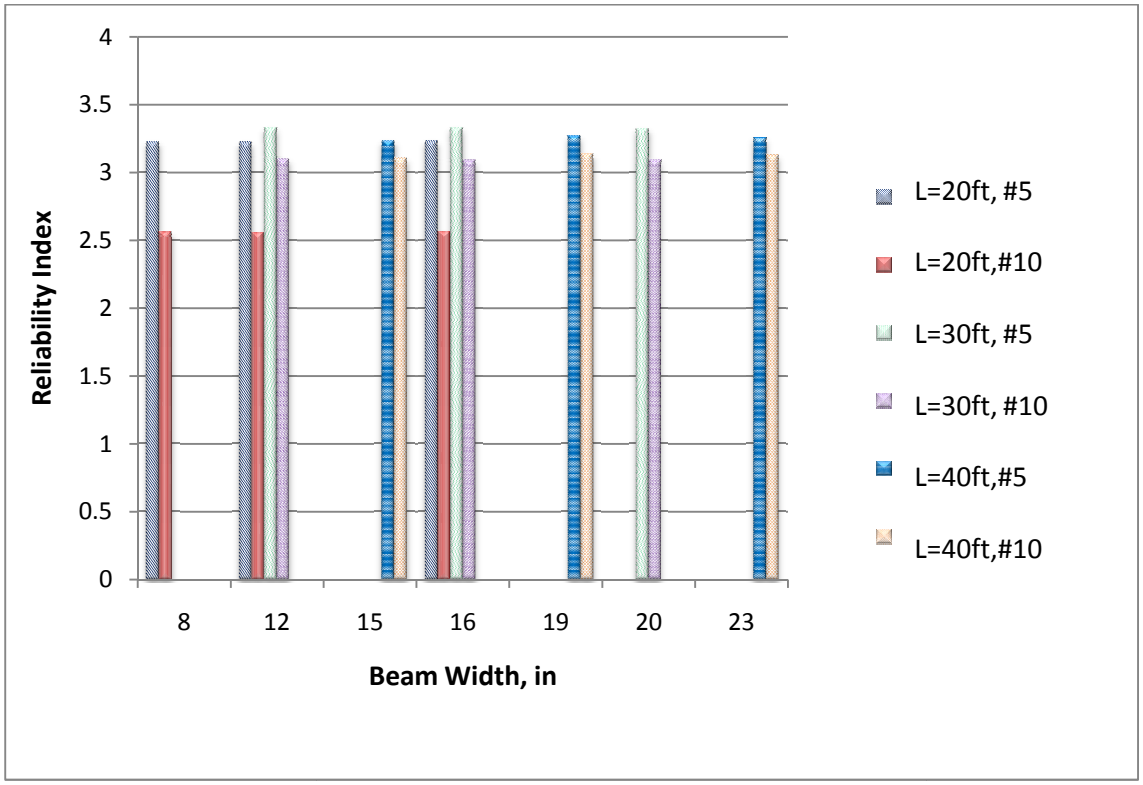

Figure 4.3: Variation of Reliability Index vs. Beam Width for both #5 and #10 Bars

4.1.2 EFFECT OF BEAM EFFECTIVE DEPTH

The second variable investigated is beam effective depth, d. A total of 243 beams for each bar size (#5 and #10, to total 486 beams) were used to analyze the effect of this variable. There are 27 beams in each span length. The effective depths were increased by 4 inches for the first increase, and 6 inches for the second increase. The data in the tables is again categorized by span length in the left vertical column and beam effective depth horizontally with average reliability index in the body. In Table 4.3, within each span length, and overall (horizontal grand total), reliability index increases as beam effective depth increases. Beta also increases as span length increases (vertical grand total), with a small exception for #5 bars at L = 40ft. Reliability index is also greater when #5 bars are used as opposed to #10 bars.

Table 4.3: Influence of Beam Effective Depth on Reliability Index

	Variation of Reliablity Index with Beam Depth (#5 bars)								
	d, in								
L, ft	16	20	22	24	28	30	34	36	Grand Total
20	3.23	3.58	3.71						3.51
30				3.33	3.57	3.65			3.52
40						3.24	3.48	3.55	3.42
Grand Total	3.23	3.58	3.71	3.33	3.57	3.44	3.48	3.55	3.48

	Variation of Reliablity Index with Beam Depth (#10 bars)								
	d, in								
L, ft	16	20	22	24	28	30	34	36	Grand Total
20	2.56	2.75	3.20						2.84
30				3.10	3.24	3.46			3.26
40						3.11	3.31	3.43	3.28
Grand Total	2.56	2.75	3.20	3.10	3.24	3.28	3.31	3.43	3.13

It can be seen in Table 4.4 that as beam effective depth increases, reliability index also increases, while standard deviation decreases and the number of beams that have reliability index less than the target decreases. With increases in effective depth, less than half the beams in each span length fail to meet the target reliability index for #5 bars,

while that number is increases for #10 bars. Again, this shows that #5 bars provide more reliable results than #10 bars. These results are supported by the corresponding graphs. The effective depth has a considerable influence on reliability index.

Table 4.4: Change in Reliability Index with Beam Effective Depth Increase

	Average Reliability Index			Standard Deviation of β			Number of $\beta < \beta_T$		
#5 Bars	Base Case	1st Increase	2nd Increase	Base Case	1st Increase	2nd Increase	Base Case	1st Increase	2nd Increase
L = 20 ft	3.23	3.58	3.71	0.81	0.64	0.57	15	10	10
L = 30 ft	3.33	3.57	3.65	0.76	0.66	0.61	16	13	11
L = 40 ft	3.24	3.48	3.55	0.75	0.68	0.64	17	14	11
# 10 Bars	Base Case	1st Increase	2nd Increase	Base Case	1st Increase	2nd Increase	Base Case	1st Increase	2nd Increase
L = 20 ft	2.56	2.74	3.20	0.94	0.83	0.74	23	22	16
L = 30 ft	3.10	3.24	3.46	0.82	0.77	0.67	18	16	14
L = 40 ft	3.10	3.31	3.43	0.68	0.63	0.59	19	17	14

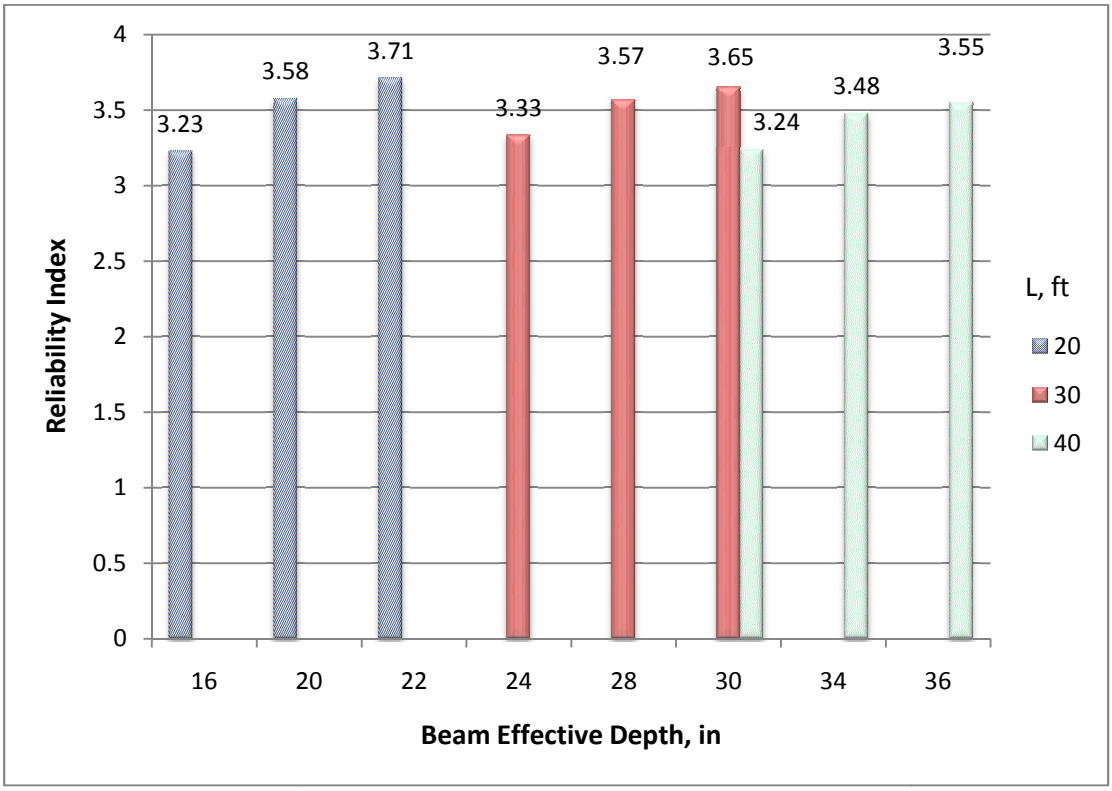

Figure 4.4: Variation of Reliability Index vs. Beam Effective Depth for #5 Bars

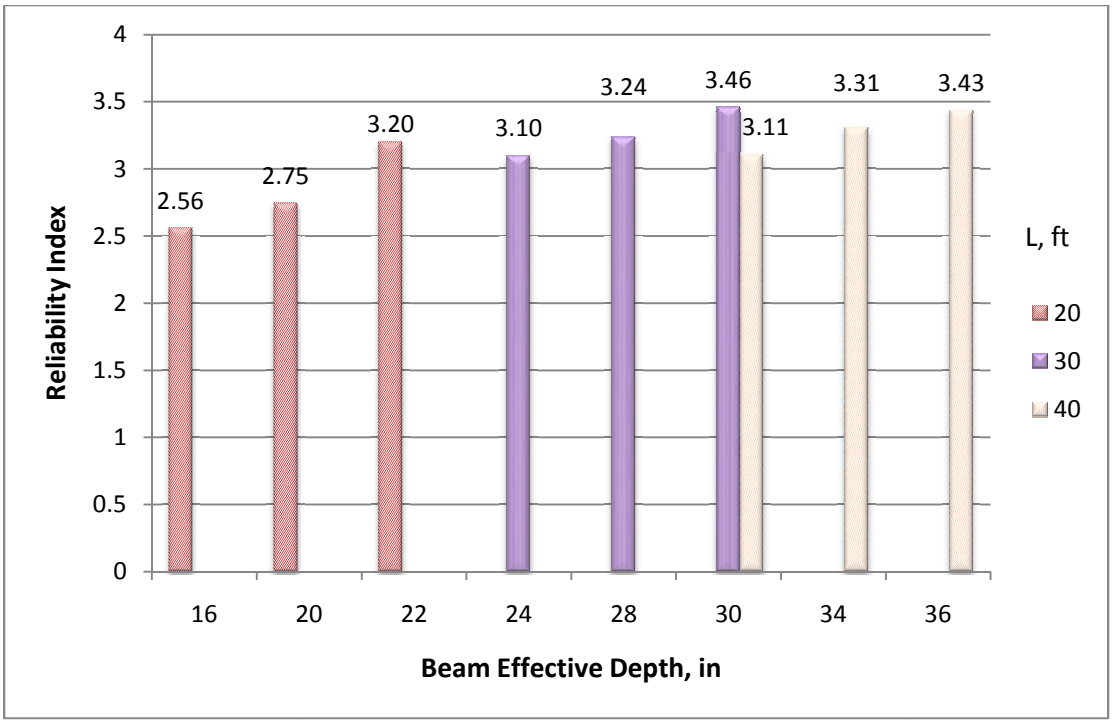

Figure 4.5: Variation of Reliability Index vs. Beam Effective Depth for #10 Bars

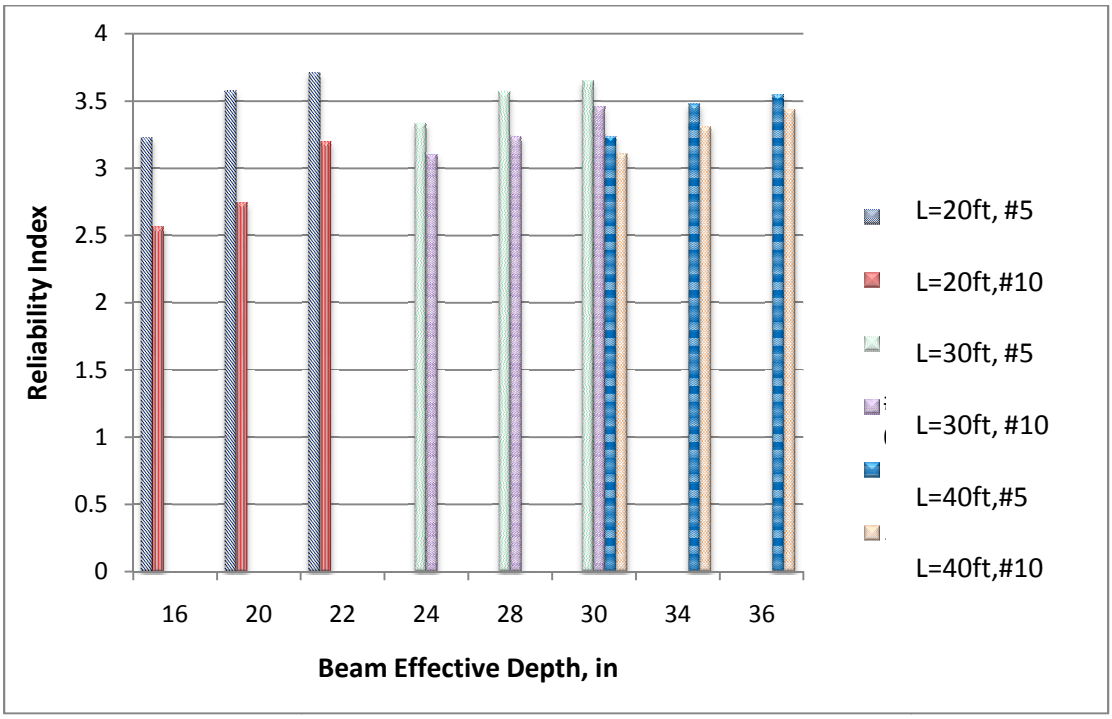

Figure 4.6: Variation in Reliability Index with Beam Effective Depth for both #5 and #10 Bars

4.1.3 EFFECT OF CONCRETE COVER

The third variable investigated is concrete cover. d_c. A total of 405 beams for each bar size (#5 and #10 to total 810 beams) were analyzed for this variable with covers of 1, 2, and 3 inches. There are 135 beams in each span length and 45 beams of each cover within each span length. The data is again categorized by span length in the left vertical column and concrete cover horizontally with average reliability index in the body. As seen in Table 4.5, within each span length, and overall (horizontal grand total), reliability index (beta) decreases as concrete cover increases. There has been great debate over the control of concrete cover. If concrete cover increases, investigators argue that this helps defend against corrosion and provide protection, but as a result, crack width increases. The debate over the level of corrosion induced from a minimal cover has not been resolved. Reliability also increases as span length increases, with the exception of #5 bars at L = 40ft. (vertical grand total). Reliability index is also greater when #5 bars are used as opposed to #10 bars. The corresponding graphs verify these results. Concrete cover has a significant effect on reliability index, as Frosch states as well.

Table 4.5: Influence of Concrete Cover on Reliability Index

Variation of Reliability Index with Concrete Cover (#5 bars)				
	dc, in			
L, ft	1	2	3	Grand Total
20	4.14	3.43	2.62	3.40
30	4.18	3.47	2.67	3.44
40	4.16	3.40	2.52	3.36
Grand Total	4.16	3.43	2.60	3.40

Variation of Reliability Index with Concrete Cover (#10 bars)				
	dc, in			
L, ft	1	2	3	Grand Total
20	3.33	2.83	2.19	2.78
30	3.85	3.25	2.55	3.22
40	3.94	3.28	2.48	3.23
Grand Total	3.70	3.12	2.41	3.08

Table 4.6 presents the reliability indices along with standard deviation and number of beams that fail to meet the target as concrete cover changes. The table shows that reliability index decreases significantly while its standard deviation increases as concrete cover increases. For a cover of 1 inch using #5 bars for all span lengths, all beams have reliability indices greater than the target of 3.5. As cover increases, the number of beams that fall below the target reliability index increases to almost half the beams in the category. When the cover reaches a value of 3 inches, all beams using both #5 and #10 bars fail to reach the target index, with an exception of 2 beams when L = 20ft for #5 bars. The influence of concrete cover on reliability index is very significant. The number of beams with reliability indices below β_T is higher when using #10 bars as opposed to #5 bars. This tapers off when cover becomes large, around 3 inches.

Table 4.6: Change in Reliability Index with Concrete Cover Increase

	Average Reliability Index			Standard Deviation of β			Number of $\beta < \beta_T$		
#5 Bars	Cover = 1"	Cover = 2"	Cover = 3"	Cover = 1"	Cover = 2"	Cover = 3"	Cover = 1"	Cover = 2"	Cover = 3"
L = 20 ft	4.14	3.43	2.62	0.23	0.38	0.55	0	23	43
L = 30 ft	4.18	3.47	2.67	0.20	0.33	0.47	0	22	45
L = 40 ft	4.16	3.40	2.52	0.17	0.25	0.36	0	29	45
# 10 Bars	Cover = 1"	Cover = 2"	Cover = 3"	Cover = 1"	Cover = 2"	Cover = 3"	Cover = 1"	Cover = 2"	Cover = 3"
L = 20 ft	3.33	2.83	2.19	0.80	0.78	0.77	21	39	45
L = 30 ft	3.85	3.25	2.55	0.53	0.56	0.61	10	27	45
L = 40 ft	3.94	3.28	2.48	0.24	0.26	0.33	3	37	45

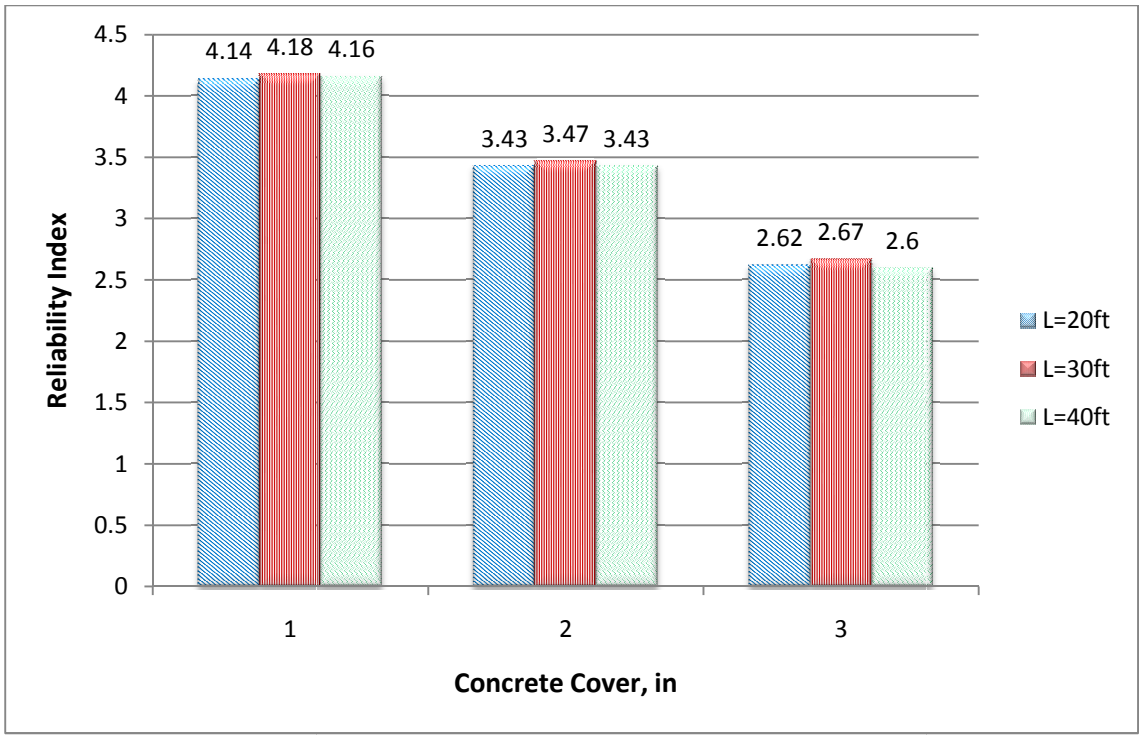

Figure 4.7: Variation of Reliability Index vs. Concrete Cover for #5 Bars

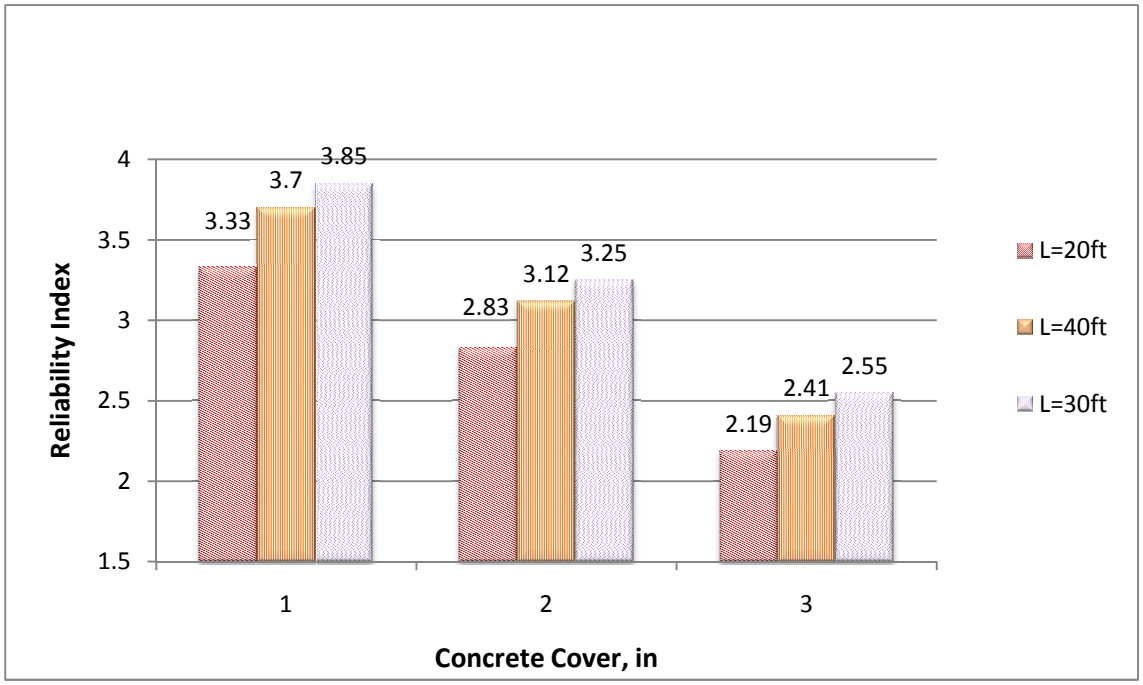

Figure 4.8: Variation of Reliability Index vs. Concrete Cover for #10 Bars

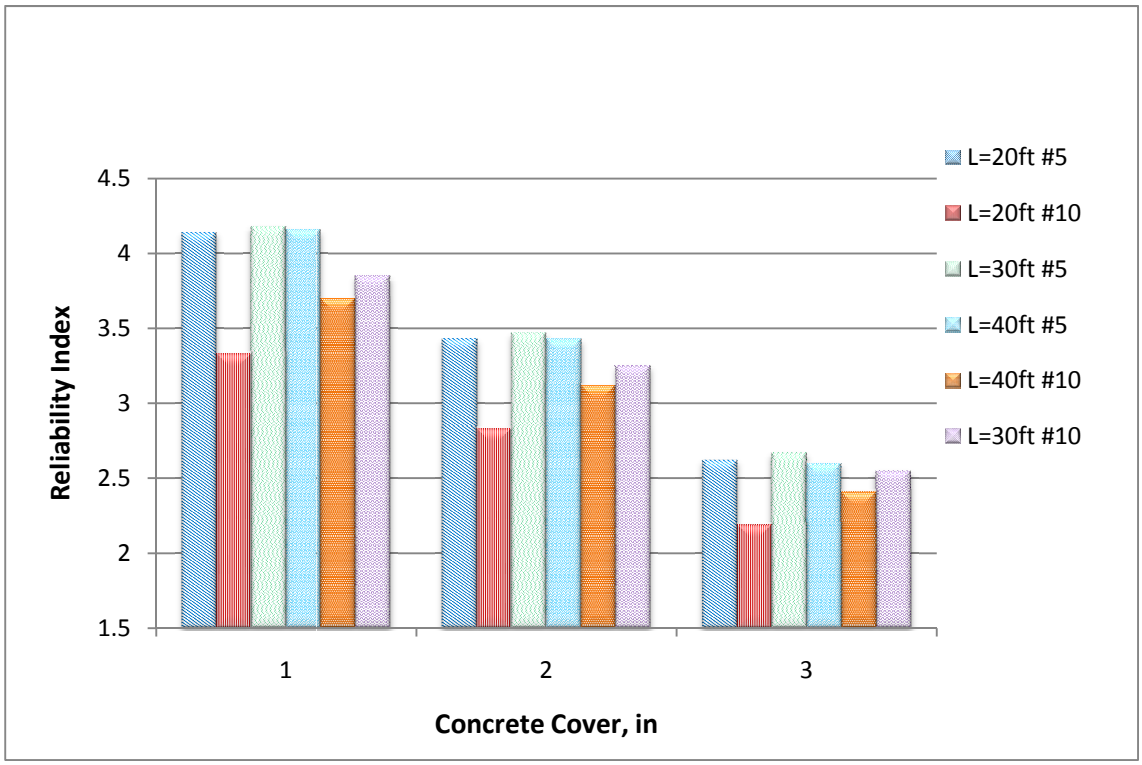

Figure 4.9: Variation of Reliability Index with Concrete Cover for both #5 and #10 Bars

4.1.4 EFFECT OF STEEL YIELD STRENGTH

The fourth variable investigated is steel reinforcement yield strength. There were 405 beams used with #5 and #10 bars to total 810 beams, with 135 beams in each span length category. The data is again categorized by span length in the left vertical column and steel yield strength horizontally with average reliability index in the body. In Table 4.7, within each span length, and overall (horizontal grand total), reliability index decreases as steel yield strength increases. There is a negligible exception when L= 20ft and f_y is 60,000 psi and a slightly larger exception when L = 40ft and f_y = 80,000 psi for #5 bars. Nevertheless, the overall trend is clear. There is also an overall trend of reliability increase as span length increases (vertical grand total). Reliability index is also greater when #5 bars are used as opposed to #10 bars. Steel yield strength has considerable influence on reliability index. Although this variable is not used in the Monte Carlo simulation, it does directly affect beam design through area of steel reinforcement required to achieve flexural adequacy but not necessarily sufficient crack width control.

Table 4.7: Influence of Steel Yield Strength on Reliability Index

Variation of Reliability Index with Steel Yield Strength (#5 bars)				
	fy, psi			
L, ft	40000	60000	80000	Grand Total
20	3.36	3.32	3.51	3.40
30	3.56	3.53	3.23	3.44
40	3.45	3.21	3.41	3.36
Grand Total	3.46	3.35	3.38	3.40

Variation of Reliability Index with Steel Yield Strength (#10 bars)				
	fy, psi			
L, ft	40000	60000	80000	Grand Total
20	3.34	2.60	2.40	2.78
30	3.62	3.38	2.65	3.22
40	3.45	3.15	3.10	3.23
Grand Total	3.47	3.04	2.72	3.08

It can be seen in Table 4.8 that reliability index decreases overall as steel yield strength increases. There are exceptions when f_y = 80 ksi at L = 20ft and 40ft. Though the change is small, overall standard deviation increases as steel yield stress increases. This is more clearly seen with #10 bars. Overall, the number of beams with reliability indices less than the target index increases as steel yield strength increases for #10 bars and remain rather constant for #5 bars. These numbers represent a little over half the beams in each category and virtually all the beams for #10 bars when steel yield strength is 80 ksi. Beams using #5 bars more often meet β_T than those beams using #10 bars. The aforementioned results can be validated by the following graphs as well.

Table 4.8: Change in Reliability Index with Steel Yield Strength Increase

	Average Reliability Index			Standard Deviation of β			Number of $\beta < \beta_T$		
#5 Bars	Fy = 40ksi	Fy = 60ksi	Fy = 80ksi	Fy = 40ksi	Fy = 60ksi	Fy = 80ksi	Fy = 40ksi	Fy = 60ksi	Fy = 80ksi
L = 20 ft	3.36	3.32	3.51	0.72	0.78	0.73	25	23	18
L = 30 ft	3.56	3.53	3.23	0.64	0.67	0.78	21	21	25
L = 40 ft	3.45	3.21	3.41	0.69	0.75	0.71	23	28	23
# 10 Bars	Fy = 40ksi	Fy = 60ksi	Fy = 80ksi	Fy = 40ksi	Fy = 60ksi	Fy = 80ksi	Fy = 40ksi	Fy = 60ksi	Fy = 80ksi
L = 20 ft	3.34	2.60	2.40	0.62	0.81	0.98	25	38	42
L = 30 ft	3.62	3.38	2.65	0.59	0.66	0.71	19	24	39
L = 40 ft	3.44	3.15	3.10	0.64	0.69	0.62	23	29	33

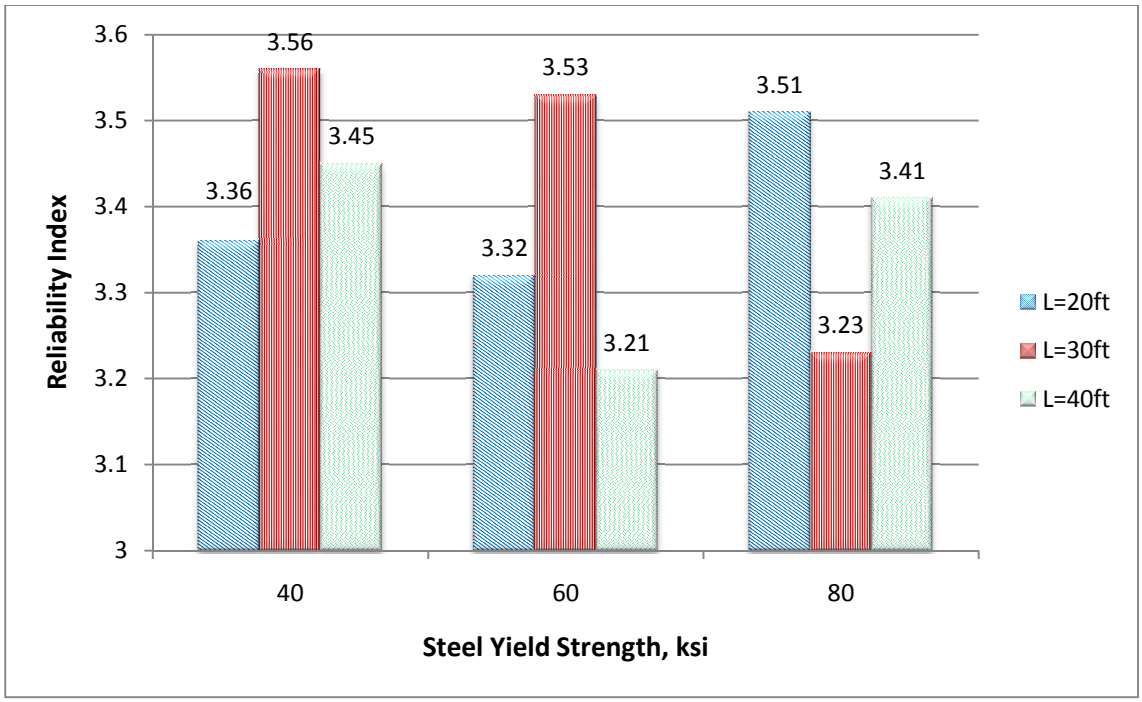

Figure 4.10: Variation of Reliability Index vs. Steel Yield Strength for #5 Bars

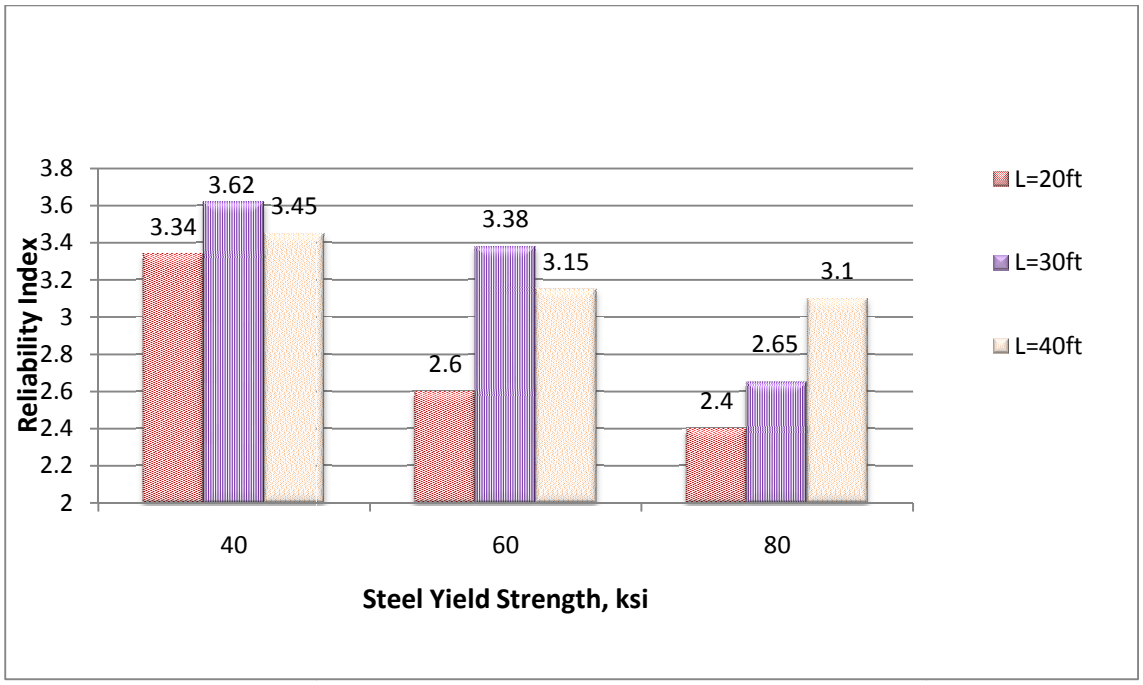

Figure 4.11: Variation of Reliability Index vs. Steel Yield Strength for #10 Bars

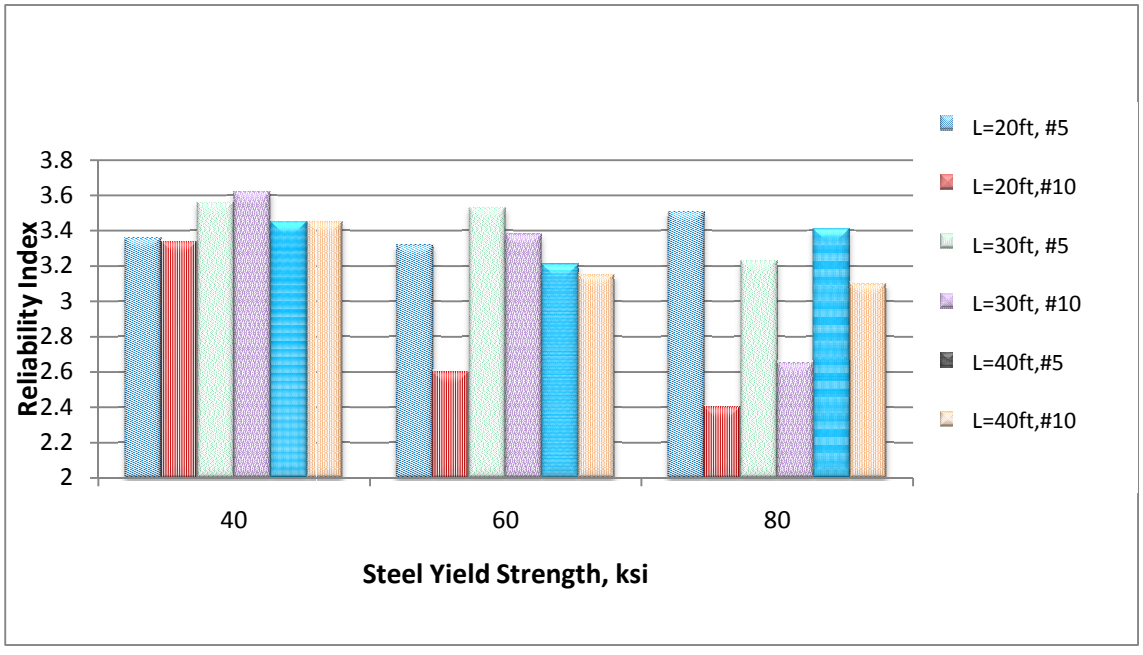

Figure 4.12: Variation of Reliability Index with Steel Strength for both #5 and #10 Bars

4.1.5 EFFECT OF CONCRETE STRENGTH

The fifth variable investigated is concrete strength. Again, 405 beams for #5 and #10 bars to total 810 beams were used to analyze the effect of this variable as it was varied from 4 to 8ksi. For each span length, there are 135 beams. In each span length, there are 45 beams within each category of concrete strength. The data is organized by span length in the left vertical column and concrete strength horizontally with average reliability index in the body. Mixed information is given in Table 4.9. There is no clear trend in reliability index as concrete strength increases. Within each span length, and overall (horizontal grand total), reliability index increases and decreases as concrete strength increases. This is also true as span length increases (vertical grand total). There are more instances, however, of reliability index increasing as concrete strength increases. This is evident with #5 bars at L = 30ft and #10 bars at span lengths of 20ft and 30ft. The span length of 40ft shows no trend in reliability index. Nevertheless, reliability index is certainly greater when #5 bars are used as opposed to #10 bars.

Table 4.9: Influence of Concrete Strength on Reliability Index

Variation of Reliability Index with Concrete Strength (#5 bars)				
	fc', psi			
L, ft	4000	6000	8000	Grand Total
20	3.39	3.26	3.53	3.40
30	3.41	3.43	3.51	3.44
40	3.54	3.21	3.32	3.36
Grand Total	3.45	3.29	3.46	3.40

Variation of Reliability Index with Concrete Strength (#10 bars)				
	fc', psi			
L, ft	4000	6000	8000	Grand Total
20	2.46	2.64	3.24	2.78
30	3.10	3.12	3.44	3.22
40	3.34	3.08	3.28	3.23
Grand Total	2.97	2.94	3.32	3.08

It can be seen in Table 4.10 there is no clear trend in reliability index as concrete strength increases. No clear trend is shown overall for the standard deviation of reliability index or the number of beams that fail to meet β_T as well. Reliability, however, does increase using #5 bars for a span length of 30ft and #10 bars for span lengths of 20ft and 30ft. Over half the beams using #5 bars do not meet the target index when concrete strength is increased. This number is even higher for #10 bars. The number of beams that meet the target reliability increases when using #10 bars for span lengths of 20ft and 30ft. Since there is no overall trend in the number of beams that meet the target reliability, changing concrete strength when designing beams will not ensure a higher reliability. However, using #5 bars certainly yields higher reliability indices than #10 bars in every category. The influence of concrete strength on reliability index is rather ambiguous as compared to other variables. This ambiguity could be due to the fact that statistical parameters for concrete strength are subject to variability when the strengths change.

Table 4.10: Change in Reliability Index as Concrete Strength Increases

	Average Reliability Index			Standard Deviation of β			Number of $\beta < \beta_T$		
#5 Bars	Fc' = 4ksi	Fc' = 6ksi	Fc' = 8ksi	Fc' = 4ksi	Fc' = 6ksi	Fc' = 8ksi	Fc' = 4ksi	Fc' = 6ksi	Fc' = 8ksi
L = 20 ft	3.39	3.26	3.53	0.74	0.81	0.67	23	24	19
L = 30 ft	3.41	3.43	3.51	0.69	0.77	0.68	24	21	22
L = 40 ft	3.54	3.21	3.32	0.67	0.76	0.71	20	28	26
# 10 Bars	Fc' = 4ksi	Fc' = 6ksi	Fc' = 8ksi	Fc' = 4ksi	Fc' = 6ksi	Fc' = 8ksi	Fc' = 4ksi	Fc' = 6ksi	Fc' = 8ksi
L = 20 ft	2.46	2.64	3.24	1.05	0.85	0.57	38	37	30
L = 30 ft	3.10	3.12	3.44	0.62	0.95	0.69	32	28	22
L = 40 ft	3.34	3.08	3.28	0.61	0.71	0.64	26	31	28

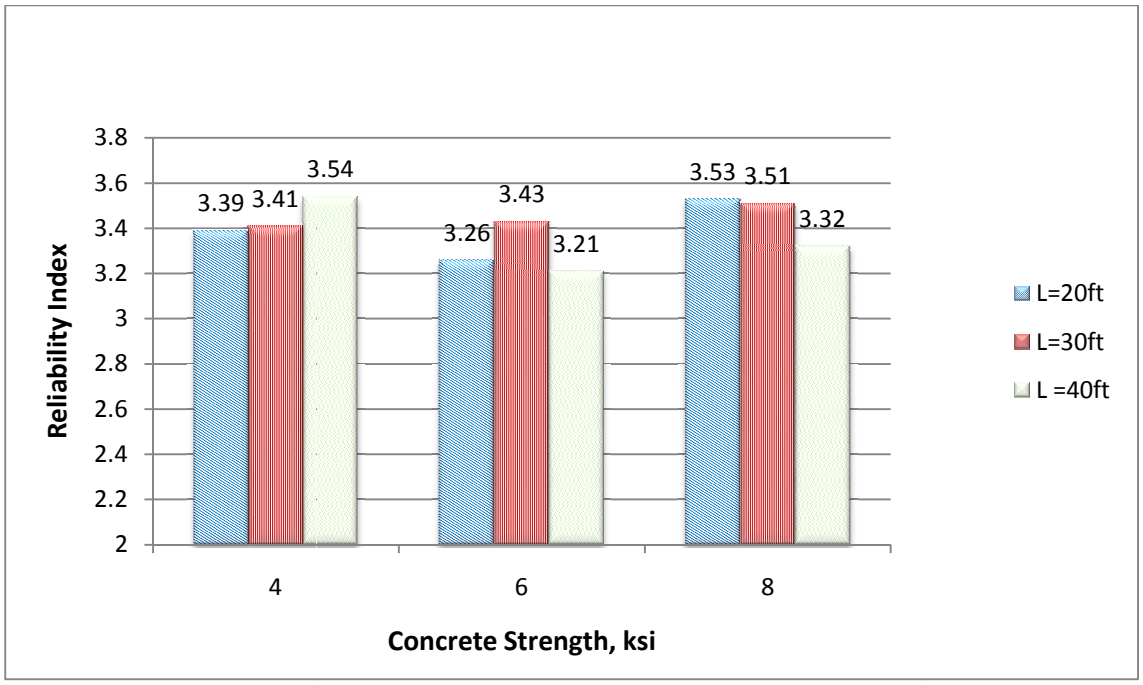

Figure 4.13: Variation of Reliability Index vs. Concrete Strength for #5 Bars

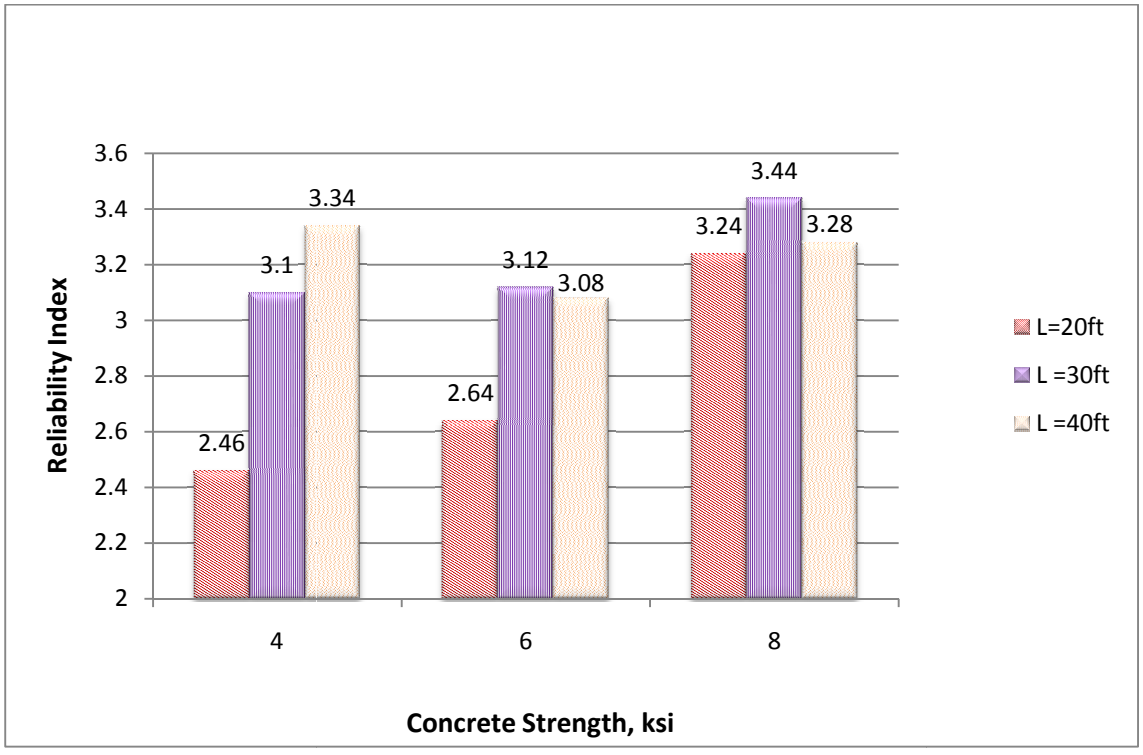

Figure 4.14: Variation of Reliability Index vs. Concrete Strength for #10 Bars

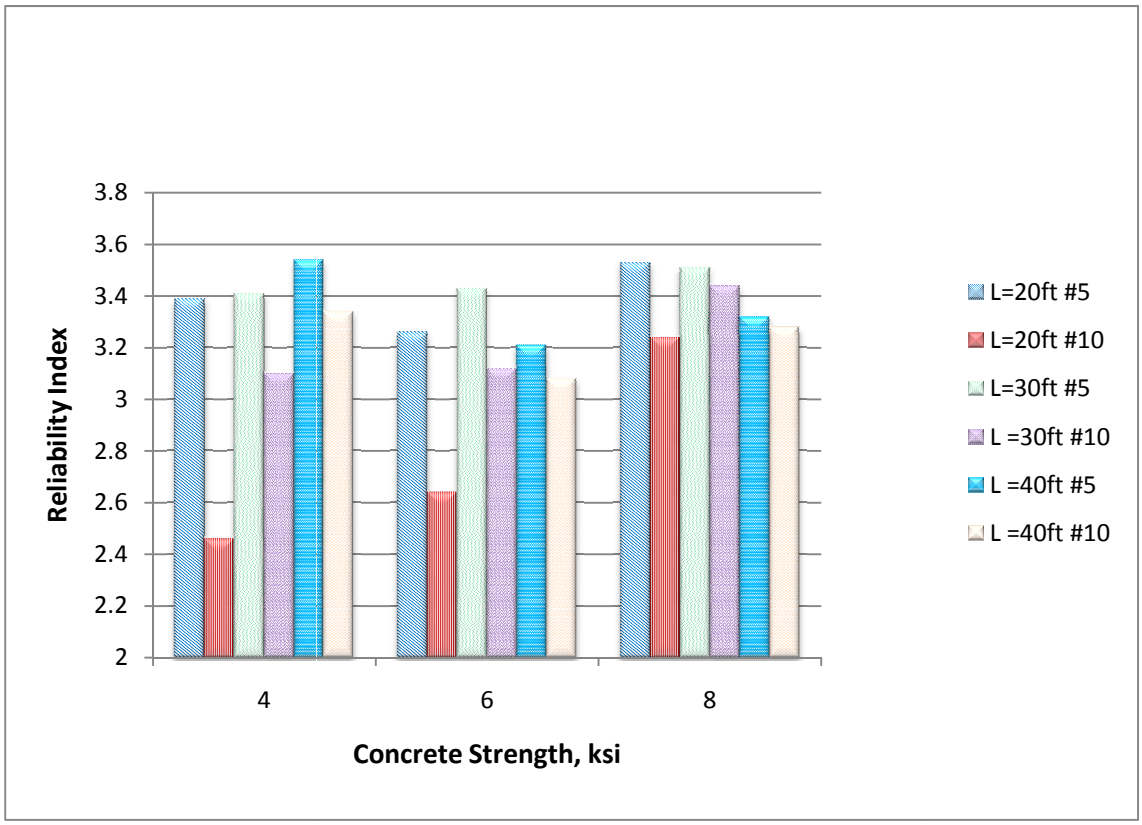

Figure 4.15: Variation of Reliability Index with Concrete Strength for both #5 and #10 Bars

4.1.6 EFFECT OF AREA OF REINFORCEMENT

The sixth variable investigated is area of steel reinforcement considered in the Monte Carlo simulation to obtain a reliability index. The area of reinforcement considered in the simulations is different than the total area of reinforcement in the beam because only the bottom most layer of reinforcement is considered to control cracking, not the full reinforcement area provided. Beams in this study had only tension reinforcement, but distributed in several layers when necessary. Beams with depth greater than 36 inches had necessary skin reinforcement, as mentioned earlier, but this again is not considered to control bottom face cracking. There were 156 beams of each bar size, #5 and #10, to total 312 beams used to analyze the influence of reinforcement area on reliability index. Area of reinforcement was decreased in the modified simulation by 0.65 in^2. A decrease in reinforcement was performed instead of an increase because for many beams, more than one layer was necessary and thus no more bars can fit in the bottom layer to directly affect crack width. Furthermore, the decrease was small to allow beams to still meet ACI flexural design adeuacy. Larger decreases would result in the elimination of many beams for the simulation since they would be inadequate in flexure. Two decreases were not performed because the change in area of reinforcement for #5 bars would not be significant.

It was observed that with the second increase of reinforcement area, the relaibility indices converged to essentially the same values as with the first increase. This is due to the fact that even though more reinforcement was added, the same amount of reinforcement can only fit at the bottom most layer of the beam. This bottom layer is the input into the Monte Carlo simulations and thus directly affects reliability index. This can

be more easily seen in the beams with #10 bars since they are a larger size. Due to this result, the first increase of reinforcement area will only be presented and 162 beams of each bar size will be analyzed.

Average original and incerased areas of reinforcement along with their respective average reliability indices for each span length are shown. In Table 4.11, the base case reinforcement area is compared with the modified, or decreased, reinforcement area. As noted earlier, the decrease is limited to ensure flexural adequacy of a sufficient number of beams. The change in reinforcement area is more evident with #10 bars, since fewer larger bars are required. Within each span length, and overall, as area of reinforcing steel decreases, reliability index decreases as well. For #5 and #10 bars, as span length increases, reliability increases, with the exception of #5 bars at a span length of 40ft. Once again, the reliability index for #5 bars is greater than that for #10 bars for both original and modified areas of reinforcement.

Table 4.11: Influence of Reinforcement Area on Reliability Index

Variation of Reliability Index with Reinforcement Area (#5 bars)				
L, ft	Base Case As, in²	Modified As, in²	Base Case β	Modified β
20	1.62	1.58	3.23	3.18
30	2.59	2.45	3.33	3.23
40	3.44	3.28	3.24	3.19
Variation of Reliability Index with Reinforcement Area (#10 bars)				
L, ft	Base Case As, in²	Modified As, in²	Base Case β	Modified β
20	3.14	2.80	2.56	2.34
30	6.54	5.86	3.10	2.70
40	8.11	7.50	3.11	2.93

It can be seen in Table 4.12 reliability index increases as reinforcement area increases. Standard deviation increases in each category as reinforcement area decreases. For both the original and modified cases, over half the beams in each span length category fail to meet the target reliability index. The number of beams that fail to meet the target index increase slightly as reinforcement area decreases. Greater changes are evident when #10 bars are used. Thus, it seems reasonable to deduce that reinforcement area considerably influences reliability index. However, there is the limitation of the total reinforcement that can fit in the beam, and the bottom layer that affects crack widths. Thus, there is a convergence on the amount of influence that reinforcement area can have on reliability index. The following graphs support these conclusions. Higher areas of reinforcement will yield higher reliability indices for the values in this study.

Table 4.12: Change In Reliability Index As Reinforcement Area Decreases

	Average Reliability Index		Standard Deviation of β		Number of $\beta < \beta_T$	
#5 Bars	Base Case	Decreased As	Base Case	Decreased As	Base Case	Decreased As
L = 20 ft	3.23	3.18	0.81	0.81	15	17
L = 30 ft	3.33	3.23	0.76	0.79	16	16
L = 40 ft	3.24	3.19	0.75	0.79	17	17
# 10 Bars	Base Case	Decreased As	Base Case	Decreased As	Base Case	Decreased As
L = 20 ft	2.56	2.34	0.94	1.09	23	24
L = 30 ft	3.10	2.70	0.82	1.08	18	20
L = 40 ft	3.10	2.93	0.68	0.76	19	21

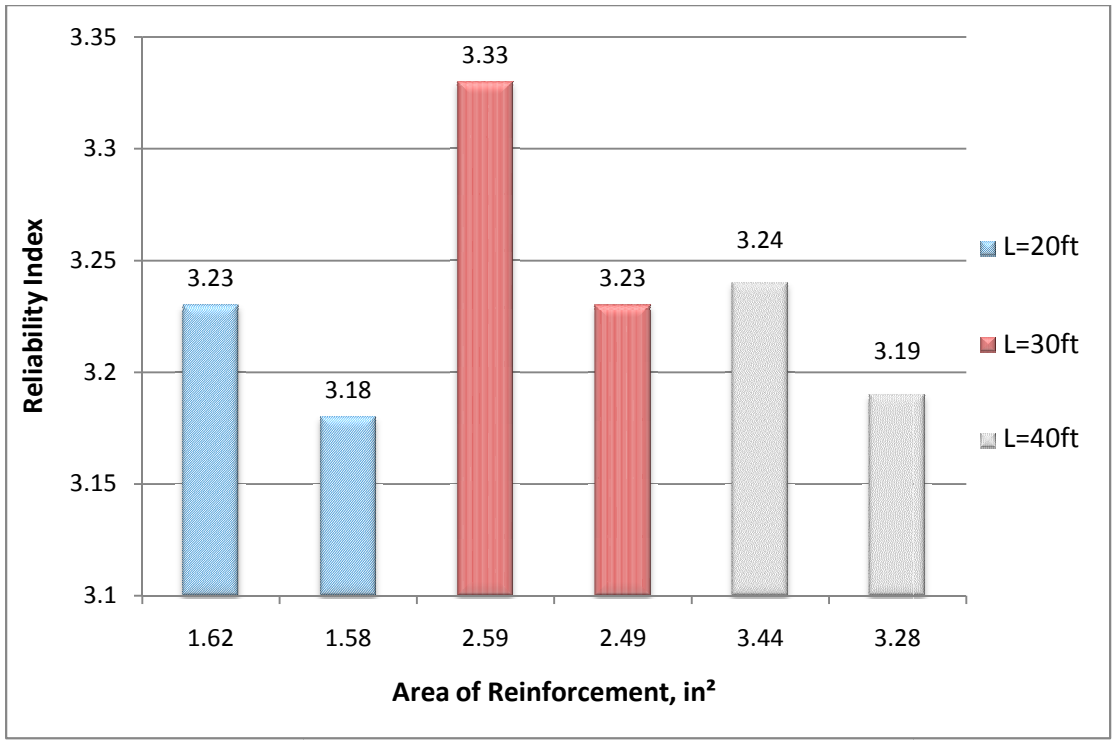

Figure 4.16: Variation of Reliability Index vs. Area of Reinforcement for #5 Bars

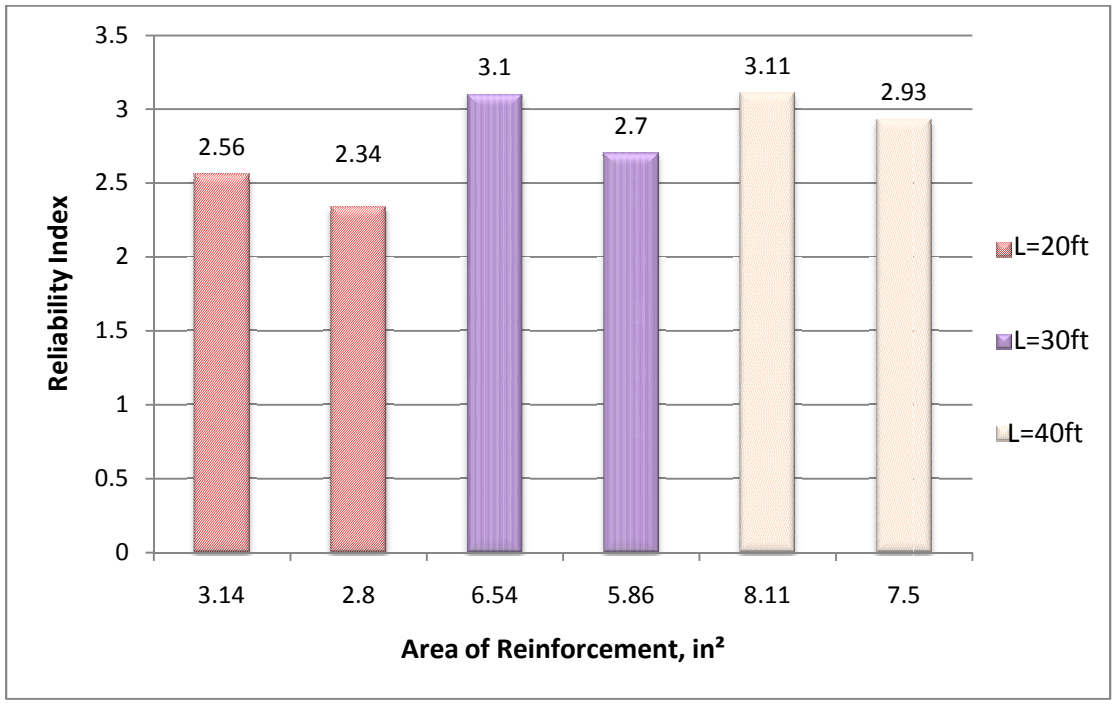

Figure 4.17: Variation of Reliability Index vs. Area of Reinforcement for #10 Bars

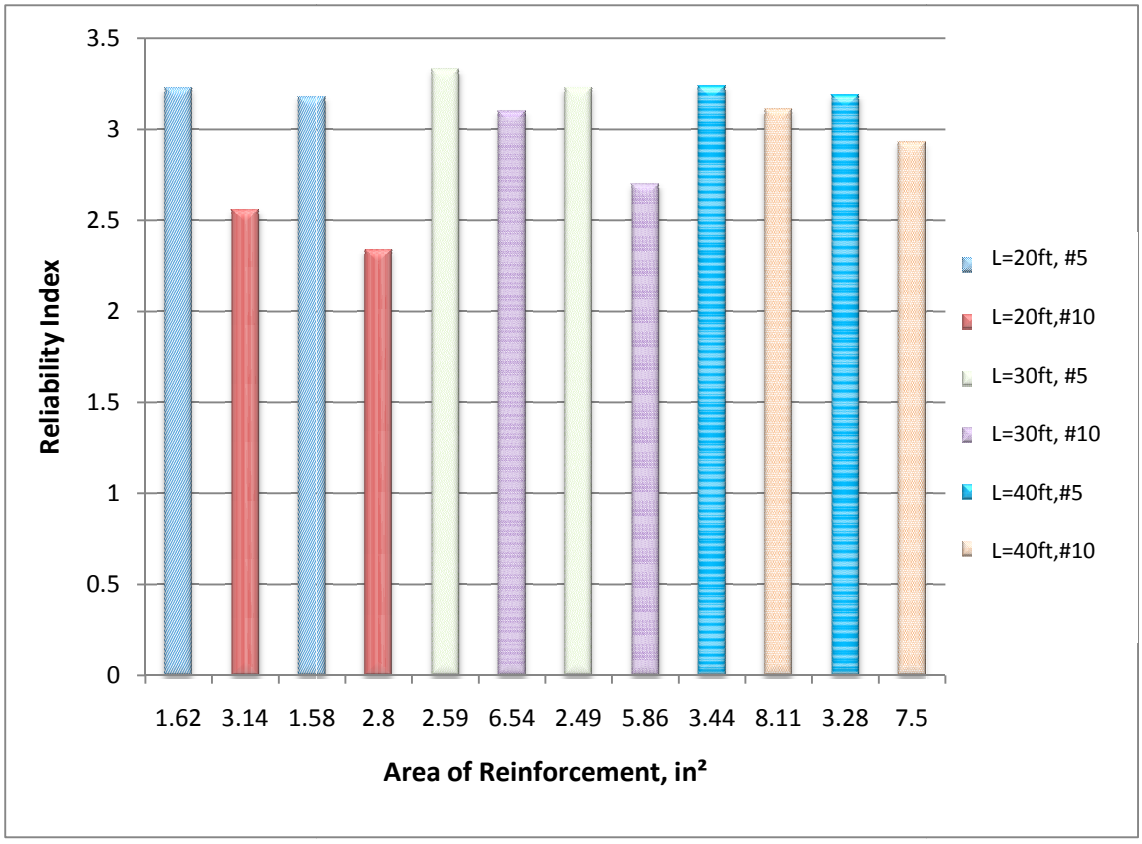

Figure 4.18: Variation of Reliability Index with Area of Reinforcement for both #5 and #10 Bars

4.1.7 EFFECT OF SPACING OF REINFORCEMENT

The seventh and eighth variables will be presented together since they are related. The seventh variable investigated is reinforcement spacing. Original spacing is the design spacing (steel adequate for flexural design) and the modified spacing is greater than original spacing by 2 inches. The eighth variable investigated is maximum allowable spacing by ACI 318-08 Section 10.6.4. This provision was discussed earlier and is based on the stress in the steel reinforcement. The actual stress, and not the recommended 2/3fy to be used, as given in ACI, resulted in very large spacings that were not reasonable. There were 243 beams for each bar size, to total 486 beams, used to analyze the effect of spacing on reliability index. The reliability indices were negative since the spacing was so large. This spacing is also not applicable to every beam since the maximum spacing is essentially dictated by the section width. Thus, this logical limitation must be applied. The maximum spacing will generally correspond to the section width in this study. To investigate these variables, 243 beams for each bar size (#5 and #10, to total 486 beams) were analyzed with 27 beams in each span length.

Using this design provision, maximum allowable spacing and the corresponding reliability index are presented in the following table. Table 4.13 presents the original, modified, and maximum spacing values along with their respective reliability indices for both #5 and #10 bars. Within each span length, and overall, the larger spacing yields considerably lower reliability indices. Reliability index increases as spacing decreases. Beta also decreases as span length increases. Reliability index is greater for #5 bars than #10 bars. Spacing using flexural design requirements yields high and positive reliability indices.

Table 4.13: Influence of Reinforcement Spacing on Reliability Index

Variation of Reliability Index with Reinforcement Spacing (#5 Bars)						
L, ft	Avg Original Spacing, in	Avg Increased Spacing, in	Avg Max Spacing, in	Original Avg β	Increased Avg β	Max Avg β
20	1.36	3.36	7.96	3.23	2.55	1.93
30	1.31	3.31	11.77	3.33	2.72	1.49
40	1.23	3.23	14.62	3.24	2.63	1.39
Variation of Reliability Index with Reinforcement Spacing (#10 Bars)						
L, ft	Avg Original Spacing, in	Avg Increased Spacing, in	Avg Max Spacing, in	Original Avg β	Increased Avg β	Max Avg β
20	4.67	6.96	7.98	2.56	2.25	2.01
30	2.87	4.87	11.85	3.10	2.39	1.57
40	2.49	4.48	14.72	3.11	2.38	1.47

In Table 4.14, it is clear that reliability index decreases as reinforcement spacing increases. Standard deviation of reliability index shows no trend, but is more spread out than other variables. The number of beams that fail to meet the target index of 3.5 average around half for the base case, and consistently increase as reinforcement spacing increases, until virtually all beams fail to meet the target reliability index when reinforcement spacing is at its maximum. Frosch argues that reinforcement spacing is among the best parameters than can control cracking in reinforced concrete structures. Spacing indirectly dictates design of several parameters. It is clear that reinforcement spacing has the strongest influence on crack control in reinforced concrete structures. The following graphs support these conclusions as well.

Table 4.14: Change in Reliability Index as Reinforcement Spacing Increases

	Average Reliability Index			Standard Deviation of β			Number of $\beta < \beta_T$		
#5 Bars	Base Case	1st Increase	Max Spacing	Base Case	1st Increase	Max Spacing	Base Case	1st Increase	Max Spacing
L = 20 ft	3.23	2.55	1.93	0.81	0.77	0.81	15	21	27
L = 30 ft	3.33	2.72	1.49	0.76	0.73	1.21	16	20	26
L = 40 ft	3.24	2.63	1.39	0.75	0.68	1.29	17	21	26
# 10 Bars	Base Case	1st Increase	Max Spacing	Base Case	1st Increase	Max Spacing	Base Case	1st Increase	Max Spacing
L = 20 ft	2.56	2.25	2.01	0.94	0.95	0.84	23	26	27
L = 30 ft	3.10	2.39	1.57	0.82	0.86	1.26	18	22	25
L = 40 ft	3.11	2.38	1.47	0.68	0.60	1.34	19	25	25

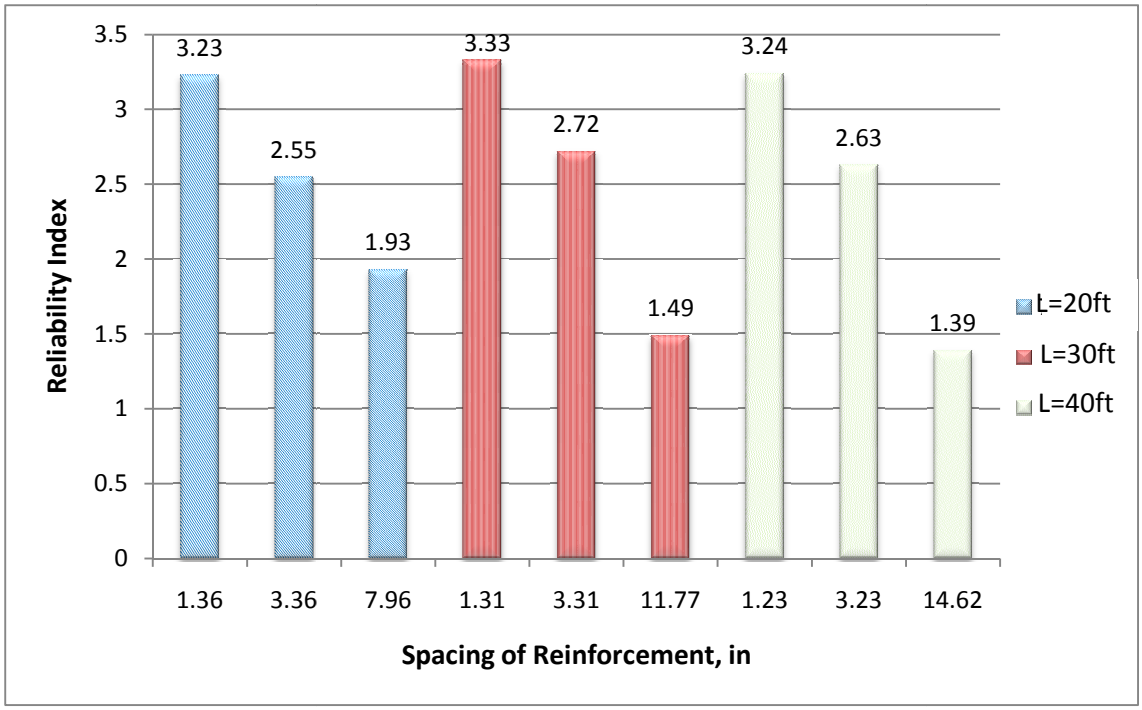

Figure 4.19: Variation of Reliability Index vs. Reinforcement Spacing for #5 Bars

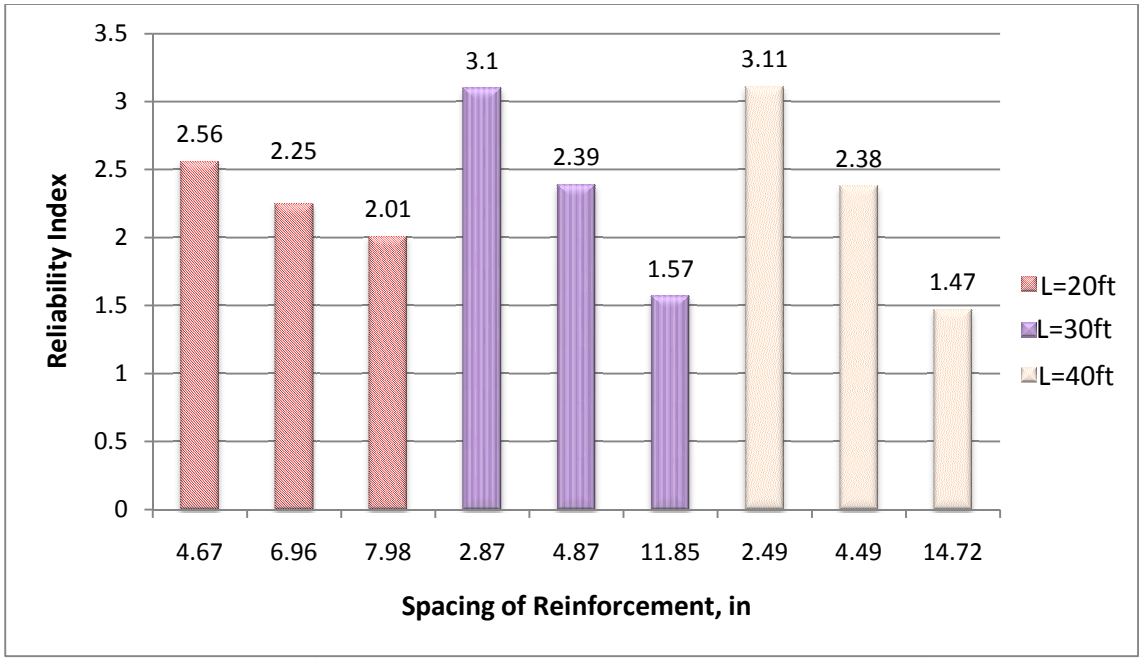

Figure 4.20: Variation of Reliability Index vs. Reinforcement Spacing for #10 Bars

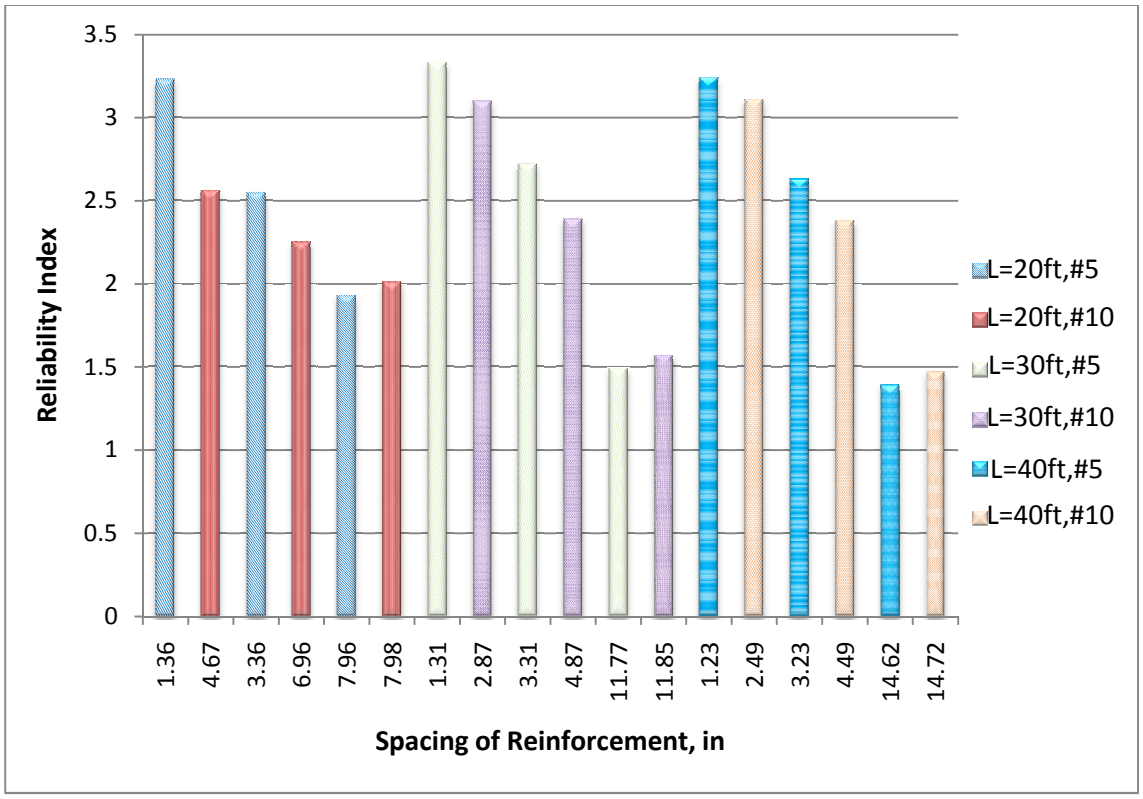

Figure 4.21: Variation of Reliability Index with Reinforcement Spacing for both #5 and #10 Bars

CHAPTER 5 CONCLUSIONS AND RECOMMENDATIONS

5.1 CONCLUSIONS AND RECOMMENDATIONS

In this study, a reliability-based approach was employed to analyze the effect of major variables on crack control in reinforced concrete beams. Probabilistic models can incorporate the level of uncertainty using available statistical information based on research and observed situations. In this thesis, the reliability of reinforced concrete structures regarding the crack control serviceability limit states was investigated. More common practice has shown a target reliability index of 3.5 is desired (Siriaksorn and Naaman, 1980). The crack control serviceability limit state was investigated to determine the most influential parameters on maximum crack width. For the base case of 81 beams, it was found that the average reliability for all span lengths using #5 bars is 3.31, while for #10 bars is 3.24.

In studying the reliability of reinforced concrete beams for the crack control limit state, the following observations or conclusions can be drawn:

(1) As beam width is increased, no significant effect results on reliability index. The average reliabilities of the beams within each span length essentially remain constant as beam width is increased. The average increase in reliability index using #5 bars is 0.31% and for #10 bars is 0.34%.

(2) As effective depth is increased, reliability index is slightly increased. The average increase in reliability index for all span lengths using #5 bars is 5.5% and for #10 bars is 7.0%.

(3) As concrete cover is increased, reliability index decreases. Frosch (1999) validates that smaller covers will reduce maximum crack widths, but researchers argue for and against the case that larger covers protect against reinforcement corrosion. The average decrease in reliability index as cover is increased is 22.9% for #5 bars and 21.1% for #10 bars. Concrete cover is certainly among the top factors influencing reliability index.

(4) In general, as steel yield strength increases, reliability decreases. The average decrease in reliability index is 1.5% for #5 bars and 12.3% for #10 bars.

(5) Also an increase in concrete strength causes a slight increase in reliability index. The average increase in reliability index is 0.59% using #5 bars and 5.8% using #10 bars.

(6) It was also found that as reinforcement area increases, reliability index also increases. The average increase in reliability index is 2.2% when using #5 bars and 11.9% when using #10 bars. This variable is limited in its influence as only a certain amount of reinforcement can fit in the bottom most layer while still adhering to ACI 318-08 code requirements for spacing of reinforcement.

(7) The seventh and eighth parameters, spacing of reinforcement and maximum allowable spacing as given by ACI 318-08 Section 10.6.4, considered in this study will be discussed together. For the beams in this study, the maximum allowable spacing was dictated by the section width, as spacing cannot logically exceed the width of the section. It is clear that decreasing spacing will result in higher reliability indices. The average reduction in reliability index when

increasing spacing is 33.2% for #5 bars and 26.7% for #10 bars. It is also evident that reinforcement spacing and concrete cover are the most significant parameters to control cracking in reinforced concrete.

(8) It was also observed that using a larger number of bars with small diameters leads to higher reliability indices than using a smaller number of bars with larger diameters. For this study, the average reliability index increased by 13.2% when using #5 bars as opposed to #10 bars.

In conclusion, reliability-based approaches should be considered to provide more realistic analyses. Reliability-based analysis models real world situations more closely than deterministic analysis. Future work can include ACI 318-08 Building Code calibration using reliability-based approaches for various serviceability limit states.

REFERENCES

1. "AASHTO LRFD Bridge Design Specifications". (2008). American Association of State Highway and Transportation Officials.

2. Abdun-Nur, Edward A. (1983). "Cracking of Concrete- Who Cares?," *ACI Concrete International*. V. 5. No. 7. pp. 27-30.

3. "*ACI* Fall Convention Debate on Crack Width, Cover, and Corrosion". (1984). New York, NY. pp 20-35.

4. ACI Committee 224. (2001). "Control of Cracking in Concrete Structures," Farmington Hills, MI. pp. 1-46.

5. "ACI 318 Building Code Requirements for Structural Concrete and Commentary". (2008). Farmington Hills, MI.

6. Base, G.D. (1971). "Causes, Control and Consequences of Cracking in Reinforced Concrete," *Australian Road Research*. V. 4. No. 7. pp. 3-13.

7. Base, G.D. (1976). "Control of Flexural Cracking in Reinforced Concrete," *Civil Engineering Transactions*. V. CE 18. No. 1. pp. 20-23.

8. Bayrak, Oguzhan. (2008). "Strength and Serviceability Design of Reinforced Concrete Deep Beams: Section 4.5 Minimum Web Reinforcement," Center for Transportation Research. Austin, TX.

9. Beeby. (1979). "The Prediction of Crack Widths in Hardened Concrete," *The Structural Engineer Part A*. V. 57A. No. 1. pp. 9-17.

10. Beeby. (2001). "Crack Control Provisions in the New Eurocode for the Design of Concrete Structures," *ACI SP 204-3*.

11. Benjamin, Jack R. and Lind, N.C. (1969). "A Probabilistic Basis for a Deterministic Code," *ACI Journal Proceedings*. V. 66. No. 11. pp. 857-865.

12. Bentz, E. and Collins, M.P. (2001). "Response 2000, Shell 2000, Triax 2000, and Membrane 2000 User Manual," http://www.ecf.utoronto.ca/~bentz/home.shtml.

13. Blackman, D.T. and Frosch, R.J. (2005)."Epoxy Coated Reinforcement and Crack Control" *ACI SP 225-11*. pp 163-178.

14. Broms, B. B. (1965). "Crack Width and Crack Spacing in Reinforced Concrete Members" by. *ACI Journal*. pp 1237-1256.

15. Carino, Nicholas J. and Clifton, James R. (2005). "Prediction of Cracking in Reinforced Concrete Structures," Report NISTIR. pp. 1-50.

16. Chowdhury, S.H. and Loo, Y.C. (2001). "A New Formula for Prediction of Crack Widths in Reinforced and Partially Prestressed Concrete Beams," *Advances in Structural Engineering*. pp. 101-110.

17. Cifuentes, C.V. and Hughes, B.P. (1988). "Comparison of Early-Age Crack Width Formulas for Reinforced Concrete," *ACI Structural Journal*. V. 85. No. 2. pp. 158-166.

18. Clark, Arthur P. (1956). "Cracking in Reinforced Concrete Flexural Members." *ACI Journal Proceedings*. V. 52. No. 4. pp. 851-862.

19. Cornell, C. Allen. (1969). "A Probability-Based Structural Code*," ACI Journal Proceedings*. V. 66. No. 12. pp. 974-985.

20. Corotis, Ross B. (1985). "Probability Based Design Codes," Concrete International. V.7, No. 4, pp. 42-49.

21. "European Standard EN 1992". (2004). *Eurocode 2: Design of Concrete Structures- Part 1-1: General rules and rules for buildings*. CEN (European Committee for Standardization).

22. Frantz, G.C., and Breen, J.E. (1978). "Control of Cracking on the Side Faces of Large Reinforced Concrete Beams," *Texas State Department of Highways and Public Transportation.* Austin, Texas.

23. Frosch, R. J. (1999). "Another Look at Cracking and Crack Control in Reinforced Concrete" *ACI Structural Journal* V. 96, No. 3, pp. 437-442.

24. Frosch, R. J. (2001). "Flexural Crack Control in Reinforced Concrete," ACI *Special Publication.* V. 204. pp. 135-154.

25. Frosch, R. J. (2002). "Modeling and Control of Side Face Beam Cracking," *ACI Structural Journal*. V.99. No. 3. pp. 376-385.

26. Gergely, P. and Lutz, L.A.. (1968). "Maximum Crack Width in Reinforced Concrete Members," *Causes, Mechanism, and Control of Cracking in Concrete*. ACI. Farmington Hills, Mich. pp 87-117.

27. Moran, J. and Lubell, A.S. (2008). "Behaviour of Concrete Deep Beams with High Strength Reinforcement. *Department of Civil and Environmental Engineering, University of Alberta.* Edmonton, Alberat, Canada.

28. Nelson, M. F. and Sexsmith, R. G. (1969). "Limitations in Application of Probabilistic Concepts," *ACI Journal Proceedings*. V. 66. No. 10. pp. 823-828.

29. Nowak, A. and Collins, K. (2000). "Reliability of Structures," McGraw Hill. pp.1-338.

30. Nowak, Andrzej S., Tabsh, Sami W. and Yamani, Ahmed S. (1994). "Probabilistic Models for Resistance of Concrete Bridge Girders," *ACI Structural Journal*. V. 91. No. 3. pp. 269-276.

31. Nowak, Andrzej S. and Szersen, Maria M. (2003). "Calibration of Design Code for Buildings (ACI 318)" *ACI Structural Journal*. V. 100. No. 3. pp. 377-391.

32. Nowak, A., Szersen, M., Szeliga, E., Szwed, A., and Podhorecki, P. (2008). "Reliability-Based Calibration for Structural Concrete, Phase 3," *Portland Cement Association.* pp. 1-110.

33. Rangan, Vijaya B. (1992). "Serviceability Design in the Current Australian Code," *ACI Special Publication*. V. 133. pp. 93-110.

34. Sexsmith, Robert G. May 1, 1969. "Reliability Analysis of Concrete Members," *ACI Journal Proceedings*. V. 66. No. 5. pp. 413-420.

35. Siriaksorn, A. and Naaman, A.E. (1980). "Reliability of Partially Prestressed Beams at Serviceability Limit states. *University of Illinois at Chicago Circle.* Chicago, IL. pp. 1-126.

36. Tammo, K. and Thelanderssen, S. (2009). "Crack Behavior Near Reinforcing Bars in Concrete Structures," *ACI Structural Journal*. V. 106. No. 3. pp. 259-267.

APPENDIX I RESISTANCE VALIDATION DATA

Clark's (1956) Specimen Data

Specimen No.	Depth, h, in	Width, b, in	Cover, dc, in	Bar Size	No. of Bars	Bar Spacing s, in	As, in²	fc', psi	fs, psi	fy, psi
6-7 1/2-3-2	6	7.5	0.69	3	3	2.5	0.3313	3720	15000	40000
6-7 1/2-4-1	6	7.5	0.75	4	2	3.75	0.3927	3550	15000	40000
6-7 1/2-4-2	6	7.5	0.75	4	2	3.75	0.3927	3570	15000	40000
6-7 1/2-4-3	6	7.5	0.75	4	2	3.75	0.3927	3810	15000	40000
6-15-6-1	6	15	0.87	6	2	7.5	0.8836	3890	15000	40000
6-9-5-5	6	9	0.81	5	2	4.5	0.6136	4300	15000	40000
6-11-6-1	6	11	0.87	6	2	5.5	0.8836	4100	15000	40000
6-11-6-2	6	11	0.87	6	2	5.5	0.8836	3750	15000	40000
6-15-7-1	6	15	0.94	7	2	7.5	1.2026	3870	15000	40000
6-15-7-2	6	15	0.94	7	2	7.5	1.2026	3850	15000	40000
6-7 1/2-7-1	6	7.5	0.94	7	1	7.5	0.6013	3600	15000	40000
6-7 1/2-7-2	6	7.5	0.94	7	1	7.5	0.6013	3460	15000	40000
6-7 1/2-5-1	6	7.5	0.81	5	2	3.75	0.6136	3330	15000	40000
6-7 1/2-5-2	6	7.5	0.81	5	2	3.75	0.6136	3200	15000	40000
6-7 1/2-5-3	6	7.5	0.81	5	2	3.75	0.6136	4190	15000	40000
6-9-8-1	6	9	1	8	1	9	0.7854	4500	15000	40000
6-9-8-2	6	9	1	8	1	9	0.7854	3780	15000	40000
6-6-7-1	6	6	0.94	7	1	6	0.6013	4250	15000	40000
6-7 1/2-6-1	6	7.5	0.87	6	2	3.75	0.8836	3980	15000	40000
6-9 1/2-7-1	6	9.5	0.94	7	2	4.75	1.2026	3410	15000	40000
6-9 1/2-7-2	6	9.5	0.94	7	2	4.75	1.2026	4100	15000	40000
15-6-8-1	15	6	2	8	1	6	0.7854	3690	15000	40000
15-6-8-2	15	6	2	8	1	6	0.7854	3750	15000	40000
15-6-6-1	15	6	1.62	6	2	3	0.8836	4360	15000	40000
15-6-6-3	15	6	1.87	6	2	3	0.8836	3940	15000	40000
15-6-7-1	15	6	0.94	7	2	3	1.2026	3890	15000	40000
15-6-7-2	15	6	1.94	7	2	3	1.2026	3250	15000	40000
15-6-7-3	15	6	1.94	7	2	3	1.2026	4280	15000	40000
15-6-7-4	15	6	1.94	7	2	3	1.2026	4210	15000	40000
15-6-7-5	15	6	1.94	7	2	3	1.2026	4040	15000	40000
15-6-10-1	15	6	2.14	10	1	6	1.2272	3570	15000	40000
15-6-10-2	15	6	2.14	10	1	6	1.2272	4160	15000	40000
15-6-8-3	15	6	2	8	2	3	1.5708	3860	15000	40000
15-6-8-4	15	6	2	8	2	3	1.5708	3870	15000	40000
15-6-9-1	15	6	1.44	9	2	3	1.988	4080	15000	40000
15-6-9-2	15	6	2.06	9	2	3	1.988	4140	15000	40000
15-6-9-3	15	6	2.06	9	2	3	1.988	3950	15000	40000
15-6-9-4	15	6	2.06	9	2	3	1.988	4140	15000	40000
15-6-9-5	15	6	2.06	9	2	3	1.988	3540	15000	40000
23-6-10-1	23	6	2.14	10	1	6	1.2272	3960	15000	40000
23-6-10-2	23	6	2.14	10	1	6	1.2272	3620	15000	40000
23-6-11-1	23	6	2.7	11	1	6	1.4849	3930	15000	40000
23-6-9-1	23	6	2.06	9	2	3	1.988	3650	15000	40000
23-6-9-2	23	6	2.06	9	2	3	1.988	3560	15000	40000
23-6-11-2	23	6	2.2	11	2	3	2.9698	3590	15000	40000
23-6-11-3	23	6	2.2	11	2	3	2.9698	4040	15000	40000

Accuracy of Crack Width Equations with Clark's Measured Crack Width (fs = 15 ksi)

Specimen No.	Max Width, in	Kaar-Mattock Error	Gergely-Lutz Error	Frosch Error
6-7 1/2-3-2	0.00073	269.8%	139.4%	113.5%
6-7 1/2-4-1	0.00068	356.8%	216.7%	225.6%
6-7 1/2-4-2	0.00109	184.9%	97.6%	103.2%
6-7 1/2-4-3	0.00166	86.8%	29.5%	33.4%
6-15-6-1	0.00226	74.5%	36.4%	88.5%
6-9-5-5	0.00214	57.4%	14.4%	23.1%
6-11-6-1	0.00278	32.6%	1.0%	14.8%
6-11-6-2	0.00266	39.2%	6.0%	20.0%
6-15-7-1	0.00246	68.5%	36.0%	74.8%
6-15-7-2	0.00278	49.2%	20.4%	54.7%
6-7 1/2-7-1	0.00342	21.7%	-1.7%	25.7%
6-7 1/2-7-2	0.00299	39.6%	12.7%	43.8%
6-7 1/2-5-1	0.00281	16.8%	-16.4%	-19.9%
6-7 1/2-5-2	0.0029	13.4%	-18.8%	-22.4%
6-7 1/2-5-3	0.00252	28.7%	-7.8%	-10.7%
6-9-8-1	0.0025	78.6%	50.2%	106.0%
6-9-8-2	0.0037	21.8%	2.4%	39.2%
6-6-7-1	0.00332	19.2%	-5.6%	5.3%
6-7 1/2-6-1	0.00198	73.9%	28.3%	15.5%
6-9 1/2-7-1	0.00484	-19.1%	-37.2%	-41.3%
6-9 1/2-7-2	0.00314	21.7%	-5.5%	-9.5%
15-6-8-1	0.00203	122.2%	141.1%	113.1%
15-6-8-2	0.00264	70.8%	85.3%	63.9%
15-6-6-1	0.00228	52.5%	43.0%	13.2%
15-6-6-3	0.00308	19.8%	19.3%	-7.4%
15-6-7-1	0.0019	51.6%	13.4%	3.6%
15-6-7-2	0.00282	35.7%	37.2%	3.9%
15-6-7-3	0.00241	56.8%	58.6%	21.6%
15-6-7-4	0.00355	6.5%	7.7%	-17.4%
15-6-7-5	0.00329	15.1%	16.4%	-10.9%
15-6-10-1	0.00442	7.3%	19.7%	1.0%
15-6-10-2	0.00513	-8.3%	2.4%	-13.0%
15-6-8-3	0.00654	-40.3%	-38.8%	-54.1%
15-6-8-4	0.00345	13.2%	15.9%	-13.0%
15-6-9-1	0.00235	45.9%	30.3%	2.1%
15-6-9-2	0.00415	-3.1%	0.5%	-26.0%
15-6-9-3	0.00302	33.7%	38.6%	1.7%
15-6-9-4	0.00292	37.7%	42.8%	5.2%
15-6-9-5	0.00443	-7.6%	-4.2%	-30.7%
23-6-10-1	0.00331	31.3%	46.5%	34.9%
23-6-10-2	0.00401	8.5%	21.1%	11.3%
23-6-11-1	0.00414	15.4%	41.9%	22.6%
23-6-9-1	0.00361	1.2%	4.9%	-14.9%
23-6-9-2	0.00332	10.1%	14.2%	-7.5%
23-6-11-2	0.0034	12.9%	20.3%	-4.7%
23-6-11-3	0.0049	-22.4%	-17.3%	-33.9%
	Avg Positive Error	**55.1%**	**39.2%**	**44.3%**
	Avg Negative Error	**-16.8%**	**-15.3%**	**-19.9%**

Accuracy of Crack Width Equations with Clark's Measured Crack Width (fs = 20

Specimen No.	Max Width, in	Kaar-Mattock Error	Gergely-Lutz Error	Frosch Error
6-9-3-1	0.0014	168.4%	76.4%	71.6%
6-9-3-3	0.00175	115.0%	41.3%	37.3%
6-7 1/2-3-2	0.00156	130.7%	49.4%	33.2%
6-7 1/2-4-1	0.00303	36.7%	-5.2%	-2.6%
6-7 1/2-4-2	0.00146	183.6%	96.7%	102.2%
6-7 1/2-4-3	0.00248	66.7%	15.6%	19.1%
6-15-6-1	0.00477	10.2%	-13.9%	19.1%
6-9-5-5	0.00337	33.3%	-3.1%	4.2%
6-11-6-1	0.00397	23.8%	-5.7%	7.2%
6-11-6-2	0.00444	11.2%	-15.3%	-4.2%
6-15-7-1	0.00417	32.6%	7.0%	37.5%
6-15-7-2	0.00499	10.8%	-10.6%	14.9%
6-7 1/2-7-1	0.00608	-8.7%	-26.3%	-5.7%
6-7 1/2-7-2	0.00497	12.0%	-9.6%	15.4%
6-7 1/2-5-1	0.0044	-0.6%	-28.8%	-31.8%
6-7 1/2-5-2	0.00432	1.5%	-27.3%	-30.6%
6-7 1/2-5-3	0.00391	10.6%	-20.8%	-23.3%
6-9-8-1	0.00407	46.3%	23.0%	68.7%
6-9-8-2	0.00496	21.2%	1.9%	38.4%
6-6-7-1	0.00531	-0.6%	-21.3%	-12.2%
6-7 1/2-6-1	0.00298	54.1%	13.7%	2.3%
6-9 1/2-7-1	0.00749	-30.3%	-45.9%	-49.4%
6-9 1/2-7-2	0.00476	7.0%	-16.8%	-20.4%
15-6-8-1	0.00464	29.6%	40.6%	24.3%
15-6-8-2	0.00459	31.0%	42.1%	25.7%
15-6-6-1	0.00441	5.1%	-1.4%	-22.0%
15-6-6-2	0.00301	54.0%	44.5%	14.3%
15-6-6-3	0.00369	33.4%	32.8%	3.0%
15-6-7-1	0.00274	40.2%	4.8%	-4.2%
15-6-7-2	0.0043	18.7%	20.0%	-9.1%
15-6-7-3	0.00362	39.2%	40.8%	7.9%
15-6-7-4	0.00431	17.0%	18.3%	-9.3%
15-6-7-5	0.00568	-11.1%	-10.1%	-31.2%
15-6-10-1	0.00659	-4.1%	7.1%	-9.7%
15-6-10-2	0.00739	-15.1%	-5.3%	-19.4%
15-6-8-3	0.0086	-39.5%	-38.0%	-53.5%
15-6-8-4	0.00515	1.1%	3.5%	-22.3%
15-6-9-1	0.00342	33.7%	19.4%	-6.5%
15-6-9-2	0.00553	-3.1%	0.5%	-26.0%
15-6-9-3	0.00409	31.6%	36.5%	0.1%
15-6-9-4	0.00444	20.7%	25.2%	-7.8%
15-6-9-5	0.00404	35.1%	40.1%	1.3%
23-6-10-1	0.00641	-9.6%	0.9%	-7.1%
23-6-10-2	0.00633	-8.3%	2.3%	-6.0%
23-6-11-1	0.00689	-7.6%	13.7%	-1.7%
23-6-9-1	0.00523	-6.9%	-3.4%	-21.7%
23-6-9-2	0.00369	32.1%	37.0%	11.0%
23-6-11-2	0.00495	3.4%	10.2%	-12.7%
23-6-11-3	0.0073	-30.5%	-25.9%	-40.8%
	Avg Positive Error	**40.0%**	**26.4%**	**25.4%**
	Avg Negative Error	**-12.6%**	**-16.7%**	**-18.2%**

Accuracy of Crack Width Equations with Clark's Measured Crack Width (fs = 25 ksi)

Specimen No.	Max Width, in	Kaar-Mattock Error	Gergely-Lutz Error	Frosch Error
6-8-3-1	0.00207	143.1%	63.7%	85.9%
6-8-3-2	0.00143	251.4%	136.6%	169.2%
6-7 1/2-3-1	0.00258	91.7%	28.4%	40.9%
6-9-3-1	0.00246	90.9%	25.5%	22.1%
6-9-3-3	0.0034	38.3%	-9.1%	-11.7%
6-7 1/2-3-2	0.00309	45.6%	-5.7%	-15.9%
6-7 1/2-4-1	0.00436	18.7%	-17.7%	-15.4%
6-7 1/2-4-2	0.00226	129.0%	58.8%	63.3%
6-7 1/2-4-3	0.00402	28.5%	-10.9%	-8.2%
6-15-6-1	0.00669	-1.8%	-23.2%	6.1%
6-9-5-5	0.00457	22.9%	-10.7%	-3.9%
6-11-6-1	0.00559	9.9%	-16.3%	-4.8%
6-11-6-2	0.00627	-1.6%	-25.0%	-15.2%
6-15-7-1	0.00616	12.2%	-9.5%	16.3%
6-15-7-2	0.00709	-2.5%	-21.3%	1.1%
6-7 1/2-7-1	0.00806	-13.9%	-30.5%	-11.1%
6-7 1/2-7-2	0.00457	52.2%	22.9%	56.8%
6-7 1/2-5-1	0.00607	-9.9%	-35.5%	-38.2%
6-7 1/2-5-2	0.00589	-6.9%	-33.4%	-36.3%
6-7 1/2-5-3	0.00508	6.4%	-23.8%	-26.2%
6-9-8-1	0.00571	30.3%	9.6%	50.3%
6-9-8-2	0.00671	12.0%	-5.9%	27.9%
6-6-7-1	0.00708	-6.9%	-26.2%	-17.7%
6-7 1/2-6-1	0.00403	42.4%	5.1%	-5.4%
6-9 1/2-7-1	0.00531	22.9%	-4.5%	-10.8%
6-9 1/2-7-2	0.00406	56.9%	21.9%	16.6%
15-6-8-1	0.00669	12.4%	21.9%	7.8%
15-6-8-2	0.00769	-2.3%	6.0%	-6.2%
15-6-6-1	0.00668	-13.3%	-18.6%	-35.6%
15-6-6-2	0.0042	38.0%	29.5%	2.4%
15-6-6-3	0.00504	22.1%	21.6%	-5.7%
15-6-7-1	0.00362	32.7%	-0.8%	-9.3%
15-6-7-2	0.00578	10.4%	11.6%	-15.5%
15-6-7-3	0.00465	35.5%	37.0%	5.0%
15-6-7-4	0.00582	8.3%	9.5%	-16.1%
15-6-7-5	0.00774	-18.5%	-17.6%	-36.9%
15-6-10-1	0.00905	-12.7%	-2.5%	-17.8%
15-6-10-2	0.00941	-16.7%	-7.0%	-20.9%
15-6-8-3	0.01053	-38.2%	-36.7%	-52.5%
15-6-8-4	0.0069	-5.7%	-3.4%	-27.5%
15-6-9-1	0.00454	25.9%	12.4%	-11.9%
15-6-9-2	0.0067	0.0%	3.7%	-23.6%
15-6-9-3	0.00537	25.3%	29.9%	-4.7%
15-6-9-4	0.00589	13.8%	18.0%	-13.1%
15-6-9-5	0.00528	29.2%	34.0%	-3.1%
23-6-10-1	0.0092	-21.3%	-12.1%	-19.1%
23-6-10-2	0.00886	-18.1%	-8.6%	-16.0%
23-6-11-1	0.00884	-9.9%	10.7%	-4.3%
23-6-9-1	0.00702	-13.3%	-10.1%	-27.1%
23-6-9-2	0.00509	19.7%	24.1%	0.5%
23-6-11-2	0.00675	-5.2%	1.0%	-20.0%
23-6-11-3	0.00967	-34.4%	-30.1%	-44.2%
	Avg Positive Error	**43.1%**	**26.8%**	**35.8%**
	Avg Negative Error	**-12.7%**	**-16.3%**	**-18.1%**

Accuracy of Crack Width Equations with Clark's Measured Crack Width (fs = 30 ksi)

Specimen No.	Max Width, in	Kaar-Mattock Error	Gergely-Lutz Error	Frosch Error
6-12-3-2	0.00147	352.4%	215.1%	357.2%
6-8-3-1	0.00304	98.7%	33.8%	51.9%
6-8-3-2	0.00281	114.6%	44.5%	64.4%
6-7 1/2-3-1	0.00492	20.6%	-19.2%	-11.3%
6-9-3-1	0.00347	62.4%	6.8%	3.9%
6-9-3-3	0.00414	36.3%	-10.4%	-12.9%
6-7 1/2-3-2	0.00322	67.7%	8.6%	-3.2%
6-7 1/2-4-1	0.00623	-0.3%	-30.9%	-28.9%
6-7 1/2-4-2	0.00329	88.8%	30.9%	34.6%
6-7 1/2-4-3	0.00517	19.9%	-16.8%	-14.3%
6-15-6-1	0.00708	11.4%	-12.9%	20.3%
6-9-5-5	0.00500	34.8%	-2.0%	5.4%
6-11-6-1	0.00732	0.8%	-23.3%	-12.8%
6-11-6-2	0.00816	-9.2%	-30.9%	-21.8%
6-15-7-1	0.00501	65.5%	33.6%	71.7%
6-15-7-2	0.00892	-7.0%	-25.0%	-3.6%
6-7 1/2-7-1	0.00615	35.4%	9.3%	39.8%
6-7 1/2-7-2	0.00609	37.1%	10.6%	41.2%
6-7 1/2-5-1	0.00506	29.7%	-7.1%	-11.1%
6-7 1/2-5-2	0.00752	-12.5%	-37.4%	-40.2%
6-7 1/2-5-3	0.00653	-0.7%	-28.9%	-31.1%
6-9-8-1	0.00654	36.6%	14.8%	57.5%
6-9-8-2	0.00840	7.3%	-9.8%	22.6%
6-6-7-1	0.00941	-15.9%	-33.4%	-25.7%
6-7 1/2-6-1	0.00502	37.2%	1.2%	-8.9%
6-9 1/2-7-1	0.00639	22.5%	-4.8%	-11.1%
6-9 1/2-7-2	0.00730	4.7%	-18.7%	-22.2%
15-6-8-1	0.00823	9.6%	18.9%	5.1%
15-6-8-2	0.00793	13.7%	23.4%	9.1%
15-6-6-1	0.00889	-21.8%	-26.6%	-42.0%
15-6-6-2	0.00536	29.8%	21.7%	-3.7%
15-6-6-3	0.00632	16.8%	16.3%	-9.8%
15-6-7-1	0.00463	24.5%	-6.9%	-14.9%
15-6-7-2	0.00735	4.1%	5.3%	-20.3%
15-6-7-3	0.00558	35.5%	37.0%	5.0%
15-6-7-4	0.00721	4.9%	6.1%	-18.7%
15-6-7-5	0.00982	-22.9%	-22.0%	-40.3%
15-6-10-1	0.01047	-9.4%	1.1%	-14.7%
15-6-10-2	0.01130	-16.7%	-7.1%	-21.0%
15-6-8-3	0.01243	-37.2%	-35.6%	-51.7%
15-6-8-4	0.00824	-5.2%	-2.9%	-27.2%
15-6-9-1	0.00572	19.9%	7.1%	-16.1%
15-6-9-2	0.00802	0.3%	4.0%	-23.4%
15-6-9-3	0.00673	20.0%	24.4%	-8.8%
15-6-9-4	0.00632	27.2%	31.9%	-2.8%
15-6-9-5	0.00666	22.9%	27.5%	-7.8%
23-6-10-1	0.01170	-25.7%	-17.1%	-23.7%
23-6-10-2	0.01104	-21.2%	-12.0%	-19.1%
23-6-11-1	0.01049	-8.9%	12.0%	-3.2%
23-6-9-1	0.00882	-17.2%	-14.1%	-30.4%
23-6-9-2	0.00626	16.8%	21.1%	-1.9%
23-6-11-2	0.00881	-12.9%	-7.2%	-26.5%
	Avg Positive Error	**40.9%**	**25.6%**	**52.7%**
	Avg Negative Error	**-14.4%**	**-17.8%**	**-18.6%**

Accuracy of Crack Width Equations with Clark's Measured Crack Width (fs = 35 ksi)

Specimen No.	Max Width, in	Kaar-Mattock Error	Gergely-Lutz Error	Frosch Error
6-12-3-1	0.00161	381.8%	235.6%	387.0%
6-12-3-2	0.00287	170.3%	88.3%	173.2%
6-8-3-1	0.00464	51.8%	2.2%	16.1%
6-8-3-2	0.00434	62.1%	9.2%	24.2%
6-7 1/2-3-1	0.00523	32.4%	-11.4%	-2.7%
6-9-3-1	0.00455	44.5%	-5.0%	-7.6%
6-9-3-3	0.00528	24.7%	-18.0%	-20.4%
6-7 1/2-3-2	0.00445	41.6%	-8.3%	-18.3%
6-7 1/2-4-1	0.00774	-6.4%	-35.1%	-33.2%
6-7 1/2-4-2	0.00616	17.6%	-18.4%	-16.1%
6-7 1/2-4-3	0.00637	13.6%	-21.3%	-18.9%
6-15-6-1	0.00888	3.6%	-19.0%	11.9%
6-9-5-5	0.00615	27.8%	-7.1%	-0.1%
6-11-6-1	0.00902	-4.6%	-27.4%	-17.4%
6-11-6-2	0.00950	-9.0%	-30.7%	-21.6%
6-15-7-1	0.00563	71.8%	38.7%	78.2%
6-15-7-2	0.01093	-11.5%	-28.5%	-8.2%
6-7 1/2-7-1	0.00734	32.4%	6.8%	36.7%
6-7 1/2-7-2	0.00765	27.3%	2.8%	31.2%
6-7 1/2-5-1	0.00618	23.9%	-11.3%	-15.1%
6-7 1/2-5-2	0.00903	-15.0%	-39.1%	-41.9%
6-7 1/2-5-3	0.00657	15.2%	-17.5%	-20.1%
6-9-8-1	0.00793	31.4%	10.5%	51.5%
6-9-8-2	0.01062	-1.0%	-16.7%	13.2%
6-6-7-1	0.01109	-16.7%	-34.0%	-26.4%
6-7 1/2-6-1	0.00651	23.4%	-8.9%	-18.0%
6-9 1/2-7-1	0.00793	15.2%	-10.5%	-16.4%
6-9 1/2-7-2	0.00924	-3.5%	-25.0%	-28.3%
15-6-8-1	0.00947	11.1%	20.6%	6.6%
15-6-8-2	0.00980	7.3%	16.5%	3.0%
15-6-6-1	0.01075	-24.6%	-29.2%	-44.0%
15-6-6-2	0.00649	25.0%	17.3%	-7.2%
15-6-6-3	0.00799	7.8%	7.3%	-16.7%
15-6-7-1	0.00557	20.7%	-9.7%	-17.5%
15-6-7-2	0.00883	1.1%	2.3%	-22.6%
15-6-7-3	0.00666	32.4%	33.9%	2.7%
15-6-7-4	0.00859	2.7%	3.9%	-20.4%
15-6-7-5	0.01170	-24.5%	-23.6%	-41.6%
15-6-10-1	0.01221	-9.4%	1.1%	-14.7%
15-6-10-2	0.01399	-21.5%	-12.4%	-25.5%
15-6-8-3	0.01427	-36.1%	-34.6%	-50.9%
15-6-8-4	0.00958	-4.9%	-2.6%	-26.9%
15-6-9-1	0.00673	18.9%	6.2%	-16.8%
15-6-9-2	0.00965	-2.8%	0.8%	-25.8%
15-6-9-4	0.00884	6.1%	10.0%	-19.0%
15-6-9-5	0.00805	18.6%	23.0%	-11.0%
23-6-10-1	0.01436	-29.4%	-21.2%	-27.5%
23-6-10-2	0.01289	-21.2%	-12.1%	-19.2%
23-6-11-1	0.01221	-8.7%	12.2%	-3.0%
23-6-9-1	0.01061	-19.7%	-16.7%	-32.5%
23-6-9-2	0.00737	15.8%	20.0%	-2.8%
	Avg Positive Error	**40.0%**	**25.9%**	**64.3%**
	Avg Negative Error	**-14.2%**	**-19.2%**	**-20.4%**

Accuracy of Crack Width Equations with Clark's Measured Crack Width (fs = 40 ksi)

Specimen No.	Max Width, in	Kaar-Mattock Error	Gergely-Lutz Error	Frosch Error
6-12-3-1	0.00440	101.5%	40.3%	103.7%
6-12-3-2	0.00455	94.9%	35.7%	96.9%
6-8-3-1	0.00637	26.4%	-14.9%	-3.3%
6-8-3-2	0.00572	40.6%	-5.3%	7.7%
6-7 1/2-3-1	0.00534	48.2%	-0.8%	8.9%
6-9-3-1	0.00588	27.8%	-16.0%	-18.3%
6-9-3-3	0.00673	11.8%	-26.5%	-28.6%
6-7 1/2-3-2	0.00579	24.3%	-19.5%	-28.2%
6-7 1/2-4-1	0.00967	-14.3%	-40.6%	-38.9%
6-7 1/2-4-2	0.00648	27.8%	-11.4%	-8.9%
6-7 1/2-4-3	0.00751	10.1%	-23.7%	-21.4%
6-15-6-1	0.01055	-0.3%	-22.1%	7.7%
6-9-5-5	0.00712	26.2%	-8.3%	-1.3%
6-11-6-1	0.01093	-10.0%	-31.5%	-22.1%
6-11-6-2	0.01166	-15.3%	-35.5%	-27.0%
6-15-7-1	0.00700	57.9%	27.5%	63.8%
6-15-7-2	0.01293	-14.5%	-31.0%	-11.3%
6-7 1/2-7-1	0.00602	84.4%	48.9%	90.5%
6-7 1/2-7-2	0.00892	24.8%	0.7%	28.6%
6-7 1/2-5-1	0.00745	17.4%	-15.9%	-19.5%
6-7 1/2-5-2	0.01069	-17.9%	-41.3%	-43.9%
6-7 1/2-5-3	0.00751	15.2%	-17.5%	-20.1%
6-9-8-1	0.00932	27.8%	7.4%	47.4%
6-9-8-2	0.02793	-57.0%	-63.8%	-50.8%
6-6-7-1	0.01428	-26.1%	-41.5%	-34.7%
6-7 1/2-6-1	0.00708	29.7%	-4.3%	-13.9%
6-9 1/2-7-2	0.01078	-5.5%	-26.6%	-29.7%
15-6-8-1	0.01099	9.4%	18.7%	5.0%
15-6-8-2	0.01388	-13.4%	-6.0%	-16.9%
15-6-6-1	0.01275	-27.3%	-31.8%	-46.0%
15-6-6-2	0.00765	21.2%	13.7%	-10.1%
15-6-6-3	0.00903	9.0%	8.6%	-15.8%
15-6-7-1	0.00663	15.9%	-13.3%	-20.8%
15-6-7-2	0.01055	-3.3%	-2.2%	-25.9%
15-6-7-3	0.00790	27.6%	29.0%	-1.1%
15-6-7-4	0.00991	1.7%	2.9%	-21.1%
15-6-7-5	0.01359	-25.7%	-24.9%	-42.5%
15-6-10-1	0.01366	-7.4%	3.3%	-12.8%
15-6-10-2	0.01638	-23.4%	-14.5%	-27.3%
15-6-8-3	0.02083	-50.0%	-48.8%	-61.6%
15-6-8-4	0.01092	-4.7%	-2.3%	-26.7%
15-6-9-1	0.00802	14.0%	1.8%	-20.2%
15-6-9-2	0.01144	-6.3%	-2.8%	-28.4%
15-6-9-4	0.01038	3.3%	7.1%	-21.1%
15-6-9-5	0.00951	14.8%	19.0%	-13.9%
23-6-10-1	0.01654	-30.0%	-21.8%	-28.0%
23-6-10-2	0.01477	-21.4%	-12.3%	-19.4%
23-6-11-1	0.01393	-8.6%	12.4%	-2.8%
23-6-9-1	0.01276	-23.7%	-20.8%	-35.8%
23-6-9-2	0.00880	10.8%	14.9%	-7.0%
	Avg Positive Error	**29.4%**	**17.2%**	**46.0%**
	Avg Negative Error	**-18.5%**	**-21.2%**	**-23.2%**

Accuracy of Crack Width Equations with Clark's Measured Crack Width (fs = 45 ksi)

Specimen No.	Max Width, in	Kaar-Mattock Error	Gergely-Lutz Error	Frosch Error
6-12-3-1	0.00709	40.7%	-2.0%	42.2%
6-12-3-2	0.00816	22.2%	-14.9%	23.5%
6-8-3-1	0.00799	13.4%	-23.7%	-13.3%
6-8-3-2	0.00714	26.7%	-14.7%	-3.0%
6-7 1/2-3-1	0.00649	37.1%	-8.2%	0.8%
6-9-3-1	0.00523	61.6%	6.3%	3.4%
6-9-3-3	0.00506	67.3%	10.0%	6.9%
6-7 1/2-3-2	0.00691	17.2%	-24.1%	-32.3%
6-7 1/2-4-3	0.01140	-18.4%	-43.4%	-41.7%
6-15-6-1	0.01377	-14.1%	-32.9%	-7.2%
6-9-5-5	0.00833	21.3%	-11.8%	-5.1%
6-11-6-1	0.01149	-3.7%	-26.7%	-16.7%
6-11-6-2	0.01451	-23.4%	-41.7%	-34.0%
6-15-7-1	0.00837	48.6%	19.9%	54.1%
6-15-7-2	0.01668	-25.4%	-39.8%	-22.7%
6-7 1/2-7-1	0.01047	19.3%	-3.7%	23.2%
6-7 1/2-7-2	0.01070	17.0%	-5.5%	20.6%
6-7 1/2-5-1	0.00884	11.3%	-20.3%	-23.6%
6-7 1/2-5-2	0.01223	-19.3%	-42.2%	-44.8%
6-7 1/2-5-3	0.00936	4.0%	-25.6%	-27.9%
15-6-8-1	0.01483	-8.8%	-1.0%	-12.5%
15-6-8-2	0.02402	-43.7%	-38.9%	-46.0%
15-6-6-1	0.01453	-28.2%	-32.7%	-46.7%
15-6-6-2	0.00916	13.9%	6.8%	-15.5%
15-6-6-3	0.01064	4.1%	3.6%	-19.6%
15-6-7-1	0.00758	14.0%	-14.7%	-22.1%
15-6-7-2	0.01186	-3.2%	-2.1%	-25.9%
15-6-7-3	0.00930	21.9%	23.3%	-5.5%
15-6-10-1	0.01624	-12.4%	-2.2%	-17.5%
15-6-10-2	0.01930	-26.9%	-18.4%	-30.6%
23-6-10-1	0.01908	5.0%	-0.8%	-11.2%
23-6-10-2	0.01693	-35.7%	-26.8%	-33.6%
	Avg Positive Error	**24.6%**	**11.7%**	**21.8%**
	Avg Negative Error	**-20.3%**	**-19.9%**	**-23.3%**

Chi's & Kirstein's (1958) Specimen Data

Specimen	b, in	h, in	d, in	dc, in	#bars	Bar #	fc', psi	fy, psi
CK1	7.5	6	5.25	0.75	2	4	5840	40000
CK2	7.5	6	5.25	0.75	2	4	2360	40000
CK3	11	6	5.12	0.88	2	6	6110	40000
CK4	11	6	5.12	0.88	2	6	2110	40000
CK5	6	15	13.06	1.94	2	7	6630	40000
CK6	6	15	13.06	1.94	2	7	6655	40000
CK7	6	15	13.06	1.94	2	7	2520	40000
CK8	6	15	13.06	1.94	2	7	2130	40000
CK9	6	15	13	2	1	8	6100	40000
CK10	6	15	13	2	1	8	5930	40000
CK11	6	15	13	2	1	8	3060	40000
CK12	6	15	13	2	1	8	2285	40000
CK13	6	23	20.87	2.13	1	10	6330	40000
CK14	6	23	20.87	2.13	1	10	2400	40000
CK15	6	23	20.94	2.06	2	9	6460	40000
CK16	6	23	20.94	2.06	2	9	2450	40000

Accuracy of Crack Width Equations with Chi & Kirstein's Measured Crack Width (fs = 15 ksi)

Specimen No.	Max Width, in	Kaar-Mattock Error	Gergely-Lutz Error	Frosch Error
CK1	0.00091	225.2%	125.5%	143.3%
CK3	0.00285	27.2%	-2.7%	12.2%
CK4	0.00375	77.0%	35.4%	-14.7%
CK5	0.00205	83.3%	85.4%	43.0%
CK6	0.0025	50.2%	51.9%	17.2%
CK7	0.00323	68.8%	70.7%	-9.3%
CK8	0.00335	103.3%	105.6%	-12.5%
CK10	0.00272	56.2%	69.5%	59.1%
CK12	0.00228	128.8%	148.3%	89.8%
CK14	0.00286	82.8%	103.6%	55.8%
CK15	0.00282	38.0%	43.1%	8.9%
CK16	0.00319	96.0%	103.2%	-3.7%
	Avg Positive Error	**86.4%**	**85.6%**	**53.6%**
	Avg Negative Error	**0.0%**	**-2.7%**	**-10.1%**

Accuracy of Crack Width Equations with Chi & Kirstein's Measured Crack Width (fs = 20 ksi)

Specimen No.	Max Width, in	Kaar-Mattock Error	Gergely-Lutz Error	Frosch Error
CK1	0.00191	106.6%	43.2%	54.6%
CK2	0.00247	93.1%	33.9%	19.5%
CK3	0.00469	3.1%	-21.1%	-9.1%
CK4	0.00535	65.4%	26.5%	-20.3%
CK5	0.0046	8.9%	10.1%	-15.1%
CK6	0.00456	9.8%	11.1%	-14.3%
CK7	0.00522	39.3%	40.8%	-25.1%
CK8	0.00334	171.9%	174.9%	17.0%
CK10	0.00497	14.0%	23.7%	16.1%
CK12	0.00416	67.2%	81.4%	38.7%
CK13	0.0061	-5.9%	4.8%	-2.6%
CK14	0.0055	26.7%	41.2%	8.0%
CK15	0.00469	10.6%	14.7%	-12.7%
CK16	0.00502	66.1%	72.2%	-18.4%
	Avg Positive Error	**52.5%**	**44.5%**	**25.6%**
	Avg Negative Error	**-5.9%**	**-21.1%**	**-14.7%**

Accuracy of Crack Width Equations with Chi & Kirstein's Measured Crack Width (fs = 25 ksi)

Specimen No.	Max Width, in	Kaar-Mattock Error	Gergely-Lutz Error	Frosch Error
CK1	0.00256	92.7%	33.6%	44.2%
CK2	0.0046	29.6%	-10.1%	-19.8%
CK3	0.00659	-8.3%	-29.8%	-19.1%
CK4	0.00669	65.3%	26.5%	-20.3%
CK5	0.00355	76.4%	78.4%	37.6%
CK6	0.00499	25.5%	26.9%	-2.1%
CK7	0.00582	56.1%	57.9%	-16.1%
CK8	0.00706	60.8%	62.6%	-30.8%
CK9	0.00541	30.6%	41.7%	33.3%
CK10	0.00736	-3.8%	4.4%	-2.0%
CK11	0.00428	83.0%	98.6%	68.5%
CK12	0.00527	65.0%	79.0%	36.8%
CK13	0.00878	-18.3%	-9.0%	-15.4%
CK14	0.00735	18.5%	32.1%	1.0%
CK15	0.00673	-3.6%	-0.1%	-24.0%
CK16	0.00659	58.1%	64.0%	-22.3%
	Avg Positive Error	**55.1%**	**50.5%**	**36.9%**
	Avg Negative Error	**-8.5%**	**-12.3%**	**-17.2%**

Accuracy of Crack Width Equations with Chi & Kirstein's Measured Crack Width (fs = 30 ksi)

Specimen No.	Max Width, in	Kaar-Mattock Error	Gergely-Lutz Error	Frosch Error
CK1	0.00353	67.7%	16.3%	25.5%
CK2	0.00621	15.2%	-20.1%	-28.7%
CK3	0.00805	-9.9%	-31.1%	-20.6%
CK4	0.00796	66.7%	27.6%	-19.7%
CK5	0.00683	10.0%	11.3%	-14.2%
CK6	0.0063	19.2%	20.6%	-7.0%
CK7	0.00698	56.2%	58.0%	-16.0%
CK8	0.00895	52.2%	53.9%	-34.5%
CK9	0.00739	14.7%	24.5%	17.1%
CK10	0.00954	-10.9%	-3.4%	-9.3%
CK11	0.00538	74.7%	89.6%	60.8%
CK12	0.00637	63.8%	77.7%	35.8%
CK13	0.01108	-22.3%	-13.4%	-19.6%
CK14	0.00903	15.8%	29.0%	-1.3%
CK15	0.00863	-9.8%	-6.5%	-28.8%
CK16	0.00821	52.3%	57.9%	-25.2%
	Avg Positive Error	**42.4%**	**42.4%**	**34.8%**
	Avg Negative Error	**-13.2%**	**-14.9%**	**-18.7%**

Accuracy of Crack Width Equations with Chi & Kirstein's Measured Crack Width (fs = 35 ksi)

Specimen No.	Max Width, in	Kaar-Mattock Error	Gergely-Lutz Error	Frosch Error
CK1	0.00449	53.8%	6.6%	15.1%
CK2	0.00783	6.6%	-26.1%	-34.0%
CK3	0.00941	-10.1%	-31.2%	-20.7%
CK4	0.00929	66.7%	27.5%	-19.7%
CK5	0.0084	4.4%	5.6%	-18.6%
CK6	0.008	9.6%	10.8%	-14.5%
CK8	0.01091	45.7%	47.3%	-37.3%
CK9	0.00991	-0.2%	8.3%	1.9%
CK10	0.0117	-15.3%	-8.1%	-13.7%
CK11	0.00672	63.2%	77.1%	50.2%
CK12	0.00775	57.1%	70.4%	30.3%
CK13	0.01298	-22.6%	-13.8%	-19.9%
CK14	0.01068	14.2%	27.2%	-2.7%
CK15	0.01049	-13.5%	-10.3%	-31.7%
CK16	0.00991	47.2%	52.6%	-27.7%
	Avg Positive Error	**36.8%**	**33.3%**	**24.4%**
	Avg Negative Error	**-12.3%**	**-17.9%**	**-21.9%**

Accuracy of Crack Width Equations with Chi & Kirstein's Measured Crack Width (fs = 40 ksi)

Specimen No.	Max Width, in	Kaar-Mattock Error	Gergely-Lutz Error	Frosch Error
CK1	0.00546	44.5%	0.2%	8.2%
CK2	0.00945	1.0%	-30.0%	-37.5%
CK3	0.01071	-9.7%	-30.9%	-20.4%
CK4	0.01062	66.6%	27.5%	-19.7%
CK5	0.01022	-2.0%	-0.8%	-23.5%
CK6	0.01	0.2%	1.3%	-21.9%
CK8	0.01257	44.5%	46.1%	-37.8%
CK9	0.01166	-3.0%	5.2%	-1.0%
CK11	0.00811	54.5%	67.7%	42.3%
CK13	0.01566	-26.7%	-18.3%	-24.1%
CK14	0.01235	12.9%	25.7%	-3.8%
CK15	0.01274	-18.6%	-15.6%	-35.7%
	Avg Positive Error	**32.0%**	**24.8%**	**25.2%**
	Avg Negative Error	**-12.0%**	**-19.1%**	**-22.6%**

Hognestad's (1962) Specimen Data

Specimen	b, in	h, in	d, in	dc, in	#bars	Bar #	fc', psi	fy, psi
H29	8	16	15.2	0.8	2	7	4030	60000
H30	8	16	14.2	1.8	2	7	3040	60000
H31	8	16	12.7	3.3	2	7	3640	60000
H32	8	16	11.2	4.8	2	7	3640	60000
H33	8	16	14.2	1.8	2	7	4360	60000
H34	8	16	14.2	1.8	2	7	4360	60000
H35	8	16	15.2	0.8	2	7	3940	60000
H36	8	16	12.7	3.3	2	7	3940	60000

Accuracy of Crack Width Equations with Hognestad's Measured Crack Width (fs = 20 ksi)

Specimen	Max Width, in	Kaar-Mattock Error	Gergely-Lutz Error	Frosch Error
H29	0.002	140.9%	72.5%	58.1%
H30	0.002	242.2%	243.5%	112.3%
H31	0.005	43.4%	85.3%	34.6%
H32	0.01	-21.3%	19.0%	-0.7%
H33	0.003	92.4%	93.2%	41.5%
H34	0.005	15.4%	15.9%	-15.1%
H35	0.005	-2.8%	-30.4%	-36.8%
H36	0.005	38.5%	79.0%	34.6%
	Avg Positive Error	**95.5%**	**86.9%**	**56.2%**
	Avg Negative Error	**-12.1%**	**-30.4%**	**-17.5%**

Accuracy of Crack Width Equations with Hognestad's Measured Crack Width (fs = 30 ksi)

Specimen	Max Width, in	Kaar-Mattock Error	Gergely-Lutz Error	Frosch Error
H29	0.004	80.7%	29.4%	18.5%
H30	0.005	105.3%	106.1%	27.4%
H31	0.012	-10.4%	15.8%	-15.9%
H32	0.019	-37.8%	-6.1%	-21.6%
H33	0.007	23.7%	24.2%	-9.0%
H34	0.006	44.3%	44.9%	6.1%
H35	0.007	4.1%	-25.5%	-32.3%
H36	0.008	29.8%	67.8%	26.1%
	Avg Positive Error	**48.0%**	**48.0%**	**19.6%**
	Avg Negative Error	**-24.1%**	**-15.8%**	**-19.7%**

Accuracy of Crack Width Equations with Hognestad's Measured Crack Width (fs = 40 ksi)

Specimen	Max Width, in	Kaar-Mattock Error	Gergely-Lutz Error	Frosch Error
H29	0.006	60.6%	15.0%	5.4%
H30	0.008	71.1%	71.8%	6.1%
H31	0.019	-24.5%	-2.5%	-29.2%
H32	0.03	-47.5%	-20.7%	-33.8%
H33	0.01	15.4%	15.9%	-15.1%
H34	0.011	4.9%	5.4%	-22.8%
H35	0.01	-2.8%	-30.4%	-36.8%
H36	0.012	15.4%	49.1%	12.1%
	Avg Positive Error	**33.5%**	**31.4%**	**7.9%**
	Avg Negative Error	**-25.0%**	**-17.9%**	**-27.5%**

Accuracy of Crack Width Equations with Hognestad's Measured Crack Width (fs = 50 ksi)

Specimen	Max Width, in	Kaar-Mattock Error	Gergely-Lutz Error	Frosch Error
H29	0.007	72.1%	23.2%	12.9%
H30	0.011	55.5%	56.2%	-3.5%
H31	0.025	-28.3%	-7.3%	-32.7%
H32	0.043	-54.2%	-30.8%	-42.3%
H33	0.012	20.2%	20.7%	-11.5%
H34	0.0115	25.5%	26.0%	-7.7%
H35	0.011	10.4%	-20.9%	-28.2%
H36	0.018	-3.8%	24.3%	-6.6%
	Avg Positive Error	**36.7%**	**30.1%**	**12.9%**
	Avg Negative Error	**-28.8%**	**-19.7%**	**-18.9%**

Kaar's and Mattock's (1963) Specimen Data

Specimen	b, in	h, in	d, in	dc, in	#bars	Bar #	fc', psi	fy, psi
KM-4.75R	4.75	17.5	13.625	3.875	8	4	3880	60000
KM-4.75T	4.75	17.5	13.625	3.875	8	4	4090	60000
KM-8R	8	16	13.625	2.375	8	4	4550	60000
KM-8T	8	16	13.625	2.375	8	4	3590	60000
KM-16R	16	16	13.625	2.375	8	4	4050	60000
KM-16T	16	16	13.625	2.375	8	4	4460	60000
KM-24R	24	16	13.625	2.375	8	4	3760	60000
KM-32R1	32	15.25	13.625	1.625	8	4	3960	60000
KM-32R2	32	16	13.625	2.375	8	4	4170	60000
KM-S1	24	8	6	2	3	6	4020	60000
KM-S2	24	8	6	2	3	4	3780	60000
KM-S3	24	8	6	2	3	10	4410	60000
KMS4	24	8	6	2	2	10	4090	60000

Accuracy of Crack Width Equations with Kaar's and Mattock's Measured Crack Width (fs = 40 ksi)

Specimen No.	Max Width, in	Kaar-Mattock Error	Gergely-Lutz Error	Frosch Error
KM-4.75R	0.013	61.5%	90.4%	8.0%
KM-4.75T	0.0104	74.1%	105.3%	35.0%
KM-8R	0.0108	-10.0%	-9.7%	-26.2%
KM-8T	0.0128	-12.1%	-11.8%	-37.8%
KM-16R	0.014	-32.6%	-28.3%	-39.6%
KM-16T	0.0148	-37.1%	-33.1%	-42.8%
KM-24R	0.0144	-31.1%	-24.2%	-36.0%
KM-32R1	0.0134	-29.7%	-32.4%	-40.1%
KM-32R2	0.0189	-45.6%	-38.7%	-46.1%
KM-S1	0.0199	-34.0%	-26.7%	-28.1%
KM-S2	0.0202	-41.6%	-35.1%	-29.2%
KM-S3	0.0266	-0.3%	10.8%	-46.2%
KMS4	0.0257	-27.2%	-16.3%	-21.3%
	Avg Positive Error	**67.8%**	**68.8%**	**21.5%**
	Avg Negative Error	**-27.4%**	**-25.6%**	**-35.7%**

Hutton's (1966) Specimen Data

Specimen	b, in	h, in	d, in	dc, in	#bars	Bar #	fc', psi	fy, psi
HU-2P-1R-1	6	5	3.5	1.5	1	5	7450	60000
HU-1P-2R-1	6	5	3.5	1.5	2	5	7000	60000
HU-0P-3R-1A	6	5	3.75	1.25	3	5	7250	60000

Accuracy of Crack Width Equations with Hutton's (1966) Measured Crack Width (All fs)

Specimen No.	Max Width, in	Kaar-Mattock Error	Gergely-Lutz Error	Frosch Error
HU-2P-1R-1	0.001	45.0%	39.6%	32.1%
HU-2P-1R-1	0.002	74.9%	68.3%	59.3%
HU-2P-1R-1	0.003	70.6%	64.2%	55.4%
HU-2P-1R-1	0.005	108.1%	100.3%	89.6%
HU-2P-1R-1	0.007	86.4%	79.5%	69.9%
HU-2P-1R-1	0.009	72.5%	66.0%	57.2%
HU-1P-2R-1	0.001	2.6%	-6.8%	-50.8%
HU-1P-2R-1	0.002	18.0%	7.2%	-43.5%
HU-1P-2R-1	0.002	105.2%	86.5%	-1.7%
HU-1P-2R-1	0.004	100.1%	81.8%	-4.1%
HU-1P-2R-1	0.006	95.0%	77.1%	-6.6%
HU-1P-2R-1	0.008	97.6%	79.5%	-5.4%
HU-1P-2R-1	0.011	74.5%	58.5%	-16.4%
HU-0P-3R-1A	0.0002	345.3%	262.5%	-27.1%
HU-0P-3R-1A	0.0005	211.7%	153.8%	-49.0%
HU-0P-3R-1A	0.0007	249.9%	184.8%	-42.8%
HU-0P-3R-1A	0.0012	326.7%	247.4%	-30.2%
HU-0P-3R-1A	0.0025	283.0%	211.8%	-37.3%
HU-0P-3R-1A	0.003	285.9%	214.2%	-36.9%
HU-0P-3R-1A	0.004	334.2%	253.4%	-29.0%
HU-0P-3R-1A	0.005	358.7%	273.4%	-25.0%
HU-0P-3R-1A	0.007	281.7%	210.7%	-37.5%
HU-0P-3R-1A	0.008	256.2%	190.0%	-41.7%
HU-0P-3R-1A	0.009	248.8%	184.0%	-42.9%
HU-0P-3R-1A	0.009	281.0%	210.1%	-37.7%
	Avg Positive Error	**176.5%**	**141.9%**	**60.6%**
	Avg Negative Error	**0.0%**	**-6.8%**	**-29.8%**

APPENDIX II BASE CASE BEAM DIMENSIONS AND RELIABILITY INDICES

Base Case: L = 20 ft: 27 Beams

L, ft	fy, ksi	fc', ksi	b, in	d, in	dc, in	h, in	As5, in²	No. #5 bars	s5, in	β5	As10, in²	No. #10 bars	s10, in	β10
20	40	4	8	16	1	17	3.37	11	1.20	**4.19**	3.68	3	3.00	**3.83**
20	40	4	8	16	2	18	3.37	11	1.20	**3.33**	3.68	3	3.00	**3.15**
20	40	4	8	16	3	19	3.37	11	1.20	**2.50**	3.68	3	3.00	**2.41**
20	60	4	8	16	1	17	1.84	6	1.20	**4.46**	2.45	2	6.00	**3.23**
20	60	4	8	16	2	18	1.84	6	1.20	**3.66**	2.45	2	6.00	**2.69**
20	60	4	8	16	3	19	1.84	6	1.20	**2.85**	2.45	2	6.00	**2.07**
20	80	4	8	16	1	17	1.23	4	2.00	**3.71**	1.23	1	8.00	**1.39**
20	80	4	8	16	2	18	1.23	4	2.00	**2.79**	1.23	1	8.00	**0.92**
20	80	4	8	16	3	19	1.23	4	2.00	**1.74**	1.23	1	8.00	**0.40**
20	40	6	8	16	1	17	4.30	14	1.38	**3.92**	4.91	4	2.00	**3.90**
20	40	6	8	16	2	18	4.30	14	1.38	**3.00**	4.91	4	2.00	**3.11**
20	40	6	8	16	3	19	4.30	14	1.38	**1.97**	4.91	4	2.00	**2.19**
20	60	6	8	16	1	17	2.45	8	1.71	**3.70**	2.45	2	6.00	**2.17**
20	60	6	8	16	2	18	2.45	8	1.71	**2.65**	2.45	2	6.00	**1.53**
20	60	6	8	16	3	19	2.45	8	1.71	**1.66**	2.45	2	6.00	**0.91**
20	80	6	8	16	1	17	1.84	6	1.20	**4.22**	2.45	2	6.00	**3.05**
20	80	6	8	16	2	18	1.84	6	1.20	**3.53**	2.45	2	6.00	**2.60**
20	80	6	8	16	3	19	1.84	6	1.20	**2.89**	2.45	2	6.00	**2.09**
20	40	8	8	16	1	17	4.91	16	1.20	**4.02**	4.91	4	2.00	**3.97**
20	40	8	8	16	2	18	4.91	16	1.20	**3.25**	4.91	4	2.00	**3.32**
20	40	8	8	16	3	19	4.91	16	1.20	**2.24**	4.91	4	2.00	**2.42**
20	60	8	8	16	1	17	3.07	10	1.33	**3.98**	3.68	3	3.00	**3.64**
20	60	8	8	16	2	18	3.07	10	1.33	**3.23**	3.68	3	3.00	**3.05**
20	60	8	8	16	3	19	3.07	10	1.33	**2.24**	3.68	3	3.00	**2.16**
20	80	8	8	16	1	17	2.15	7	1.00	**4.46**	2.45	2	6.00	**3.48**
20	80	8	8	16	2	18	2.15	7	1.00	**3.76**	2.45	2	6.00	**2.96**
20	80	8	8	16	3	19	2.15	7	1.00	**3.21**	2.45	2	6.00	**2.55**

Base Case: L = 30ft: 27 Beams

L, ft	fy, ksi	fc', ksi	b, in	d, in	dc, in	h, in	As5, in²	No. #5 bars	s5, in	β5	As10, in²	No. #10 bars	s10, in	β10
30	40	4	12	24	1	25	7.36	24	1.30	**4.08**	7.36	6	2.00	**4.01**
30	40	4	12	24	2	26	7.36	24	1.30	**3.37**	7.36	6	2.00	**3.38**
30	40	4	12	24	3	27	7.36	24	1.30	**2.38**	7.36	6	2.00	**2.48**
30	60	4	12	24	1	25	4.30	14	1.54	**3.95**	4.91	4	3.33	**3.49**
30	60	4	12	24	2	26	4.30	14	1.54	**3.14**	4.91	4	3.33	**2.84**
30	60	4	12	24	3	27	4.30	14	1.54	**2.15**	4.91	4	3.33	**1.97**
30	80	4	12	24	1	25	2.76	9	1.25	**4.33**	3.68	3	5.00	**3.45**
30	80	4	12	24	2	26	2.76	9	1.25	**3.48**	3.68	3	5.00	**2.79**
30	80	4	12	24	3	27	2.76	9	1.25	**2.79**	3.68	3	5.00	**2.26**
30	40	6	12	24	1	25	9.51	31	1.00	**4.29**	9.82	8	1.43	**4.29**
30	40	6	12	24	2	26	9.51	31	1.00	**3.74**	9.82	8	1.43	**3.79**
30	40	6	12	24	3	27	9.51	31	1.00	**3.01**	9.82	8	1.43	**3.13**
30	60	6	12	24	1	25	5.52	18	1.18	**4.42**	6.14	5	2.50	**4.19**
30	60	6	12	24	2	26	5.52	18	1.18	**3.45**	6.14	5	2.50	**3.35**
30	60	6	12	24	3	27	5.52	18	1.18	**2.73**	6.14	5	2.50	**2.69**
30	80	6	12	24	1	25	3.68	12	1.82	**3.67**	3.68	3	5.00	**2.53**
30	80	6	12	24	2	26	3.68	12	1.82	**2.77**	3.68	3	5.00	**1.95**
30	80	6	12	24	3	27	3.68	12	1.82	**1.67**	3.68	3	5.00	**1.15**
30	40	8	12	24	1	25	11.04	36	1.14	**4.20**	11.04	9	1.25	**4.27**
30	40	8	12	24	2	26	11.04	36	1.14	**3.50**	11.04	9	1.25	**3.65**
30	40	8	12	24	3	27	11.04	36	1.14	**2.54**	11.04	9	1.25	**2.76**
30	60	8	12	24	1	25	6.44	21	1.00	**4.24**	7.36	6	2.00	**4.15**
30	60	8	12	24	2	26	6.44	21	1.00	**3.78**	7.36	6	2.00	**3.73**
30	60	8	12	24	3	27	6.44	21	1.00	**3.06**	7.36	6	2.00	**3.06**
30	80	8	12	24	1	25	4.30	14	1.54	**4.04**	4.91	4	3.33	**3.56**
30	80	8	12	24	2	26	4.30	14	1.54	**3.06**	4.91	4	3.33	**2.77**
30	80	8	12	24	3	27	4.30	14	1.54	**2.15**	4.91	4	3.33	**1.98**

Base Case: L = 40ft: 27 Beams

L, ft	fy, ksi	fc', ksi	b, in	d, in	dc, in	h, in	As5, in²	No. #5 bars	s5, in	β5	As10, in²	No. #10 bars	s10, in	β10
40	40	4	15	30	1	31	11.35	37	1.08	**4.28**	12.27	10	1.44	**4.27**
40	40	4	15	30	2	32	11.35	37	1.08	**3.34**	12.27	10	1.44	**3.40**
40	40	4	15	30	3	33	11.35	37	1.08	**2.62**	12.27	10	1.44	**2.73**
40	60	4	15	30	1	31	6.44	21	1.30	**4.08**	7.36	6	2.60	**3.79**
40	60	4	15	30	2	32	6.44	21	1.30	**3.25**	7.36	6	2.60	**3.09**
40	60	4	15	30	3	33	6.44	21	1.30	**2.32**	7.36	6	2.60	**2.24**
40	80	4	15	30	1	31	4.30	14	1.00	**4.22**	4.91	4	4.33	**3.58**
40	80	4	15	30	2	32	4.30	14	1.00	**3.66**	4.91	4	4.33	**3.19**
40	80	4	15	30	3	33	4.30	14	1.00	**2.94**	4.91	4	4.33	**2.57**
40	40	6	15	30	1	31	15.03	49	1.08	**4.10**	15.95	13	2.17	**3.95**
40	40	6	15	30	2	32	15.03	49	1.08	**3.49**	15.95	13	2.17	**3.43**
40	40	6	15	30	3	33	15.03	49	1.08	**2.56**	15.95	13	2.17	**2.58**
40	60	6	15	30	1	31	8.59	28	1.44	**3.93**	8.59	7	2.17	**3.80**
40	60	6	15	30	2	32	8.59	28	1.44	**2.88**	8.59	7	2.17	**2.87**
40	60	6	15	30	3	33	8.59	28	1.44	**1.95**	8.59	7	2.17	**2.02**
40	80	6	15	30	1	31	5.83	19	1.44	**3.85**	6.14	5	3.25	**3.36**
40	80	6	15	30	2	32	5.83	19	1.44	**2.97**	6.14	5	3.25	**2.66**
40	80	6	15	30	3	33	5.83	19	1.44	**2.01**	6.14	5	3.25	**1.84**
40	40	8	15	30	1	31	17.18	56	1.18	**4.16**	17.18	14	2.00	**4.08**
40	40	8	15	30	2	32	17.18	56	1.18	**3.12**	17.18	14	2.00	**3.14**
40	40	8	15	30	3	33	17.18	56	1.18	**2.28**	17.18	14	2.00	**2.37**
40	60	8	15	30	1	31	9.82	32	1.26	**4.01**	9.82	8	1.86	**3.94**
40	60	8	15	30	2	32	9.82	32	1.26	**3.21**	9.82	8	1.86	**3.23**
40	60	8	15	30	3	33	9.82	32	1.26	**2.26**	9.82	8	1.86	**2.35**
40	80	8	15	30	1	31	6.75	22	1.24	**4.11**	7.36	6	2.60	**3.86**
40	80	8	15	30	2	32	6.75	22	1.24	**3.42**	7.36	6	2.60	**3.28**
40	80	8	15	30	3	33	6.75	22	1.24	**2.37**	7.36	6	2.60	**2.29**

Note: L = span length
f_y = steel yield strength
f_c' = concrete strength
b = beam width
d = beam effective depth
d_c = concrete cover
h = beam height
As5/10 = area of steel reinforcement using #5/#10 bars, respectively
No. #5/#10 bars = number of #5/#10 bars, respectively
s5/10 = spacing of #5/#10 bars, respectively
β5/10 = reliability index using #5/#10 bars, respectively

APPENDIX III MATLAB DESIGN AND SIMULATION CODES

BEAM DESIGN CODE: Base Case

```
%CODE TO DESIGN BEAMS%
%INPUT Span Length L (ft), fy (psi), fc'(psi), dc (in)%
%INPUT Data
input = xlsread('beaminput.xls');
L=input(:,1)';
fy=input(:,2)';
fc=input(:,3)';
dc=input(:,4)';

%Permute Input Matrix
I=npermutek([1 2 3],4);
V = [L(I(:,1))' fy(I(:,2))' fc(I(:,3))' dc(I(:,4))'];


%RUN FOR NUMBER OF CASES N;  INPUT N
N=81;
i=1;

for i=1:N

%Design Beams for all combinations
d(i)=ceil(V(i,1)*12/16);

if mod(d(i),2)==1
   d(i)=d(i)+1;
end

b(i)=ceil(d(i)/2);
h(i) = V(i,4) + d(i);

selfwt = (b(i)*h(i)/144*150)/1000;
wu = 1.2*selfwt + 1.6*1;
Mu(i) = [wu*(V(i,1))^2]/8*12;

cb = d(i)*87000/(87000+(V(i,2)));
c = 0.5*cb;

if (V(i,3) <= 4000)
   B1 = 0.85;
else
   B1 = 0.85-0.05*((V(i,3)-4000)/1000);
end

a = c*B1;

As(i) = (0.85*V(i,3)*b(i)*a)/(V(i,2));

NumberofNo5bars(i)=ceil(As(i)/0.307);
NumberofNo10bars(i)=ceil(As(i)/1.227);
```

```
As5(i)=NumberofNo5bars(i)*(.097656*pi);
MAs5(i) = As5(i);
Layers5(i)= 1;

As10(i)=NumberofNo10bars(i)*(.390625*pi);
MAs10(i) = As10(i);
Layers10(i) = 1;

if NumberofNo5bars(i) > 1
s5(i) = (b(i)-2)/(NumberofNo5bars(i)-1);
else s5(i) = b(i);
end

d5(i) = d(i);

if ((s5(i) < 1) | (s5(i)*(NumberofNo5bars(i)-1)) > b(i))
   MAs5(i) = As5(i)/2;
   s5(i) = 2*s5(i);
   Layers5(i) = 2;
   d5(i) = d(i)- 5/16 - 0.5;
   if ((s5(i) < 1) | (s5(i)*(NumberofNo5bars(i)-1)/2) > b(i))
      MAs5(i) = As5(i)/3;
      s5(i) = 3/2*s5(i);
      Layers5(i) = 3;
      d5(i) = d(i) - 5/8-1;
   end
   if ((s5(i) < 1) | (s5(i)*(NumberofNo5bars(i)-1)/3) > b(i))
      MAs5(i) = As5(i)/4;
      s5(i) = 4/3*s5(i);
      Layers5(i) = 4;
      d5(i) = d(i) -1.5*5/8-1.5;
   end
   if ((s5(i) < 1) | (s5(i)*(NumberofNo5bars(i)-1)/4) > b(i))
      MAs5(i) = As5(i)/5;
      s5(i) = 5/4*s5(i);
      Layers5(i) = 5;
      d5(i) = d(i)-2*5/8-2;
   end
   if ((s5(i) < 1) | (s5(i)*(NumberofNo5bars(i)-1)/5) > b(i))
      MAs5(i) = As5(i)/6;
      s5(i) = 6/5*s5(i);
      Layers5(i) = 6;
      d5(i) = d(i)-2.5*5/8-2.5;
   end

end


if NumberofNo10bars(i) > 1
s10(i) = (b(i)-2)/(NumberofNo10bars(i)-1);
else s10(i) = b(i);
end
```

```
d10(i) = d(i);
if ((s10(i) < 10/8) | (s10(i)*(NumberofNo10bars(i)-1)) > b(i))
   MAs10(i) = As10(i)/2;
   s10(i) = 2*s10(i);
   Layers10(i) = 2;
   d10(i) = d(i) - 10/16-0.5;
   if ((s10(i) < 10/8) | (s10(i)*(NumberofNo10bars(i)-1)/2) > b(i))
      MAs10(i) = As10(i)/3;
      s10(i) = 3/2*s10(i);
      Layers10(i) = 3;
      d10(i) = d(i) - 10/8-1;
   end
   if ((s10(i) < 10/8) | (s10(i)*(NumberofNo10bars(i)-1)/3) > b(i))
      MAs10(i) = As10(i)/4;
      s10(i) = 4/3*s10(i);
      Layers10(i) = 4;
      d10(i) = d(i) - 10/8-1.5;
   end

end



a5(i) = (As5(i))*V(i,2)/(0.85*V(i,3)*b(i));
a10(i) = (As10(i))*V(i,2)/(0.85*V(i,3)*b(i));

c5 = a5(i)/B1;
c10 = a10(i)/B1;

e5=0.003*((d(i)-c5)/c5);

if  e5 > 0.005
     phi5(i) = 0.9;
elseif (0.002 <= e5) & (e5 <= 0.005)
       phi5(i) = 0.65 + (e5-0.002)*250/3;
else
   phi5(i) = 0.65;

end

Mu5(i) = phi5(i)*((As5(i))*V(i,2)*(d5(i)-a5(i)/2))/1000;

if Mu5(i) > Mu(i)
   Design5(i) = 1;
else
   Design5(i) = 0;
end

e10=0.003*((d(i)-c10)/c10);



if  e10 > 0.005
   phi10(i)= 0.90;
elseif (0.002 <= e10) & (e10 <= 0.005)
```

```
        phi10(i) = 0.65 + (e10-0.002)*250/3;
else
        phi10(i)=0.65;

end

Mu10(i) = phi10(i)*((As10(i))*V(i,2)*(d10(i)-a10(i)/2))/1000;

if Mu10(i) > Mu(i)
   Design10(i) = 1;
else
   Design10(i) = 0;
end

Vu(i) = (1.6*1000*V(i,1) + 1.2*b(i)*h(i)/144*150*V(i,1))/24;
Vn5(i) = 2*sqrt(V(i,3))*b(i)*d5(i);
Vn10(i) = 2*sqrt(V(i,3))*b(i)*d10(i);

if Vn5(i) > Vu(i)
   Shear5(i) = 1;
else
   Shear5(i) = 0;
end

if Vn10(i) > Vu(i)
   Shear10(i) = 1;
else
   Shear10(i) = 0;
end

i=i+1;
end
```

RANDOM NUMBER GENERATOR CODE FOR EACH VARIABLE: Base Case

```
%Code to Generate Random Numbers%

rel= xlsread('designoutput.xls');

i=1;

for i=1:81
   b_mu(i)= rel(i,4);
   b_sigma(i)= b_mu(i)*0.04;

   As5_mu(i)= rel(i,11)*.9;
   As5_sigma(i)= As5_mu(i)*0.015;
```

```
As10_mu(i) = rel(i,17)*0.9;
As10_sigma(i)= As10_mu(i)*0.015;

if rel(i,3)== 4000
fc_mu(i)= log(rel(i,3)*1.21);
fc_sigma(i)= sqrt(0.155);
elseif rel(i,3) == 6000
   fc_mu(i)= log(rel(i,3)*1.22);
   fc_sigma(i)= sqrt(.075);
elseif rel(i,3)== 8000
   fc_mu(i)= log(rel(i,3)*1.093);
   fc_sigma(i)= sqrt(.088);
end

CEc_mu(i)= 33.6;
CEc_sigma(i)= 4.08912;

w_mu(i)= 150;
w_sigma(i)= 4.5;

Es_mu(i)= 29000;
Es_sigma(i)= Es_mu(i)*0.024;

fy_mu(i)= log(rel(i,2)*1.13);
fy_sigma(i)= sqrt(.03);

d5_mu(i)= rel(i,9)*.99;
d5_sigma(i)= d5_mu(i)*0.04;

d10_mu(i)= rel(i,15)*.99;
d10_sigma(i)= d10_mu(i)*0.04;

if  rel(i,1)== 20
P_mu(i)= 83.33;
P_sigma(i)= 83.333*0.19;
elseif  rel(i,1) == 30
   P_mu(i)= 83.33;
   P_sigma(i)= 83.333*0.18;
elseif   rel(i,1) == 40
   P_mu(i)= 83.33;
   P_sigma(i)= 83.333*0.17;
end

dc_mu(i)= rel(i,6);
dc_sigma(i)= dc_mu(i)*0.04;

h_mu(i)= rel(i,7);
h_sigma(i)= 0.15625;

wc_mu(i)= 0.016;
wc_sigma(i)= 0.0032;
```

```
   Length(i)= rel(i,1)*12;
   spacing5(i)= rel(i,13);
   spacing10(i)= rel(i,19);

   i=i+1;
end
```

MONTE CARLO SIMULATION CODE: Base Case

```
%Monte Carlo Simulation

reliRA;
i=1;
for i=1:81


b = normrnd(b_mu(i),b_sigma(i),1,2000);
As5 = normrnd(As5_mu(i),As5_sigma(i),1,2000);
As10 = normrnd(As10_mu(i),As10_sigma(i),1,2000);
fc = lognrnd(fc_mu(i),fc_sigma(i),1,2000);
CEc = normrnd(CEc_mu(i),CEc_sigma(i),1,2000);
w = normrnd(w_mu(i),w_sigma(i),1,2000);
Es = normrnd(Es_mu(i),Es_sigma(i),1,2000);
fy = lognrnd(fy_mu(i),fy_sigma(i),1,2000);
d5 = normrnd(d5_mu(i),d5_sigma(i),1,2000);
d10 = normrnd(d10_mu(i),d10_sigma(i),1,2000);
u=rand(1,2000);
k=1;
for k=1:2000
P(k)=((83.333-0.45*28.33)-(log(-log(u(k)))/(1.282/20.833)));
k=k+1;
end

dc = normrnd(dc_mu(i),dc_sigma(i),1,2000);
h = normrnd(h_mu(i),h_sigma(i),1,2000);
wc = normrnd(wc_mu(i),wc_sigma(i),1,2000);
L=Length(i);
s5=spacing5(i);
s10=spacing10(i);

j=1;
for j = 1:2000;
   Beta(j)=1+.08*dc(j);
   Ec(j)=CEc(j)*(w(j)^1.5)*sqrt(fc(j));
   fs5(j)=
[3*(As5(j)*Es(j)+3*Ec(j)*b(j)*d5(j)+sqrt(As5(j)^2+Es(j)^2+2*As5(j)*Es(j)*Ec(j)*b(j)*d5(j)))*P(j)*L^2]/[
8*d5(j)*(4*As5(j)*Es(j)+9*Ec(j)*b(j)*d5(j))*As5(j)];
   fs10(j)=
[3*(As5(j)*Es(j)+3*Ec(j)*b(j)*d10(j)+sqrt(As5(j)^2+Es(j)^2+2*As5(j)*Es(j)*Ec(j)*b(j)*d10(j)))*P(j)*L^
2]/[8*d10(j)*(4*As5(j)*Es(j)+9*Ec(j)*b(j)*d10(j))*As5(j)];
```

```
    resistance5(j)= [wc(j)*1000*Es(j)]/[2*Beta(j)*sqrt(dc(j)^2+(s5/2)^2)];
    resistance10(j)= [wc(j)*1000*Es(j)]/[2*Beta(j)*sqrt(dc(j)^2+(s10/2)^2)];
    G5(j)=resistance5(j)-fs5(j);
    G10(j)=resistance10(j)-fs10(j);

    j=j+1;
end

Gmean5= mean(G5);
Gmean10= mean(G10);
Gstdev5= std(G5);
Gstdev10= std(G10);
RelIndex5(i)= Gmean5/Gstdev5;
RelIndex10(i) = Gmean10/Gstdev10;
i=i+1;
end
```